

# A Practical Framework for Component-Level Structural Health Monitoring of the Gerald Desmond Bridge

Mehran Rahmani, PhD, PE  
Andrea Calabrese, PhD

Vesna Terzic, PhD  
Brittany Campbell



# MINETA TRANSPORTATION INSTITUTE

Founded in 1991, the Mineta Transportation Institute (MTI), an organized research and training unit in partnership with the Lucas College and Graduate School of Business at San José State University (SJSU), increases mobility for all by improving the safety, efficiency, accessibility, and convenience of our nation's transportation system. Through research, education, workforce development, and technology transfer, we help create a connected world. MTI leads the [Mineta Consortium for Transportation Mobility \(MCTM\)](#) and the [Mineta Consortium for Equitable, Efficient, and Sustainable Transportation \(MCEEST\)](#) funded by the U.S. Department of Transportation, the [California State University Transportation Consortium \(CSUTC\)](#) funded by the State of California through Senate Bill I and the Climate Change and Extreme Events Training and Research (CCEETR) Program funded by the Federal Railroad Administration. MTI focuses on three primary responsibilities:

## Research

MTI conducts multi-disciplinary research focused on surface transportation that contributes to effective decision making. Research areas include: active transportation; planning and policy; security and counterterrorism; sustainable transportation and land use; transit and passenger rail; transportation engineering; transportation finance; transportation technology; and workforce and labor. MTI research publications undergo expert peer review to ensure the quality of the research.

## Education and Workforce Development

To ensure the efficient movement of people and products, we must prepare a new cohort of transportation professionals who are ready to lead a more diverse, inclusive, and equitable transportation industry. To help achieve this, MTI sponsors a suite of workforce development and education opportunities. The Institute supports educational programs offered by the Lucas Graduate School of Business: a Master of Science in Transportation Management, plus graduate certificates that include High-Speed and Intercity Rail Management and Transportation Security Management. These flexible programs offer live online classes so that working transportation professionals can pursue an advanced degree regardless of their location.

## Information and Technology Transfer

MTI utilizes a diverse array of dissemination methods and media to ensure research results reach those responsible for managing change. These methods include publication, seminars, workshops, websites, social media, webinars, and other technology transfer mechanisms. Additionally, MTI promotes the availability of completed research to professional organizations and works to integrate the research findings into the graduate education program. MTI's extensive collection of transportation-related publications is integrated into San José State University's world-class Martin Luther King, Jr. Library.

---

## Disclaimer

The contents of this report reflect the views of the authors, who are responsible for the facts and accuracy of the information presented herein. This document is disseminated in the interest of information exchange. MTI's research is funded, partially or entirely, by grants from the U.S. Department of Transportation, the U.S. Department of Homeland Security, the California Department of Transportation, and the California State University Office of the Chancellor, whom assume no liability for the contents or use thereof. This report does not constitute a standard specification, design standard, or regulation.

Report 23-34

# A Practical Framework for Component-Level Structural Health Monitoring of the Gerald Desmond Bridge

Mehran Rahmani, PhD, PE

Vesna Terzic, PhD

Andrea Calabrese, PhD

Brittany Campbell

December 2023

A publication of the  
Mineta Transportation Institute  
Created by Congress in 1991  
College of Business  
San José State University  
San José, CA 95192-0219

# TECHNICAL REPORT DOCUMENTATION PAGE

<b>1. Report No.</b> 23-34	<b>2. Government Accession No.</b>	<b>3. Recipient's Catalog No.</b>	
<b>4. Title and Subtitle</b> A Practical Framework for Component-Level Structural Health Monitoring of the Gerald Desmond Bridge		<b>5. Report Date</b> December 2023	
		<b>6. Performing Organization Code</b>	
<b>7. Authors</b> Mehran Rahmani, PhD, PE Vesna Terzic, PhD Andrea Calabrese, PhD Brittany Campbell		<b>8. Performing Organization Report</b> CA-MTI-2155	
<b>9. Performing Organization Name and Address</b> Mineta Transportation Institute College of Business San José State University San José, CA 95192-0219		<b>10. Work Unit No.</b>	
		<b>11. Contract or Grant No.</b> ZSB12017-SJAUX	
<b>12. Sponsoring Agency Name and Address</b> State of California SB1 2017/2018 Trustees of the California State University Sponsored Programs Administration 401 Golden Shore, 5th Floor Long Beach, CA 90802		<b>13. Type of Report and Period Covered</b>	
		<b>14. Sponsoring Agency Code</b>	
<b>15. Supplemental Notes</b>			
<b>16. Abstract</b> Bridges serve as critical transportation infrastructure, but traditional maintenance inspection to ensure their safety is time-consuming, costly, and labor-intensive, especially for larger and more complex structures. This study presents a practical framework for the instrumentation, data acquisition, and remote condition assessment of the Gerald Desmond Bridge, California's largest cable-stayed bridge. The framework aims to establish a foundation for real-time or near real-time remote health monitoring of the bridge's critical elements. Through a comprehensive literature review, best practices and recent advancements in sensing technologies and instrumentation strategies utilized in similar cable-stayed bridges worldwide were examined. The study emphasizes the importance of understanding the bridge's load path, structural redundancy, and the failure mechanisms of critical elements to design an effective monitoring regime. The proposed instrumentation includes a wide range of cutting-edge and sustainable monitoring sensors, addressing challenges related to data acquisition for a large sensing network. A set of requirements was gathered to guide the design process, covering wireless sensing technologies, local response monitoring, scalability, cable tension analysis, energy-saving techniques, fatigue life estimation, and compensation for thermal effects. Element-specific instrumentation and layout designs tailored to the critical elements of the bridge were proposed. The study highlights the advantages of remote monitoring in terms of efficiency, cost-effectiveness, and early detection of damage. Verification and calibration of the sensing network are crucial steps, involving field tests, data analysis, and the determination of thresholds for healthy or anomalous responses. The study underscores the importance of these verifications and calibrations in enhancing the system's reliability and accuracy for early damage detection.			
<b>17. Key Words</b> Bridge health monitoring, Cable-stayed, Wireless sensors, Accelerometers, Strain gauges	<b>18. Distribution Statement</b> No restrictions. This document is available to the public through The National Technical Information Service, Springfield, VA 22161.		
<b>19. Security Classif. (of this report)</b> Unclassified	<b>20. Security Classif. (of this page)</b> Unclassified	<b>21. No. of Pages</b> 119	<b>22. Price</b>

Copyright © 2023

by **Mineta Transportation Institute**

All rights reserved.

DOI: 10.31979/mti.2023.2155

Mineta Transportation Institute College of Business  
San José State University San José, CA 95192-0219

Tel: (408) 924-7560

Fax: (408) 924-7565

Email: [mineta-institute@sjsu.edu](mailto:mineta-institute@sjsu.edu)

[transweb.sjsu.edu/research/2155](http://transweb.sjsu.edu/research/2155)

# ACKNOWLEDGMENTS

This research study was supported by California State University Transportation Consortium (CSUTC) via funding provided through California's Senate Bill 1 (SB 1). We express our sincere gratitude for this support.

We would also like to thank the Mineta Transportation Institute (MTI) at San José State University (SJSU) for their leadership in allocating the grants and their role in promoting transportation research in California. We also thank Dr. Hilary Nixon from MTI for her support for this project.

We would also like to express our gratitude for the generous support provided by Ms. Tanya Wyckoff from Caltrans, who supplied the research team with the structural drawings and reports.

# CONTENTS

Acknowledgments .....	vi
List of Figures .....	ix
List of Tables .....	xiv
Executive Summary.....	1
1. Introduction .....	3
1.1. Problem Statement .....	3
1.2. Project Objectives .....	7
1.3. Proposed Monitoring Strategy and Devices: Process and Major Steps.....	8
2. Sensors and Sensing Technologies Used for Civil Engineering Applications: A Detailed Review .....	11
2.1 Strain Gages.....	12
2.2 Accelerometers.....	20
2.3 Displacement Sensors .....	23
2.4 Tiltmeters and Inclinometers.....	25
2.5 Load Cells.....	26
2.6 Anemometers.....	27
2.7 Temperature Sensors .....	28
2.8 Humidity Sensors .....	30
3. Cable-Stayed Bridge Health Monitoring: A Literature Review .....	32
3.1 Instrumentation Approaches and Sensing Technologies Used for Monitoring Cable- Stayed Bridges.....	32
3.2 A review of Bridge Health Monitoring Methodologies: The Post- Processing Attemp.....	53

4. The Case-Study Cable-Stayed Bridge: Description and Dynamic Response.....	56
4.1. Bridge Structural System, Design Considerations, and Critical Elements .....	56
4.2. Codes and Guidelines for the Design of Bridges and Their Maintenance .....	60
4.3. Existing Monitoring System on the Bridge and Recorded Response During Carson 2021 Earthquake .....	63
5. Proposed Instrumentation Framework for the Bridge.....	76
5.1. Monitoring Strategy and Proposed Sensing Network.....	76
5.2. Recommended Sensor Types, Placement, and Naming Convention.....	82
6. Summary, Conclusion, and Future Work .....	94
Bibliography .....	97
About the Authors .....	103

# LIST OF FIGURES

Figure 1.1. A bird's eye view of the old (front) and the new (rear) Gerald Desmond Bridge (Source: Port of Long Beach) .....	5
Figure 1.2. Main elements of a structural health monitoring (SHM) system for bridges.....	7
Figure 2.1. A detailed view of conventional foil strain gauges (reprinted from Michigan Scientific Corp: <a href="http://www.michsci.com">www.michsci.com</a> ).....	13
Figure 2.2. a) Strain gages attached to the top and bottom of a bridge floor beam (Bischoff et al. 2009), b) a strain gage welded to a steel reinforcing bar prior to construction (Dong et al. 2010) .....	14
Figure 2.3. The principal technology behind Fiber Optic Intensity sensors when subject to deformation: A) using two in-line optical fibers, B) using an optical fiber and a mirror (reprinted from Massaroni et. al 2015).....	16
Figure 2.4. Schematic illustration of change in light intensity in a fiber optic intensity sensor as a function of measured strain.....	16
Figure 2.5. The principle behind Fiber Bragg Grating (FBG) optical sensors (e.g., strain gages). The wavelength of reflected light from the vertical gratings (shown in blue) changes as the sensor deforms axially. The spectrum of colors is indicative of wavelength variation (reprinted from Massaroni et al. 2015) .....	17
Figure 2.6. a) FBG strain gage and its input/output wires (source: <a href="http://polytec.com">polytec.com</a> ), b) internal structure of a FBG strain gage (Wang et al. 2013) .....	18
Figure 2.7. A schematic view of internal components of a vibrating wire strain gage (Woszczyński et al. 2022) .....	19
Figure 2.8. Examples of vibrating wire strain gages for monitoring steel structures. a) steel profile with welded VW strain gages (source: <a href="http://geo-instruments.com">geo-instruments.com</a> ), b) VW strain gages attached to steel joint plates of a bridge (source: <a href="http://spectotechnology.com">spectotechnology.com</a> ) .....	20
Figure 2.9. Inside view of SMA-1 analog accelerograms (courtesy of Mihailo Trifunac) .....	21
Figure 2.10. Internal structure of a typical spring-mass accelerometer (reprinted from Li et al. 2018).....	22
Figure 2.11. Components of a piezoelectric accelerometer (reprinted from Ghemari et al. 2018). .....	22

Figure 2.12. a) Internal structure of a LVDT displacement sensor (reprinted from Greif et al. 2006), b) an image of two commercial LVDT sensors manufactured by Megatron Elektronik GmbH & Co. (source: directindustry.com).....	24
Figure 2.13. a) Image illustrating a LVDT gage attached to a masonry stone of a historic tower (Said et al. 2005), b) displacement sensor attached at a steel bridge joint (source: resensys.com).....	24
Figure 2.14. a) A tilt beam rotational sensor, b) a zoomed in view of the tilt sensor at the center of the casing rod (source: soilinstruments.com) .....	26
Figure 2.15. Illustration of Fiber Bragg Grating tiltmeter technology (reprinted from Guo et al. 2015) .....	26
Figure 2.16. a) A view of compression strain-gaged load-cell (source: sensocar.com), b) a view of a S-type tension/compression load cell (source: sensocar.com) .....	27
Figure 2.17. Conventional anemometer mounted on a pole for wind speed measurement (source: munroinstruments.com) .....	28
Figure 2.18. a) Internal structure of a thermocouple temperature sensor (reprinted from Thamrin et al. 2007), b) components of two types of Resistive Temperature Detector (RTD) sensors (source: electrical4u.com) .....	29
Figure 2.19. The principle behind a Fiber Bragg Grating (FBG) temperature sensor (reprinted from Chen et al. 2018).....	30
Figure 2.20. a) Diagram illustrating a capacitive humidity sensor (reprinted from Lee and Lee, 2005), b) example of a commercial capacitive humidity sensor (source: TZT Teng store).....	31
Figure 3.1. Sensors layout for Wuhan bridge (No.2). Str: strain gauges; T: temperature sensors; Vib: vibration sensors; CCD: displacement monitoring system. Reprinted from Shengchun and Desheng (2008) .....	37
Figure 3.2. Strain gauge sensors layout for Tsing Ma Bridge. Reprinted from Ye et al. (2012) .....	38
Figure 3.3. Sensor types and layout for Third Bridge at Panama Canal. Reprinted from Arlin and Melendez (2017) .....	40
Figure 3.4. Flowchart of a wireless sensor network (WSN) components and communication order for bridge health monitoring. Reprinted from Noel et al. (2017).....	43

Figure 3.5. Sensor types and layout for the Yonghe Bridge. Reprinted from Kaloop and Hu (2016) .....	45
Figure 3.6. Sensor types and layout for the new Jindo Bridge. Reprinted from Joe et al. (2011) .....	46
Figure 3.7. Hierarchical data coordination in a cluster-based topology. Reprinted from Joe et al. (2011).....	48
Figure 3.8. Number of responsive wireless sensors as a function of their distance from the gateway node. Reprinted from Jang et al. (2010).....	49
Figure 3.9. Application of a magnetic frictional strain gauge produced by Sokki Kenkyujo Co (right) attached to the bottom flange of the Jindo Bridge (left). Reprinted from Jo et al. (2013).....	50
Figure 3.10. Use of solar panel for energy harvesting at the cable node (left), rechargeable battery (middle), use of wind turbine at girder's bottom flange. Reprinted from Jo et al. (2011).....	52
Figure 3.11. Status of sensor node solar rechargeable battery voltage over time. The black curve belongs to a solar battery installed under the deck. Reprinted from Jo et al. (2011) .....	52
Figure 4.1. A rendering of the completed Gerald Desmond Bridge (Source: Port of Long Beach) .....	57
Figure 4.2. The main span, towers and stay cables arrangement (Source: structural drawings supplied by the Caltrans) .....	57
Figure 4.3. Stay cables' connection to the tower (left) and a close view of steel anchor boxes and concrete corbels (right) (Source: structural drawings supplied by the Caltrans) .....	58
Figure 4.4. Aerial view of the bridge deck framing including girders, floor beams, stringers, and cable anchorage (Source: Bing map bird's eye view) .....	59
Figure 4.5. Existing Accelerometers layout on the main-span of the bridge – CSMIP station 14703 (source: <a href="https://www.strongmotioncenter.org">https://www.strongmotioncenter.org</a> ).....	64
Figure 4.6. Existing Accelerometers placement on the West Tower – CSMIP station 14703 (source: <a href="https://www.strongmotioncenter.org">https://www.strongmotioncenter.org</a> ) .....	65

Figure 4.7. Existing Accelerometers placement on the East Tower – CSMIP station 14703 (source: <a href="https://www.strongmotioncenter.org">https://www.strongmotioncenter.org</a> .....	66
Figure 4.8. Cross-section view of existing Accelerometers placement on the edge girders – CSMIP station 14703 (source: <a href="https://www.strongmotioncenter.org">https://www.strongmotioncenter.org</a> ).....	66
Figure 4.9. ShakeMap of the Carson 2021 earthquake and the shaking intensity contours (a). Location of the earthquake epicenter relative to the bridge (b). (source: <a href="https://www.strongmotioncenter.org">https://www.strongmotioncenter.org</a> ) .....	69
Figure 4.10. Recorded acceleration and estimated displacement response on the bridge deck and foundation level during Carson 2021 earthquake. The recorded motion is in longitudinal direction (i.e., along the bridge) .....	70
Figure 4.11. Recorded acceleration and estimated displacement response on the bridge deck and foundation level during Carson 2021 earthquake. The recorded motion is in transverse direction (i.e., perpendicular to the bridge).....	71
Figure 4.12. Fourier transform amplitudes (FT) of acceleration response at the deck level (top) and foundation level (bottom) along the longitudinal direction.....	72
Figure 4.13. Power Spectral Density (PSD) of acceleration response at the deck level (top) and foundation level (bottom) along the longitudinal direction .....	73
Figure 4.14. Fourier transform amplitudes (FT) of acceleration response at the deck level (top) and foundation level (bottom) along the transverse direction .....	74
Figure 4.15. Power Spectral Density (PSD) of acceleration response at the deck level (top) and foundation level (bottom) along the transverse direction. ....	75
Figure 5.1. The proposed wireless sensors network topology for the Gerald Desmond Bridge .....	81
Figure 5.2. Recommended cables’ accelerometers placement and naming convention.....	83
Figure 5.3. Recommended strain gages placement(s) and naming convention(s) for girders.....	84
Figure 5.4. Layout of recommended accelerometers on girders and towers .....	85
Figure 5.5. Displacement transducer at select girders’ splice joints, and loadcells at the east and west bents.....	86

Figure 5.6. Tiltmeters, GPS sensors and anemometers layout recommended for installation on the bridge girders and towers..... 87

Figure 5.7. Layout of FBG fiber optic strain gages recommended for the anchor boxes. The strain gages should be installed near the top flange of stiffener plate..... 89

Figure 5.8. Layout of corrosion and temperature sensors recommended at steel anchor boxes. Humidity sensors will be placed on the interior and exterior of tower..... 90

Figure 5.9. Displacement transducers for installation on the viscous dampers at deck..... 91

# LIST OF TABLES

Table 3.1. A comparison between wired and wireless sensor networks for use in bridge health monitoring, adopted from Noel et al. (2017).....	42
Table 5.1. Recommended sensor types for monitoring the critical elements of the bridge ....	80
Table 5.2. Summary of the monitoring network, including critical elements, sensing clusters, and associated unique sensors' IDs .....	93

# Executive Summary

This study presents a practical framework for instrumentation and data acquisition and aggregation for the new Gerald Desmond Bridge. The recommended instrumentation is intended to serve as the basis for a remote condition assessment of the bridge's critical elements. The bridge, located at the Port of Long Beach and completed in 2020, is California's first cable-stayed bridge that serves as a critical transportation link in the region. The iconic bridge features a unique 2,000-foot-long cable-stayed segment. This very large structure demands frequent inspection and monitoring to ensure the health of its critical elements, such as its towers, girders, and stay cables. The framework presented in this study will be effective in creating a foundation for real-time, or near real-time, remote health monitoring of the bridge. The framework primarily targets the monitoring of the bridge's critical elements. As part of this study, a comprehensive literature review on best practices and recent advancements in both sensing technologies and instrumentation strategies utilized in similar cable-stayed bridges worldwide was performed. The framework identifies and recommends appropriate sensor types for each critical element, optimal sensor placements, and provides a consistent naming convention for all sensing channels across the monitoring network.

The structural system of the bridge and its design reports, such as load rating reports, have been reviewed, and the existing array of 44 accelerometers on the main span of the bridge, deployed by the California Geological Survey (CGS), is discussed in detail in Chapter 4. For reference, the response of the bridge during a local earthquake (Carson 2021) has been analyzed in the time and frequency domain. A comprehensive understanding of the load path and structural redundancy within the bridge is crucial when designing an effective monitoring regime. This knowledge allowed us to explain the failure mechanisms of critical elements and their potential impact on adjacent elements. The proposed instrumentation in this study will go beyond accelerometer arrays to encompass a wide range of cutting-edge and sustainable monitoring sensors, including Fiber Bragg Grating (FBG) friction strain gauges, displacement transducers, fiber optic temperature sensors, FBG tiltmeters, ultrasonic anemometers, and more. Challenges associated with data acquisition for a large sensing network have been thoroughly examined, and practical solutions have been proposed to ensure the resiliency of the network.

In this study, all the crucial factors associated with the design of a successful remote monitoring system have been thoroughly examined. We gathered a set of requirements that serve as guiding principles for the design process, including (1) wireless sensing technologies and their advantages, (2) element-level local response monitoring, (3) scalability of the network, (4) cables' tension analysis, (5) energy saving and harvesting, (6) fatigue life estimation of fracture-critical elements, (7) compensation of response for thermal effects, (8) decentralization of the data acquisition, and more. Each factor was carefully reviewed to ensure the establishment of a monitoring system for the bridge that is both reliable and resilient. Subsequently, we proposed element-specific instrumentation and layout designs tailored to the bridge's critical elements.

Traditional visual inspection involves several challenges for a complex and exceptionally large structure like the Gerald Desmond Bridge. These challenges include (1) labor intensity, (2) time consumption, (3) cost, and (4) subjectivity. Considering these challenges, alternative methods such as monitoring the bridge's critical elements using sensory data and detecting damage or deterioration in its early stages are highly desirable for inspectors and operators. The remote monitoring of bridge elements offers significant advantages in facilitating emergency responses in large cities. Providing early warnings for unsafe routes as soon as damage is detected enables a fast response to ensure public safety.

Verification and calibration of the sensing network are key steps after the proposed sensors have been partially or fully deployed on the bridge. A series of recordings can be collected during heavy and light traffic hours, as well as on windy days. The recorded responses of members under each sensing cluster must be reviewed, and the accuracy of the values should be confirmed. Calculated responses should be compared with results obtained from the finite element model to verify and calibrate the sensor network and the post-processing algorithm based on actual on-site data. Furthermore, thresholds for healthy responses and anomalous responses at critical elements should be determined using the field tests. Response variabilities in the parameter of interest (e.g., strain or displacement) and their sensitivity to various environmental, operational, or non-damage related phenomena (such as creep, shrinkage cracks, thermal expansion, or contraction) should be investigated and filtered out. These verifications and calibrations are crucial for early damage warning systems, as they enhance the system's reliability and prevents future false positive alerts.

# 1. Introduction

## 1.1. Problem Statement

The new Gerald Desmond Bridge, completed in 2020, is California's first cable-stayed bridge, situated in the city of Long Beach. It serves as a critical transportation link and contributes significantly to the economy of Southern California. Spanning over the back channel of the Port of Long Beach's inner harbor, this six-lane bridge features a unique 2,000-foot-long cable-stayed segment. The main span, stretching 1,000 feet, crosses the channel, while the east and west sides are supported by two 500-foot back spans. Figure 1.1 shows a view of the old and the new bridges. The cable-stayed segment of the Gerald Desmond Bridge is supported by two tall reinforced concrete towers, each measuring 515 feet in height. In total, there are 80 stay cables, with 40 cables attached to each tower. These stay cables play a crucial role in connecting the edge girders of the bridge deck to the towers' structures.

Cable-stayed bridges have become an increasingly popular option for the design of long-span bridges. One of the main reasons for their popularity is the economic advantage they offer. Cable-stayed bridges require fewer materials compared to other bridge types, resulting in cost savings. Additionally, the construction time for cable-stayed bridges is often shorter, further contributing to their economic feasibility. The design of the Gerald Desmond Bridge faced a significant challenge due to seismic activity in the southern California region. This necessitated special considerations and seismic design measures to ensure the bridge's immediate serviceability even during small- to moderate-level earthquakes. In order to accommodate large displacements caused by seismic events, the bridge's design incorporated horizontal and vertical dampers, also known as "shock absorbers," as well as an innovative swivel joint at two ends of the cable-stayed bridge. The purpose of these dampers is to activate only when the bridge undergoes significant movement, dissipating energy and minimizing the impact of seismic forces on the bridge's structural integrity.

This relatively complex bridge requires frequent inspection and monitoring to ensure the health of its critical elements, such as its deck, girders, and stay cables. It is essential to facilitate early detection of any damage or deterioration in these elements. The bridge accommodates a daily traffic volume of approximately 66,000 vehicles, with about one-third of them being heavy trucks. Regular structural monitoring will enable timely and more manageable repairs of the affected elements, ensuring uninterrupted service to the Port and meeting the regional transportation demand. Traditional visual inspection has been the preferred method for assessing bridge components in many cases. However, this approach involves several challenges for a complex and exceptionally large structure like the Gerald Desmond Bridge. These challenges include:

*Labor Intensity:* Frequent visual inspections require a significant amount of human effort, making them labor-intensive. Due to this limitation, bridge inspections are performed by Structure Maintenance and Investigations (SM&I) engineers approximately once every two years, per federal and state bridge maintenance guidelines ([dot.ca.gov](http://dot.ca.gov)).

*Time Consumption:* Due to the bridge's size and complexity, visual inspections can be time-consuming, leading to increased costs and making the inspection a less repeatable action for maintaining a large bridge.

*Cost:* The extensive manpower and resources required for visual inspections contribute to higher costs associated with bridge condition assessment, as partially emphasized in previous items.

*Subjectivity:* Assessing the condition of bridge elements through visual inspection introduces a subjective element that can vary from one inspector to another. This subjectivity may lead to inconsistencies and potential human errors in evaluating the bridge's health.

Considering these challenges, alternative methods for monitoring the integrity of a bridge's structure and its critical elements, such as using sensory data, and detecting damage and deterioration in their early stages are highly desirable for inspectors and operators. A carefully chosen set of sensors with desired cost, sensitivity, and ease of installation, along with an appropriate data acquisition strategy and on-site post-processing capability, can provide bridge inspectors with an advantage in conducting more frequent, more accurate, and more reliable inspections of bridge elements, without the need to have their boots on the bridge. The sensor-based condition assessment also enables the monitoring of the structure's integrity in the aftermath of major natural disasters, such as earthquakes or strong winds, when physical access to bridge elements may be limited.

The remote monitoring of bridge elements offers significant advantages in facilitating emergency response in large cities. By providing early warnings for unsafe routes as soon as damage is detected, it enables a fast response to ensure public safety. Additionally, this proactive approach helps minimize monetary losses caused by unnecessary closures of structurally sound bridges. By utilizing remote monitoring systems, cities can enhance the resilience of their transportation grid and improve their overall efficiency in managing critical infrastructure.



Figure 1.1. A bird's eye view of the old (front) and the new (rear) Gerald Desmond Bridge  
(Source: Port of Long Beach).

Structural identification and health monitoring through sensory data have gained significant interest over the past four decades. One notable initiative is the California Strong Motion Instrumentation Program (CSMIP),<sup>1</sup> which has installed sensors on more than 80 bridges across the state. This program has played an important role in promoting the utilization of data for assessing the condition of structures. The instrumentation deployed by CSMIP typically includes accelerometers that are securely mounted on the bridges. After each earthquake event, the agency collects and organizes data from these accelerometers, making it available to the public for research purposes within a few weeks. This study's authors have utilized these datasets for over fourteen years, finding them invaluable for calibrating and validating their analytical models.

The new Gerald Desmond Bridge has recently joined the roster of stations equipped with CSMIP's instrumentation (refer to Chapter 4 for more details). As part of this installation, the agency has deployed 44 accelerometer channels, including 15 triaxial sensors, placed on the bridge's girders, towers, and foundation. While these accelerometers offer valuable insights into the bridge's overall vibrational characteristics, such as mode shapes and modal frequencies, their primary purpose is not to directly assess the condition of individual bridge elements (e.g., cables or girders). Detecting damage or anomalies at the component level using the global response of the bridge (i.e., absolute acceleration) is challenging due to various sources of operational noise (e.g., traffic, construction) and environmental noise (e.g., temperature, wind). Achieving accurate and reliable identification of damage or anomalies at the bridge component-level requires additional measures beyond the global response data.

---

<sup>1</sup> <http://www.conservation.ca.gov/cgs/smip>

Furthermore, the accelerometers deployed by CSMIP are not designed to be triggered by wind vibrations or service limit state loads, such as combinations of traffic, temperature variations, or seasonal wind gusts. Additionally, the data collected from these sensors are typically not immediately available. These additional limitations further complicate real-time condition assessment at the component level of the bridge. Therefore, there is a growing need for a proprietary and dense monitoring network that specifically targets the critical elements of the bridge and provides real-time or near real-time data on their condition. In this study, we aim to develop such a health monitoring network for the bridge, as elaborated in subsequent chapters.

Figure 1.2 shows the main elements of a Bridge Health Monitoring (BHM) system. As highlighted in the figure, the project is focused on proposing the sensing and recording system for the Gerald Desmond Bridge. The sensing system consists of an array of sensors attached to structural elements with potentially some limited on-the-spot pre-processing capabilities, as well as a data acquisition system (DAQ), as illustrated in the figure. Other elements of a BHM system include data transmission to a remote office, typically via the internet; data post-processing; and the elements' condition assessment and reporting. In this project, we have proposed a framework for effectively sensing and monitoring the response of critical elements in the bridge, with the goal of promptly detecting any signs of deterioration. The framework encompasses the selection of appropriate sensor types for each critical element, optimal sensor placement, and a consistent naming convention. Detailed information regarding these aspects will be provided in the subsequent chapters.

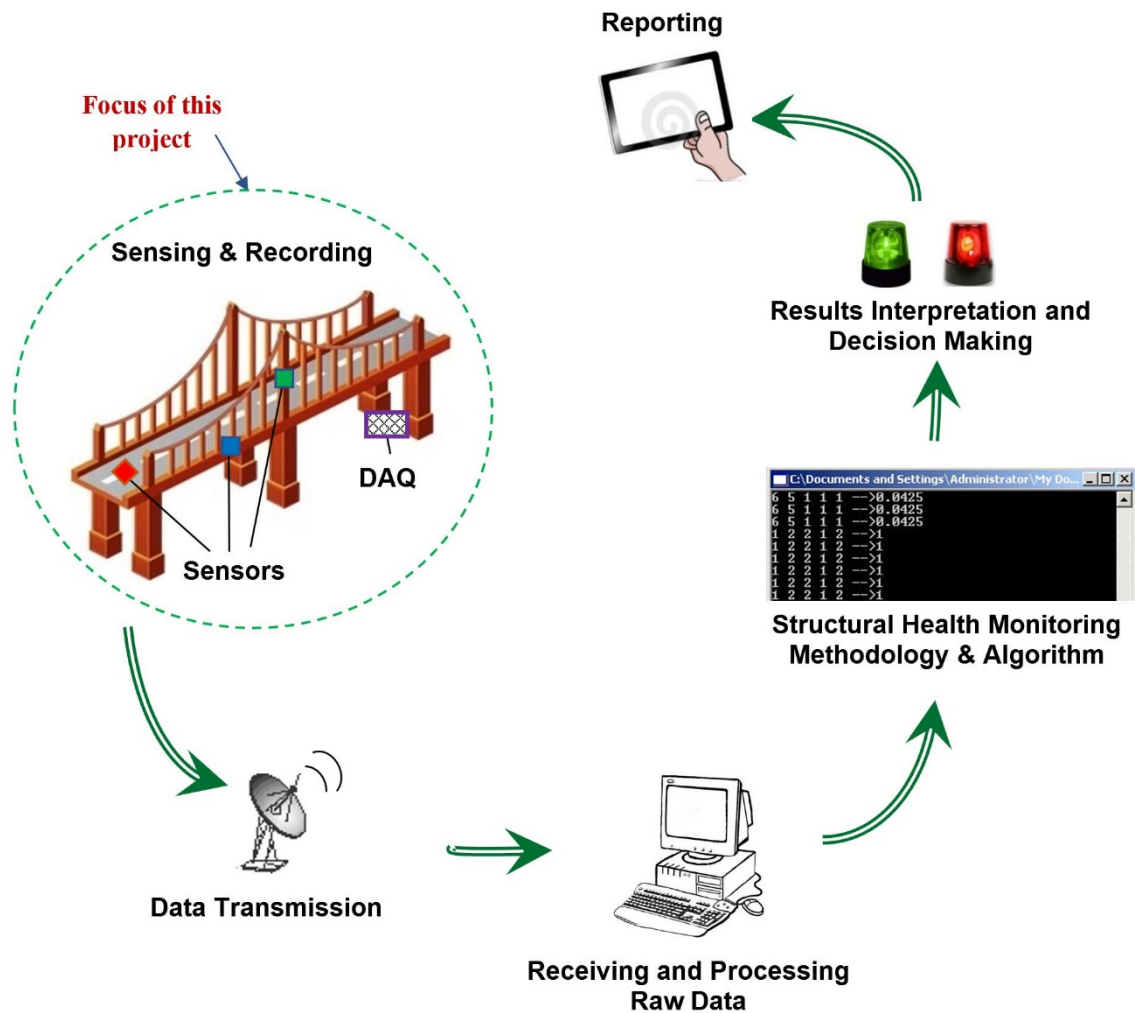


Figure 1.2. Main elements of a structural health monitoring (SHM) System for bridges.

## 1.2. Project Objectives

The main objectives of this project have been as follows:

- 1) to implement a practical framework for instrumentation and data acquisition and aggregation of the new Gerald Desmond Bridge. The framework will be effective in creating a solid foundation for real-time or near real-time remote health monitoring and condition assessment of the bridge. The framework primarily targets the monitoring of the bridge's critical elements.
- 2) to perform a comprehensive literature review on best practices and recent advancements in both sensing technologies and instrumentation strategies utilized in similar cable-stayed bridges worldwide.

3) to identify and propose appropriate sensor types for each critical element, recommend optimal sensor placements, and provide a consistent naming convention for the sensing channels.

What sets the instrumentation framework discussed in this report apart is its comprehensive and bridge-specific instrumentation layout. The instrumentation will go beyond accelerometer arrays to encompass a wide range of cutting-edge and sustainable monitoring sensors, including Fiber Bragg Grating (FBG) friction strain gauges, LVDT displacement transducers, fiber optic temperature sensors, tiltmeters, ultrasonic anemometers, and more. The extensive and tailored sensor layout enables element-level bridge monitoring. Furthermore, data recording and transmission in the proposed framework will be conducted in real-time or near real-time, allowing for frequent daily monitoring of the structure. The challenges associated with data acquisition for a large sensing network have been thoroughly examined, and practical solutions have been proposed to ensure the resiliency of the network.

### 1.3. Proposed Monitoring Strategy and Devices: Process and Major Steps

When designing a health monitoring system specific to a bridge, there are several choices and challenges that need to be considered. To better organize all the factors involved in our monitoring strategy, we can divide them into two main categories: (1) available approaches for instrumentation and state-of-the-art sensing technologies and data acquisition, and (2) methodologies for post-processing the recorded data and detecting anomalies. The first category addresses questions regarding the sensing aspect of bridge monitoring, such as which parameters should be measured, what type of sensors should be deployed, whether a wireless or wired network should be used, and what data acquisition system and strategy should be employed. The second category focuses on the analysis of the collected data using algorithms and surrogate models to assess the health of critical elements. This report primarily emphasizes recent advancements in the first category, specifically instrumentation and sensing technologies for cable-stayed bridges, and aims to transform the lessons from real-world examples into practical guidelines for the instrumentation of the Gerald Desmond Bridge. In this section, we provide a preview of the discussion in this report's upcoming chapters.

The development of a practical and reliable bridge health monitoring (BHM) system, one of the main objectives of this study, was achieved by leveraging best practices and successful case studies. Various factors were considered, including the identification of critical bridge elements, the determination of relevant monitoring parameters, the selection of suitable sensor types and acquisition equipment, ensuring the durability of the monitoring network, cost, and more. Additionally, for long-span cable-stayed bridges, the deployment of diverse sensor types was crucial to enable comprehensive monitoring and obtain a thorough understanding of the bridge's condition.

As the first step, it is essential to perform a review of state-of-the-art sensing technologies and the various types of sensors available and suitable for monitoring civil structures. We also try to

highlight those sensors successfully used in bridge monitoring efforts. In Chapter 2 of this report, we introduce some of the most popular types of instruments for measuring structural response parameters, e.g., strain, acceleration, displacement, and temperature, and provide a brief overview of their sensing technologies and some of their best applications. The second step in this project, discussed in Chapter 3, involves a comprehensive observational study on practical in-use health monitoring systems on cable-stayed bridges around the world, specifically those that have been instrumented and monitored at their component level (e.g., cables, towers). The presented review allows us to examine successful examples of such projects and extract valuable lessons from their experiences, highlighting both effective strategies and areas that may require improvement. The observational information is valuable for designing and tuning our BHM system for the Gerald Desmond Bridge, and it ensures its practicality and resiliency in long-term monitoring regimes.

Each structure possesses unique characteristics in terms of its geometry, structural design, seismic design, and construction details. Therefore, conducting a thorough examination of existing structural drawings and design reports, such as load rating reports, is essential to comprehend the behavior of different elements of the bridge under various limit states induced by dead load, traffic, earthquake, and wind loads. Furthermore, it is crucial to gain a comprehensive understanding of the load path and the redundancies in the bridge's structure. This knowledge helps us explain the failure mechanisms of critical elements and their impact on adjacent elements. By acquiring these details, we can develop a tailored system that suits the specific requirements of our case study. For instance, within the proposed bridge health monitoring (BHM) system, it is important to monitor fracture-critical elements, such as steel box girders, as well as the stay cables. While the bridge is expected to exhibit elastic behavior under routine service loads, such as traffic and mild earthquakes, it is important to acknowledge that damage and deterioration are inevitable. Fatigue, for example, can lead to cracks in fracture-critical members, and the presence of large cyclic loads can exacerbate the fatigue damage within these elements. Chapter 4 of this report delves into the structural system and load path of the case study bridge, reviews the requirements specified by the relevant codes and guidelines, and offers an overview of the bridge's response during a local earthquake that was recorded by the existing accelerometers installed on the bridge.

In this study, our approach to tackling this challenge relies on two factors: (a) the resolution of the instruments installed on the bridge elements, and (b) the accuracy of the identification (regression) model used to detect changes or damage in an element. The first factor will be addressed through an extensive examination of state-of-the-art sensing technologies, including fiber optic sensors, laser sensors, LVDTs, and strain gauges, among others. The selection of appropriate instruments for each element is crucial for the overall success of the BHM system. It is important that the sensors' readings remain relatively unaffected by environmental conditions such as temperature or humidity. The second factor, identification accuracy, necessitates a thorough analysis of the variations in the parameter of interest (e.g., strain or displacement) and their sensitivity to different environmental or non-damage-related factors (such as creep, shrinkage cracks, and thermal expansion or contraction). It is important to distinguish between non-damage-related changes and actual damage signals, treating the former as noise and filtering them out from the signal. While

the post-processing efforts are not within the scope of this study, being aware of the challenges associated with this phase will assist us in designing our remote monitoring network effectively.

In Chapter 5 of this report, we thoroughly examine all the crucial factors involved in designing a successful remote monitoring system. We gather a set of requirements that serve as guiding principles for the design process, ensuring the establishment of a reliable and resilient monitoring system for the bridge. Subsequently, we propose element-specific instrumentation and layout designs tailored to the bridge's critical elements.

## 2. Sensors and Sensing Technologies Used for Civil Engineering Applications: A Detailed Review

A closed loop for the monitoring of a structure comprises the sensors, data acquisition units, data collection, pre-processing and transmission units, as well as a base station equipped with a software application for the post-processing of data. In this chapter, we emphasize the state-of-the-art sensing technologies and common sensors used for bridge monitoring in the US and around the globe. The sensors presented in this section could be categorized based on the engineering parameter they measure (e.g., acceleration, displacement, or force). One could place the sensors in different groups based on their best application for monitoring specific bridge elements. The latter groups are discussed in Chapter 4 where real-world application of the sensors and sensing technologies are reviewed.

Engineering parameters measured by sensor gages on a bridge are:

- i) Strain: presenting elements' deformation normalized by its initial length subjected to a load. Its linear relationship with engineering stress in an elastic domain has made strain a popular measurement parameter for structural monitoring purposes. The measured strain can be converted to an element's stress which can then be compared with member's capacity or expected design stress. Moreover, continuous strain measurement can be used to detect and count hysteresis cycles induced at a steel element for its fatigue life assessment.
- ii) Acceleration: acceleration was one of the earliest engineering measurements in full-scale structures. For example, building and free-field earthquake acceleration were recorded in the 1970s using a popular accelerogram, namely SMA-1. To date, measuring structural acceleration, in its absolute form, has been the most widely monitored structural response. California Geological Survey (CGS) has instrumented and maintained more than 80 bridges across California, using a network of accelerometers on each. The new Gerald Desmond Bridge also has been instrumented by CGS using 62 channels, which we will discuss in more detail in Chapter 4 of this report.
- iii) Displacement: measuring an element's or structure's displacement could be critical for some health monitoring applications. Displacement can be calculated from a double integration of acceleration data; however, noise in the data can lead to a larger error in the calculated displacement. Therefore, sensors that directly measure a structure's displacement could provide valuable data for the monitoring of a structure.
- iv) Tilt/Rotation: measuring the rotation (i.e., tilt) of main elements in a large structure has become a very useful condition assessment parameter. The rotation of an element (e.g., mid-span of a girder and the tower) could provide insight into the magnitude of the movements of the elements at a given time. In contrast to displacement, accurate rotation

measurement is more practical, and it could be used as a supplementary parameter for validating recorded displacements on an element.

- v) Loads: measured directly or indirectly, the element's forces (e.g., cable tension) is another useful parameter for monitoring an element's condition. In addition, being able to measure the load exerted by a moving mass on a bridge could be a useful monitoring parameter to detect any oversized load caused by traffic and could be combined with other recorded data for a more robust condition assessment.
- vi) Temperature: temperature fluctuation during a day or a season can noticeably affect the bridge response. In addition, such fluctuation could affect sensors' readings. Therefore, recording temperature periodically is necessary for condition assessment and the processing of recorded data.
- vii) Humidity: humidity can increase the pace of corrosion in a steel structure, which in turn can cause structural failure. Humidity in air surrounding the structure as well as humidity inside the bridge cables' protective sleeves must be measured periodically to better estimate the possibility and extent of corrosion. Given the proximity of the Gerald Desmond Bridge to the port's harbor and the Pacific Ocean, measuring the humidity becomes even more important.
- viii) Wind Speed: wind-induced vibration in the structures can cause or exacerbate damage in a bridge structure. Strong wind load could cause large lateral and vertical movements in the deck. In addition, it can cause prolonged large-strain cables' vibration. The taller a bridge, the greater the wind effect. Anemometers and new sensing techniques for measuring wind speed are necessary for understanding the extent of the wind-induced vibration of a bridge structure.

The rest of this section will introduce some of the most popular types of instruments for measuring each of the abovementioned parameters, presenting a brief overview of their sensing technologies and some of their best uses. Among these sensors, strain gages and accelerometers are the most widely used instruments for structural response measurements. Hence, a greater weight will be assigned to these types of sensors in the discussion to follow.

## 2.1. Strain gages

Strain gages are among the contact sensors which must be attached to a point or section of an object (e.g., a structural element). These relatively small sensors are attached to the element of interest by adhesives, magnets, or welding (on metallic surfaces). The gage will react to any deformation induced in the element and sends a low-amplitude time-series signal to a convertor where the signal is amplified and transduced to the internal strain in the element. As a result, the connection between the sensor and the element surface must be non-slipping. The very small gage

comprises a miniature coil encompassed by two plates. Herein, a brief overview of some of the most popular strain gages and their technologies will be provided.

2.1.1 Conventional Foil Strain Gages

A foil strain gage (also known as a resistive foil strain gage) is comprised of a metallic foil as shown in Fig. 2.1. The foil is flexible and could deform along with the element it is attached to. The deformation changes the electrical resistance in the foil. The change in the electrical resistance, which is a very weak signal, is recorded, amplified, and converted to the element's strain using a factor known as the *gage factor*. The idea behind this set up originated more than 80 years ago (Keil, 2017), making foil strain gages one of the earliest strain measurement tools in the industry. Figures 2.2a and b show two examples of strain gages attached to structural elements. Figure 2.2a shows a strain gage attached to a bridge floor-beam using adhesive and Figure 2.2b shows a strain gage welded to a steel reinforcing bar (before embedment in concrete). Note that the use of adhesive is the preferred bonding choice for strain gauges unless the surface is rough and chance of slippage is high, in which case welding could be a viable option.

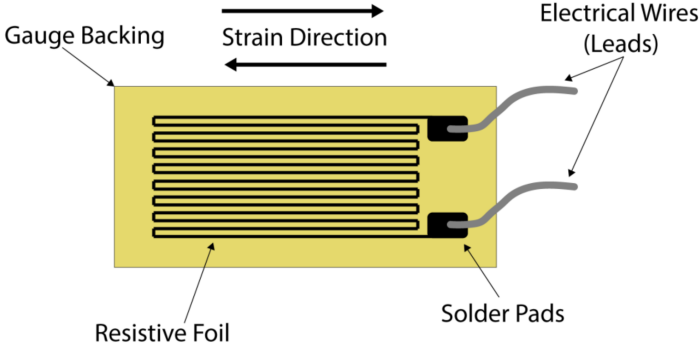


Figure 2.1. A detailed view of conventional foil strain gauges (reprinted from Michigan Scientific Corp: [www.michsci.com](http://www.michsci.com)).

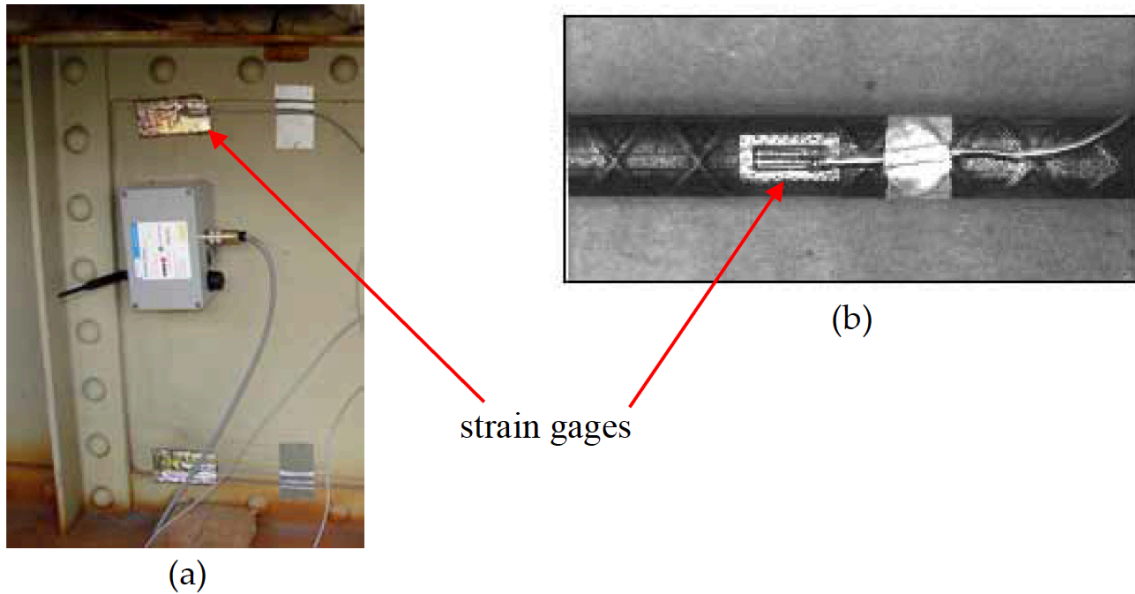


Figure 2.2. a) Strain gages attached to the top and bottom of a bridge floor beam (Bischoff et al., 2009), b) a strain gage welded to a steel reinforcing bar prior to construction (Dong et al., 2010)

The very weak (i.e., low amplitude) signal generated by the foil strain gages makes them less suitable for long structures. In long structures, the length of wires extending from the gage to the reading unit could be significant, leading to additional noises being introduced to the generated signal. These noises comprise electromagnetic and electrostatic noises induced from the environment along the network. These noises could be more challenging when the sensor is recording a high-frequency vibration (relatively stiff elements) where the original signal could be heavily contaminated by the high-frequency noises. From a durability standpoint, the foil strain gages are susceptible to corrosion in humid environment and could be damaged by harsh environmental effects if not protected and maintained. This will make them less favorable for long-term monitoring schemes.

### 2.1.2. Fiber Optic Sensors (FOS)

In the past two decades, Fiber Optic Sensors (FOSs) have gained significant interest for civil infrastructure monitoring. The FOSs are largely used for measuring the strain and temperature of an object and provide several advantages compared to conventional *foil* strain gages. As their technologies have been advanced in the recent years, their application for bridge health monitoring has grown significantly, such that they can be found in almost all large-scale health monitoring projects. In this section, we briefly discuss the basic physics behind the FOSs and highlight some of their main advantages.

Before digging into the Fiber Optic Sensors, it will be helpful to review the optical fibers first. Optical fibers are thin transparent strings (i.e., fibers) of glass, made from silica, which provide a

path for light to travel from one end to another. The optical fibers can transmit data (i.e., light wave signals) at a much higher rates than metallic wire cables. Moreover, over a long distance, the loss of transmitted signals in optical fibers is much less than metal wires. An additional advantage of optical fiber is their insensitivity to electromagnetic fields (e.g., the presence of a high-voltage source) which could introduce extra noise in the metal wires. These benefits have made optical fibers the first choice for most long-distance communication and ethernet data transmission. By introducing an innovative design, optical fibers were used to fabricate fiber optic sensors (FOSs) for aerospace and civil engineering applications.

In a fiber optic sensor, the light is transmitted via optical fibers (i.e., cables) into the optic sensor at any given time, and the sensor returns the light signal back to a measuring station. Deformation in an element and the sensor that is attached to it will cause the incoming optic signal to change (also referred to as “being modulated”) within the sensor, and hence, a changed optic signal is sent back to the measurement device, where the change in signal is interpreted as the object’s deformation. This could result in precise strain measurement on the structure due to the abovementioned benefits the optical fibers offer compared to metallic wires.

In recent years, different fiber optic sensors have been developed. The differences between them lie in the way light signals are modulated within the sensor or to which application they are customized for. Some of the most popular fiber optic sensors for civil structures monitoring are as follows:

**i) Fiber Optic Intensity Sensors:**

The Fiber Optic *intensity* sensors measure change (i.e., loss or gain) in the intensity of transmitting light through the optical fiber sensor due to deformation. The loss/gain in intensity could be directly related to deformation in the sensor. Figure 2.3 shows two technologies for measuring this change. Figure 2.3a illustrates the optical fiber sensor comprising two in-line optical fibers situated at a distance of  $d$ . If the strain sensor is expanded (i.e., elongated) due to deformation, the distance ( $d$ ) between the two fibers increases which consequently results in a loss in the intensity of transmitted light. This relation is illustrated in Figs. 2.3a and 2.4. The other technology for intensity strain sensors, as illustrated in Fig. 2.3b, replaces the second in-line optical fiber by a mirror situated at a distance of  $d$ . The mirror reflects the incoming light, and as the sensor deforms, the distance between the mirror and the inlet fiber changes which results in the change in the intensity of reflected light. The change in the intensity is then translated into strain at the location of the sensor. There exist other principles for detecting light intensity, which has led to the emergence of other types of intensity FOSs. Reviewing those technologies is outside the scope of this project.

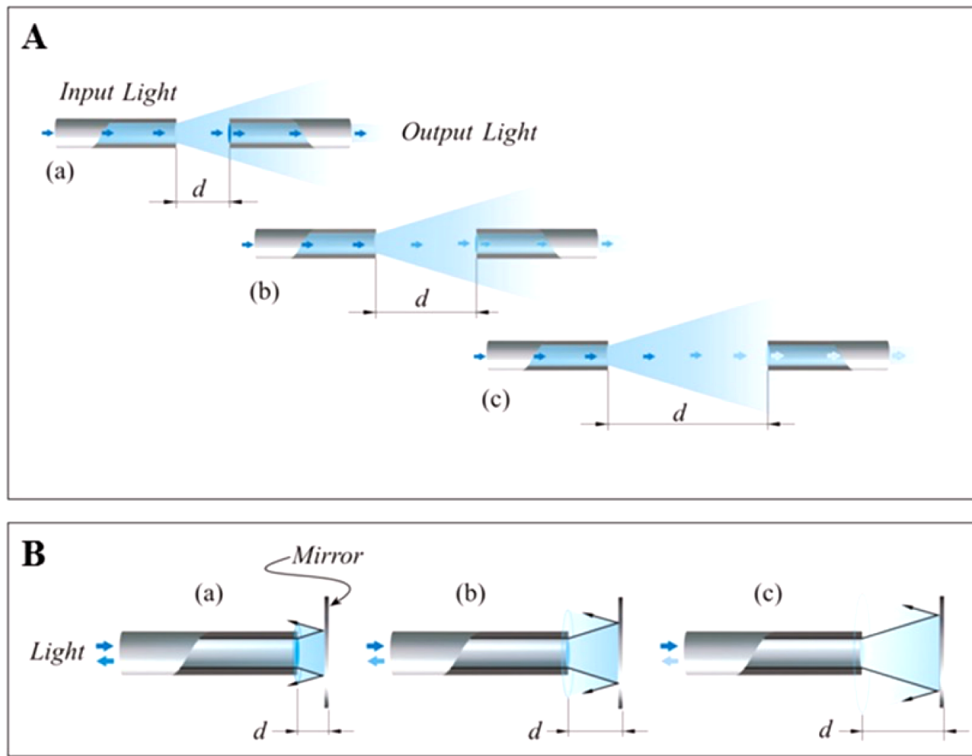


Figure 2.3. The principal technology behind Fiber Optic *Intensity* sensors when subject to deformation: A) using two in-line optical fibers, B) using an optical fiber and a mirror (reprinted from Massaroni et al., 2015).

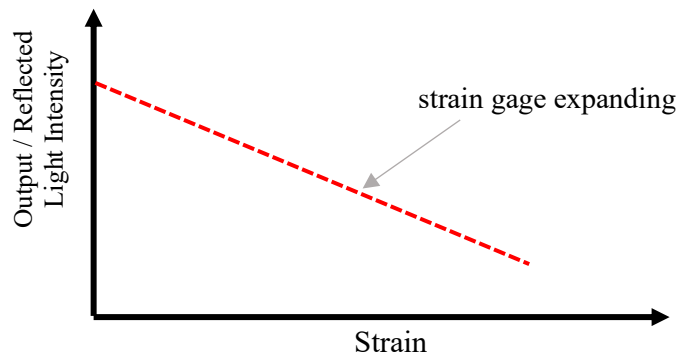


Figure 2.4. Schematic illustration of change in light intensity in a fiber optic intensity sensor as a function of measured strain.

## ii) Fiber Bragg Grating (FBG) Sensor:

Fiber Bragg Grating (FBG) optical sensors are a subgroup of a family of sensors known as *Spectrometric* sensors. The transmitting light in the optical sensor is a spectrum represented by a range of wavelengths. The sensitive physical parameter that is measured in the optical sensor is the wavelength of the reflected light from the *Bragg gratings*. As illustrated in Figure 2.5, the input light in the sensor is partially reflected from vertical Bragg gratings (shown as blue disks). The reflected light contains a relatively constant wavelength when the sensor is unstrained. Once the sensor deforms, the distance between the gratings changes which leads to a change in the wavelength of reflected light (see Fig. 2.5). Using secondary calculations, such change is translated into deformation (i.e., strain) in the sensor and the element it is attached to. The FBG optical strain sensors have become very popular in recent years due to their benefits compared to conventional sensors. Their high sensitivity and accuracy in measurement is their foremost benefit. Although, similar to most other sensors, their readings could be affected by a change in ambient temperature, requiring the measurements to be corrected for temperature effects. It is noteworthy that the FBG temperature sensors are also popular and that they utilize the same physics and principles described above to measure temperature. Figures 2.6a and 2.6b illustrate a real world FBG strain gage and its internal structure, respectively.

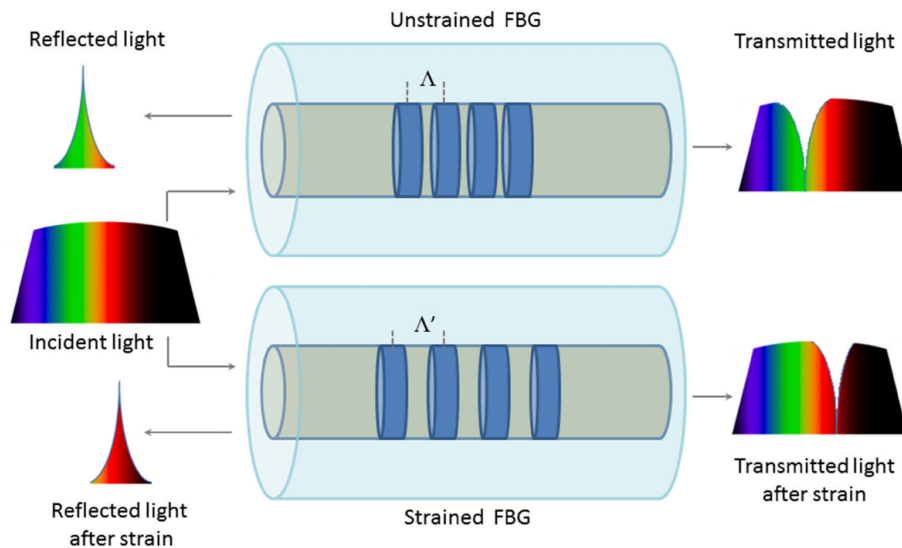


Figure 2.5. The principle behind Fiber Bragg Grating (FBG) optical sensors (e.g., strain gages). The wavelength of reflected light from the vertical gratings (shown in blue) changes as the sensor deforms axially. The spectrum of colors is indicative of wavelength variation (reprinted from Massaroni et al., 2015).

**Benefits of FOSs compared to conventional foil strain gages:**

*Transmission Speed and Signal Loss:* The speed of the transmission of light in fiber optic sensors, as noted earlier in this section, is much higher than in metallic wire cables. In addition, over a long distance, the loss of transmitted signals in optical fiber sensors is much less than in the metal wires used in conventional foil sensors. These are important advantages for monitoring long structures such as cable-stayed bridges.

*Sensitivity to Electromagnetic Fields:* Unlike metallic foil strain gages, optical strain gages are not impacted by magnetic fields near them. This results in transmitted signals with much less noise (i.e., larger signal to noise ratio).

*Durability:* Metallic-foil strain gages are susceptible to corrosion which could impact their measurement over time. On the other hand, the optical sensors are less impacted by moisture and could provide more robust readings over a long monitoring scheme. This becomes more essential for large bridges, where replacing sensors periodically is not plausible.

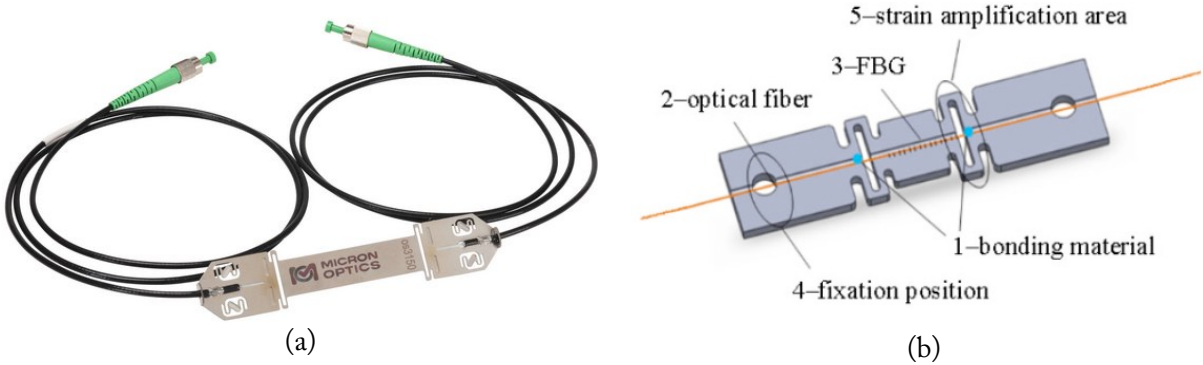


Figure 2.6. a) FBG strain gage and its input/output wires (source: polytec.com), b) internal structure of a FBG strain gage (Wang et al. 2013).

*2.1.3. Vibrating wire strain gauges*

Another class of strain measurement technology is vibrating wire (VW) strain gages. These sensors comprise a vibrating wire anchored at two ends and under tension. There is also a coil or a magnet near the mid-span of the wire. The wire in the set up vibrates at a certain frequency due to the magnetic field induced by the coil. The frequency is directly related to the tension in the wire. The VW strain gage must be attached on the surface of an object where the points of fixation are the two ends of the vibrating wire. When the object is deformed, the VW is deformed with it which will directly affect the frequency of the vibrating wire. Such change in frequency is then processed

to infer deformation in the gage and the object it is attached to. Figure 2.7 illustrates the technology and components of VW strain gages.

The VW strain gages are relatively bulky compared to other types of strain gages. Depending on the location of their end fixture, these gages could monitor a relatively large length on an object when compared to conventional strain gages attached to a *point* on the object. Figure 2.8 illustrates two examples of VW sensors being used for monitoring a stretch of steel element near structural joints or where fracture or buckling is imminent. It is noteworthy that the coil and wires in the gage can expand or contract with changes in temperature as this makes these sensors very sensitive to ambient temperature. Hence, a temperature sensor must be included in these sensors to allow for correction to the strain readouts. Given the metallic casing of these gages, if welded to steel sections, temperature correction may not be necessary.

As discussed earlier, relying on the tension and vibrational frequency of the wires, the vibrating-wire sensing technologies can be expanded for monitoring other parameters such as temperature and displacement. These applications will be discussed further in this section.

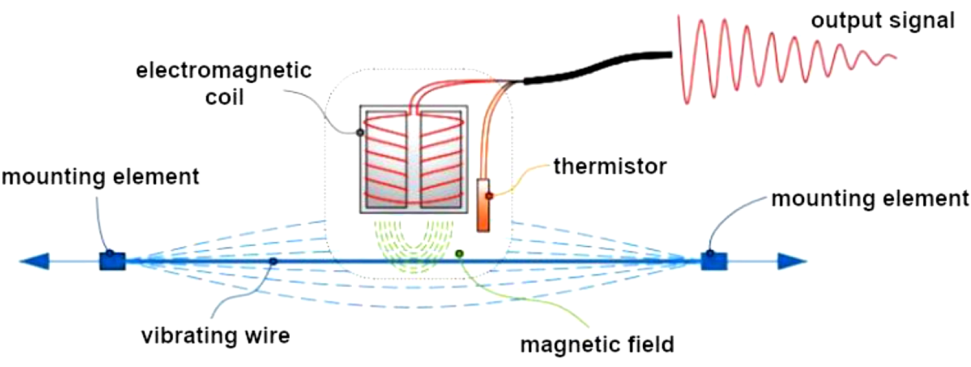


Figure 2.7. A schematic view of internal components of a vibrating wire strain gage (Woszczyński et al., 2022).



Figure 2.8. Examples of vibrating wire strain gages for monitoring steel structures. a) steel profile with welded VW strain gages (source: geo-instruments.com), b) VW strain gages attached to steel joint plates of a bridge (source: spectotechnology.com).

## 2.2. Accelerometers

Accelerometers are among the most popular and widely used sensing technologies in engineering. In civil engineering, accelerometers have been used for monitoring buildings and bridges to measure structural vibration due to natural or manmade events for more than a century. Unlike the strain gages which provide a direct measurement for the point of an element they are adhered to, accelerometers provide the absolute acceleration measurement for both the element as well as the entire structural system. Acceleration signals have been used to calculate modal frequencies and mode shapes (i.e., vibrational signatures) of building and bridges. It is noteworthy that the case-study bridge is currently instrumented by 62 accelerometers (refer to Chapter 4 for details) across its deck and east approach. In Chapter 4, we discuss the current instrumentation of the bridge and provide its acceleration response to a local earthquake.

Accelerometers measure an element's acceleration relative to the gravitational acceleration,  $g$ . Their technologies have been developed extensively since the very early devices used in civil structures. The early devices to measure Earth's or a building's motion or acceleration were called seismographs. Before computers and the fast digital computing chips era, accelerometers were analog devices with mechanical moving arms requiring a paper or film roll on which to record the earthquake's motion. SMA-1 (manufactured by Kinemetrics) was one of the most popular analog accelerometers in 1970s. It was used to record multiple regional earthquakes in California. Figure 2.9 shows a picture of the seismograph. The basic components of SMA-1 are mirrors, a light source, a trigger switch, light sensitive film, a lightproof case, and resistors for damping. The instrument is set up at the desired site. Once the switch detects significant ground motion, the machine is activated. The light source is turned on, and the film begins to rotate by way of a battery-powered motor. The initial light source beams light into a mirror and reflects from two others until the light source becomes a point and exposes the light-sensitive film to it. The box

movement, due to external excitation, moves the mirrors in order to obtain a reading of acceleration on the film. The major shift from analog accelerograms to digital accelerometers occurred in the late 1980s when computers became more accessible and less expensive to use.

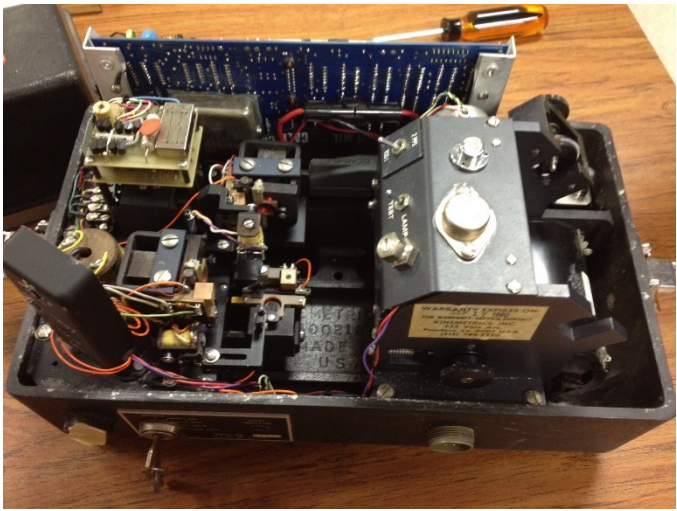


Figure 2.9. Inside view of SMA-1 analog accelerograms (courtesy of Mihailo Trifunac).

2.2.1. *Spring-Mass Accelerometers*

The technology behind most accelerometers, also known as spring-mass accelerometers, is relatively simple. As shown in Figure 2.10, typical accelerometers consist of a mass (a.k.a. a seismic mass) attached to a fixed frame via an elastic spring and a dashpot. The rigidity of the spring is known and can vary from one sensor to another. Acceleration induced to the box exerts force on the mass, based on Newton’s law, causing the mass to displace and deform the spring. The displacement of the mass is then measured and, given the stiffness of the spring, the acceleration signal is digitally emitted. The stiffer the spring, the higher the acceleration that the sensor can detect; however, with a stiffer spring, the sensor’s sensitivity may be reduced. The spring-mass sensors are large, but are very sensitive to small amplitude accelerations, making them suitable for ambient vibration monitoring of structures.

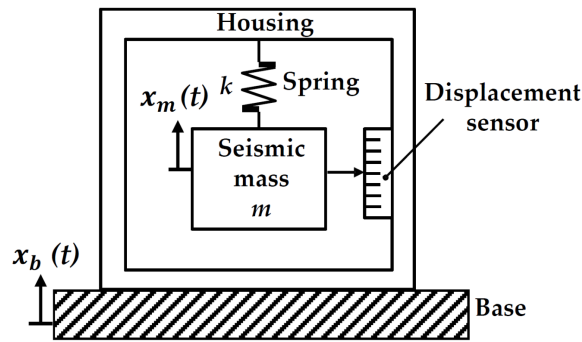


Figure 2.10. Internal structure of a typical spring-mass accelerometer (reprinted from Li et al. 2018).

### 2.2.2. Piezoelectric Accelerometers

A newer class of accelerometers known as *piezoelectric* accelerometers has gained interest in recent years. The technology behind these sensors is similar to a spring-mass accelerometer in which the spring is replaced by a *piezoelectric crystal*. Figure 2.11 illustrates a schematic view of a piezoelectric sensor structure. Once the sensor box is excited, the inertial force induced in the mass deforms the piezoelectric crystal beneath. The deformation of the crystal generates electrical charges that will be measured by a readout unit. The electrical signal is translated to the magnitude of the force induced on the crystal. Given the amount of the mass and the force, the acceleration can be back-calculated.

The piezoelectric sensors are much smaller and lighter than spring-mass sensors, which is considered their main advantage. They can also operate and measure a larger range of acceleration. However, they are generally less sensitive to small-amplitude acceleration when compared to spring-mass sensors.

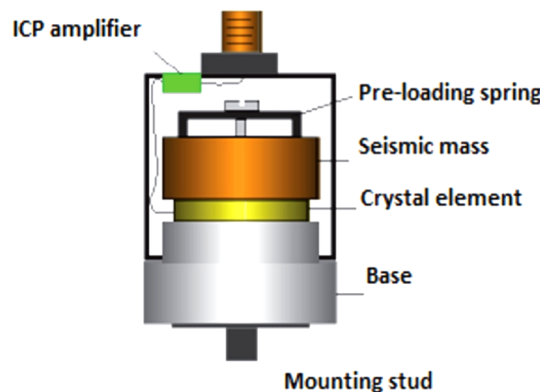


Figure 2.11. Components of a piezoelectric accelerometer (reprinted from Ghemari et al. 2018).

Given the large applications of accelerometers in engineering industries (e.g., aerospace, civil, robotics, and automotive), very small sized electro-mechanical accelerometers have gained significant interest in recent years and have dominated the market. These modern, small, and relatively inexpensive accelerometers, like those deployed in most smartphones, fall under the broader category of devices known as micro-electro-mechanical systems (MEMS). A MEMS accelerometer has a moving mass, similar to a piezoelectric sensor, but at a microscopic level. In these sensors, the mass is typically attached to the tip of a micro cantilever beam. The acceleration will cause inertial force in the mass which leads to deflection of the beam. The deflection results in a signal that is measured and converted to acceleration. For the MEMS accelerometers, there is a trade-off between sensitivity and the range of measured acceleration. The high dynamic range sensors typically have lower sensitivity. Low sensitivity MEMS accelerometers are not useful for low-amplitude vibration (i.e., ambient noise) monitoring applications.

### 2.3. Displacement Sensors

Displacement is a popular engineering measurement when the health of an element is investigated. Given the rigidity of a structure or portion thereof, displacement can be used to calculate the true load-effect on the structure. In civil structures, the maximum drift ratio is a widely used indicator of the extent of stress a structure has gone through during a loading regime. Drift is a dimensionless measure calculated using lateral displacement of a vertical structure normalized by its height. In addition, at a smaller scale, displacement sensors could be deployed to measure deformation at the element level. For instance, the amount of opening and closing of structural joints and splices or the progression of an existing crack/damage could be monitored by a displacement sensor.

Displacement response can alternatively be calculated by a double integration of recorded acceleration response. However, this method might lead to a degree of error in the calculated displacement due to unknown initial conditions (e.g., calculating integration constants from the two integrals). Therefore, a direct displacement measurement would be a more accurate approach, but the cost of displacement sensors is higher than modern accelerometers, being a prohibitive factor for the large deployment of displacement sensors.

Displacement sensing technologies partially overlap with those of the accelerometers discussed earlier. Two of the most popular technologies are as follows.

#### *2.3.1. Linear Variable Differential Transducers (LVDT)*

LVDTs are among the most popular displacement sensors in the laboratory environment for accurate displacement measurement with very high precision. They are often used for measuring small deformations in an object under mostly static loading. These sensors consist of a metallic shaft that is housed in a cylindrical casing and can freely move along the axis of the sensor (i.e., height of the cylinder). Within the cylindrical casing exists a coil within which the metallic shaft can slide. Movement of the shaft within the coil generates differential voltage which is linearly

correlated with the movement of the shaft. The measured voltage is then transformed into displacement with very high precision. Figures 2.12a and 2.12b illustrate the internal structure of a LVDT sensor as described above and a picture of a typical commercial LVDT, respectively.

LVDT displacement sensors are popular for long term monitoring of *relative* displacement near structural joints or on the sides of a crack developing on an element. Figures 2.13a and 2.13b illustrate two on-site applications of LVDT displacement sensors for monitoring cracks on a masonry structure as well as the relative movements between two adjoining beams in a bridge, respectively.

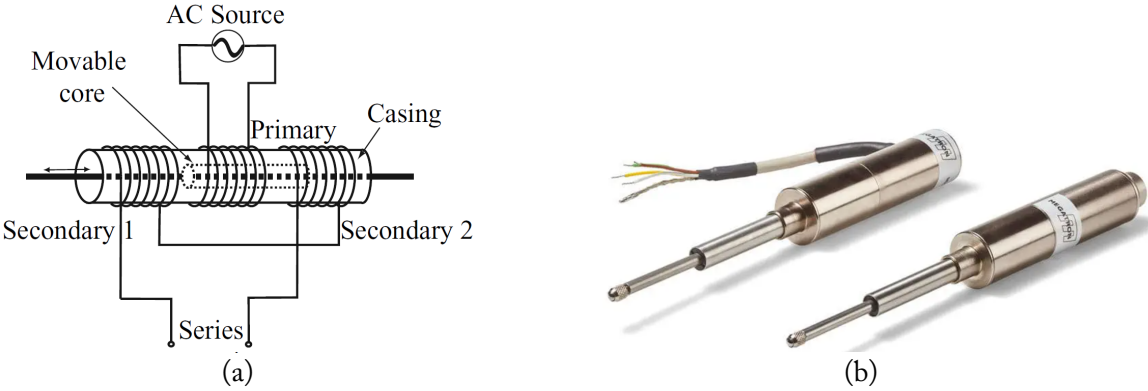


Figure 2.12. a) Internal structure of a LVDT displacement sensor (reprinted from Greif et al. 2006), b) an image of two commercial LVDT sensors manufactured by Megatron Elektronik GmbH & Co. (source: directindustry.com).

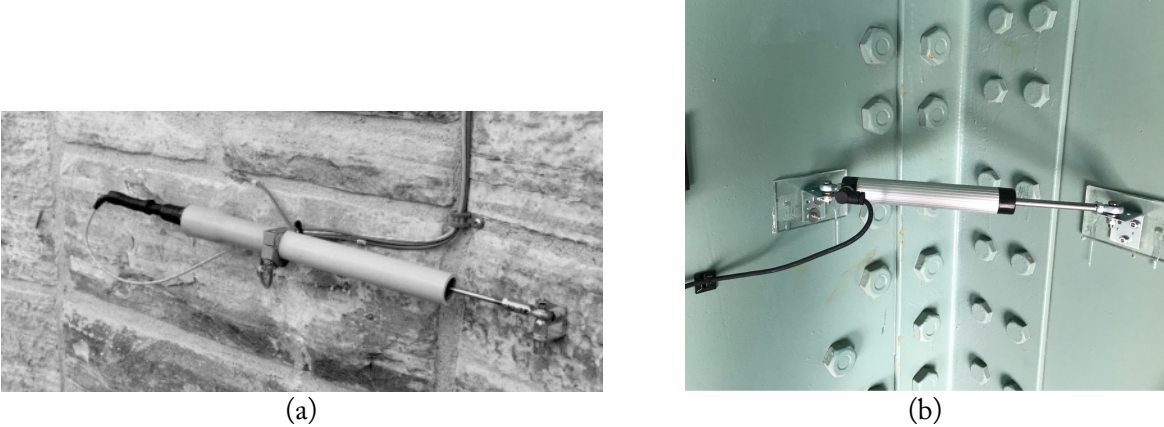


Figure 2.13. a) Image illustrating a LVDT gage attached to a masonry stone of a historic tower (Said et al. 2005), b) displacement sensor attached at a steel bridge joint (source: resensys.com).

### 2.3.2. Laser-based Displacement Sensors

Laser-based displacement devices are among non-contact sensors which measure the displacement of an object from a distance. The sensor emits a light beam towards the object. Once hitting a reflective surface, the light is reflected toward the sensor and detected via a *photodiode* receiver on it. Knowing the speed of light and measuring the travel time to and from the object, the distance of the sensor to the object can be measured. If the laser-based sensor is kept stationary, the change in the distance can indicate that the object has been displaced. Laser-based sensors are useful for measuring displacement when access to the object is limited or wiring is not a feasible option. The technique could also be very useful during the construction process of certain structures, such as bridges or walls, to constantly monitor the position and displacement of various nodes on the structure in a non-contact manner (without direct deployment of a sensor on the element under construction).

It is noteworthy that the accuracy of laser-based sensors in an outdoor environment could be about 1.5mm, which is much lower than that of LVDT sensors. Their measurement accuracy can be greatly impacted by the surface of the element and its reflectivity.

## 2.4. Tiltmeters and Inclometers

Tiltmeters and inclinometers (also known as rotational sensors) are popular devices that can provide direct measurement of the deformation of an element in the form of its rotation with respect to its axis. An element's rotation (e.g., of the mid-span of a girder or a tower) could provide insight into the magnitude of vertical or lateral movements of the elements at a given time. These readings can be performed at a node on the structure with relatively high accuracy, which can help infer an element's displacement during a loading scenario.

Tilt beam sensors are among rotational sensing technologies in the industry. They are used extensively to monitor differential movement, including settlement, in the structure. The technology is similar to that of a liquid bubble level, where a tilt sensor in the level can move as the beam (casing rod) is tilted. The movement generates voltage proportional to the rotation of the casing rod. The casing in these conventional tilt beams could be as long as three meters, making them suitable for measuring the differential settlement of a foundation or lateral movement of a vertical column or wall element. Figure 2.14 shows a tilt beam rotational sensor's internal configuration.

Modern tiltmeters utilize the fiber optic sensing technology, as described in Section 2.1.2. An example of such tiltmeters is the Fiber Bragg Grating (FBG) tiltmeter, which can provide accurate readings of a rotational angle for long-term condition assessment (Xiao et al. 2017). The technology measures the light reflecting from tilted grating planes to infer rotation in the sensor. Figure 2.15 illustrates FBG tiltmeter technology (Guo et al. 2015). More details about fiber optic sensing technologies can be found in Section 2.1.2.



Figure 2.14. a) A tilt beam rotational sensor, b) a zoomed in view of the tilt sensor at the center of the casing rod (source: soilinstruments.com).

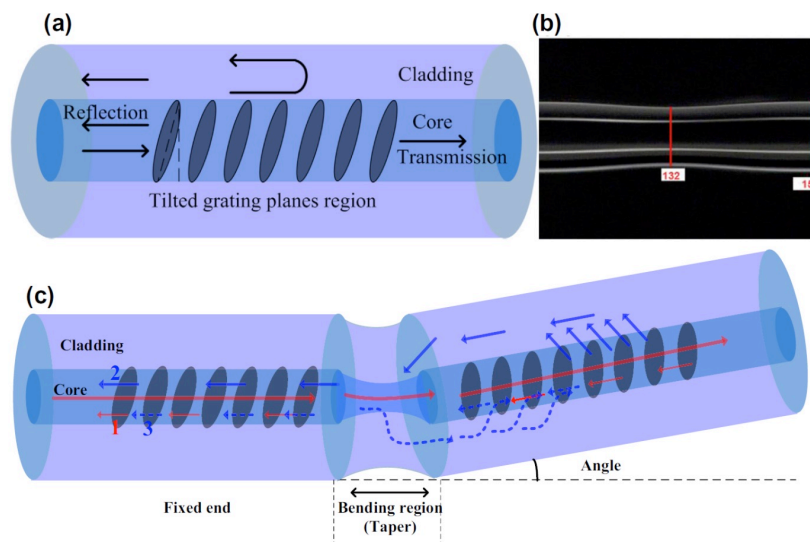


Figure 2.15. Illustration of Fiber Bragg Grating tiltmeter technology (reprinted from Guo et al. 2015).

## 2.5. Load Cells

A load cell is a transducer that directly measures the force induced in an object. The load cells should be placed in series (i.e., along) with the direction of loading. There are three types of load cells: hydraulic, pneumatic, and strain-gage load cells. The hydraulic and pneumatic load cells are the early technologies in this category which utilize the force-balance principle to measure load. For instance, the hydraulic load cell comprises a fluid chamber and a piston. As the loading platen is compressed, the fluid in the chamber is compressed, which moves the piston. The readings of a hydraulic load cell are not as precise as strain-gage load cells, which are most common these days.

The majority of modern load cells use one or more strain gages in their structure. Hence, their technology is very similar to those of bonded foil strain gages, where deformation results in an electrical signal proportional to the magnitude of the applied load. One application of the strain-gaged load cells is found in digital bathroom scales. Figure 2.16 shows an industrial compression load cell and a S-type load cell. In bridge health monitoring, employing compression load cells to measure the load imposed by moving masses on a bridge can serve as a valuable monitoring parameter. It enables the detection of oversized loads resulting from traffic and allows for their integration with other recorded data, thereby enhancing the overall robustness of condition assessment.

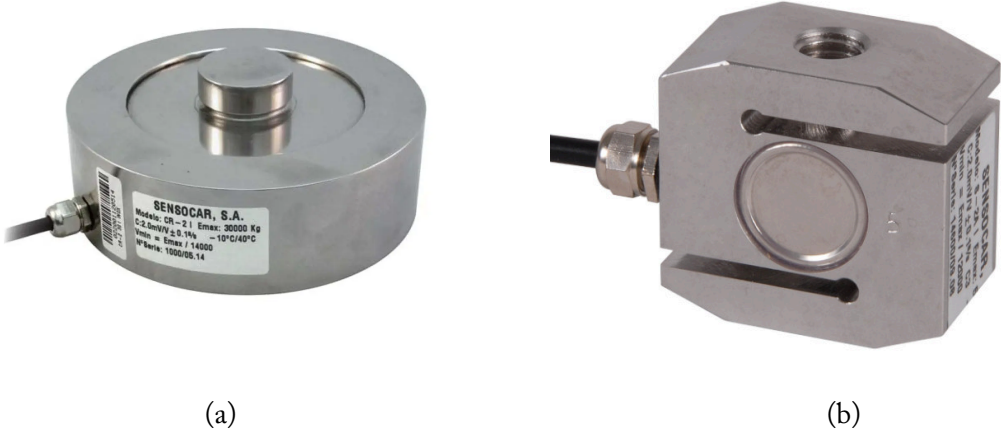


Figure 2.16. a) A view of compression strain-gaged load-cell (source: sensocar.com), b) a view of a S-type tension/compression load cell (source: sensocar.com).

### 2.6. Anemometers

A large-span bridge built over a wide channel with open (i.e., unobstructed) surrounding terrain could experience strong wind loads during its service life. Although the southern California region is safe from superstorms and hurricanes, strong seasonal winds are frequent in the region, which requires attention when monitoring a bridge. Wind load effect on a bridge structure in aggregate with other concurrent loads, such as heavy traffic, rain, and thermal load, could increase the strain in critical elements for a sustained period of time. As such, the critical elements will become more susceptible to damage from fatigue load. Hence, measuring wind speed at the bridge site and near the critical elements is essential for estimating its load-effect during monitoring.

Conventional anemometers are relatively simple devices that measure wind and gust speed via a rotating horizontal arm. Figure 2.17 illustrates an anemometer with a three-pronged rotating arm. As shown in the figure, the horizontal arm is equipped with three side-facing cups. Wind will force the horizontal arm to spin and consequently rotate the vertical shaft it is mounted on. The shaft's rotational speed is proportional to the wind speed. The figure also shows a wind vane located at the lower segment, helping with the identification of wind direction. Anemometers are installed

on top of a pole or top of a structure, such that the wind path around them is not obstructed. Wind speed is a key parameter in bridge health monitoring under service loads, as well as in quantitative modeling for fatigue life predictions. Once a large strain is detected on a bridge, the wind speed could help us segregate the effect of wind load from other operational loads on the bridge and help with avoiding false alerts during the monitoring efforts.



Figure 2.17. Conventional anemometer mounted on a pole for wind speed measurement (source: munroinstruments.com).

### 2.7. Temperature Sensors

Temperature can impact both the structure and the instrument that are deployed on it. Particularly, for a large structure such as a bridge, the effect of temperature on the dynamic characteristics of the structure (e.g., frequencies of vibration and mode shapes) could be noticeably large (Catbas et al. 2008). In addition, a bridge element’s deformation due to temperature could be multiple times larger than deformation induced by traffic (Catbas et al. 2008), making it challenging to detect damage-related changes in the monitored element. On the instrument side, the temperature can directly impact the measurement for strain, acceleration, or displacement. This effect is present for almost all modern sensors, including MEMS accelerometers and fiber bragg grating (FBG) strain gages. For instance, the effect of temperature on FBG strain gage or tiltmeter measurements is quite significant, such that most of these sensors are equipped with a built-in temperature compensator sensor, usually of the same FBG technology, to correct the measurement for the change in temperature during a day (Xiao et al. 2017).

Conventional thermometers include *thermocouple* and *Resistive* temperature sensors. New technologies that have improved both the accuracy and precision of temperature measurements include fiber optic technology such as FBG thermometers. Here we briefly discuss the technologies behind each of these sensors.

A *thermocouple* comprises two metallic wires of different materials and different thermal expansion features. The two metals are adjoined at one point, and when the ambient temperature changes, the difference in their expansion or contraction will generate a voltage signal corresponding to the change in the temperature. Although very inexpensive, these thermometers have the low accuracy of about 0.5 degree Celsius.

The *resistive* temperature sensor is another popular temperature sensing technology in engineering. It works on the principle that change in the temperature changes the electrical resistance of a base material in the sensor, such as a platinum plate or a ceramic semiconductor. This method of measurement provides higher accuracy than thermocouples but at a higher price for the sensor. One important caveat for using the *Resistive* sensor is that the electrical current generated in the sensor could lead to the self-heating of the device and consequently, result in measurement error in the measured temperature. Looking more broadly, the self-heating of a device (e.g., strain, tilt, or displacement sensors) is also an issue when we deal with event-triggered measurements because the sensors could be cold before they are triggered to start the measurement and, as they continue the measurement and as the generated data is transferred, they self-heat internally, which introduces measurement error. As a result, reading temperature within the sensor itself or in its proximity is essential for correcting the temperature-induced error in the measured response parameter (e.g., strain or tilt). Figures 2.18a and b illustrates internal structures and components of a thermocouple as well as a resistive temperature sensor.

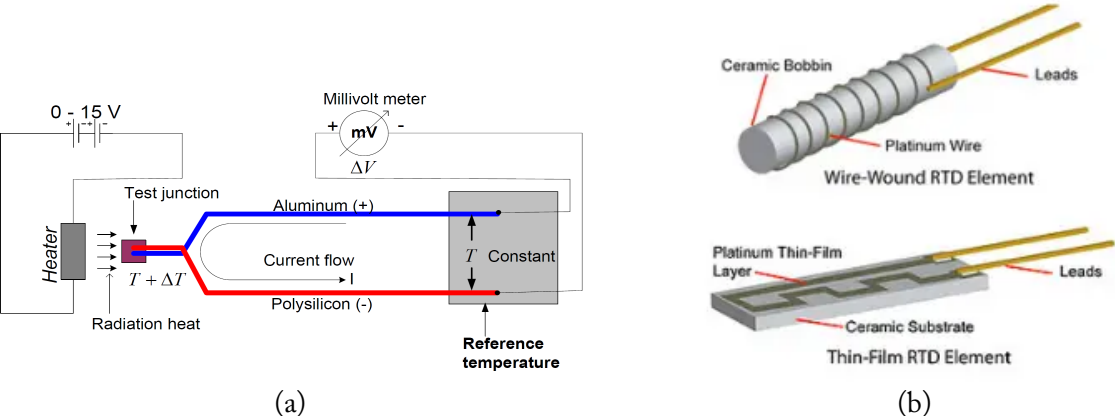


Figure 2.18. a) Internal structure of a thermocouple temperature sensor (reprinted from Thamrin et al. 2007), b) components of two types of Resistive Temperature Detector (RTD) sensors (source: electrical4u.com).

With the presence of fiber optic technologies and their relatively high accuracy and precision of measurement, a comparable level of accuracy in temperature measurement is necessary to enable a correction of readings by these modern sensors. The Fiber Bragg Grating (FBG) temperature sensors are among the newer and highly accurate sensors used in the industry. The principle behind the FBG temperature sensor is the same as those of FBG strain gages discussed in earlier sections of this chapter. As shown in Figure 2.19, temperature change causes the Bragg Grating to stretch

which, in turn, results in a shift in the wavelength of reflected optical signal in the sensor. The shift is related to a change in temperature. These optical sensors provide high accuracy readings and offer several advantages compared to conventional sensors, as discussed in Section 2.1.2.

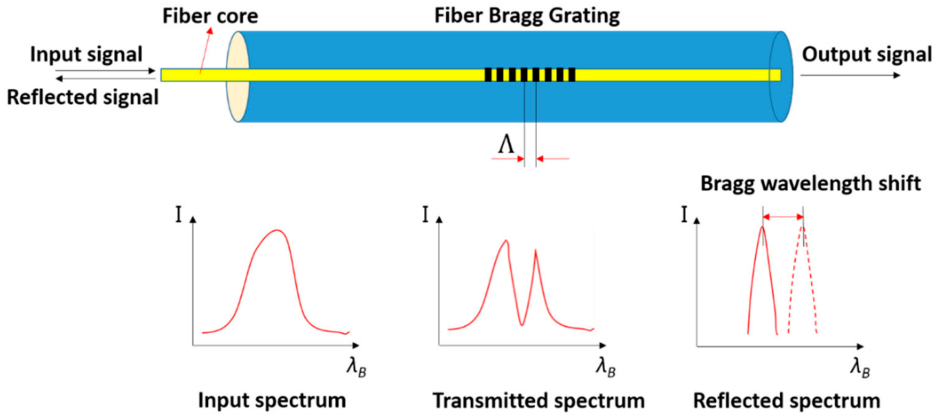


Figure 2.19. The principle behind a Fiber Bragg Grating (FBG) temperature sensor (reprinted from Chen et al. 2018).

### 2.8. Humidity Sensors

Humidity sensors are among the most widely used sensors humans use to monitor the relative humidity in the environment or in their homes. Nowadays, small, low-cost humidity sensors with a very low energy consumption are available for monitoring indoor relative humidity. The word “relative” refers to the value reported by these sensors, which is a percentage calculated based on the amount of water vapor in air relative to a saturated state (100%). The two most common sensing technologies for measuring relative humidity are (1) capacitive humidity sensors and (2) resistive humidity sensors. Other technologies that are newer and more precise in their measurements and more sensitive in detecting change in humidity include piezoresistive humidity sensors and optical humidity sensors. The higher sensitivity comes at a higher expense and bulkier size for the sensors. In this research project, we aim to measure humidity at the proximity of critical steel elements, such as cables and girders. The frequency of measurements will be low (a few times a day) and a reasonable level of precision and accuracy would be acceptable. Hence, conventional humidity sensors would suffice for the bridge monitoring framework in this project. In this section, we briefly review the technology behind the most common humidity sensors (i.e., the capacitive and the resistive).

#### i) Capacitive Humidity Sensors

More than 75% of humidity sensors used around the world are based on capacitive sensing technology (Lee and Lee, 2005). These sensors are low cost and have low energy consumption. They can also be of a relatively small size, suitable for fitting into narrow spaces in a structure. The capacitive humidity sensors comprise two electrodes covered by a polymer-based dielectric layer

that is sensitive to change in humidity. Some examples of these moisture-sensitive layers are Polyimide films (Story et al. 1995) and porous silicon (O'Halloran et al. 1997). When the dielectric layer is exposed to humidity, the capacitance in the circuit changes, which then is transduced into a change in humidity. Figure 2.20a illustrates the internal structure of a capacitive humidity sensor, with the two electrodes shown in black lines, and Figure 2.20b shows a commercially available capacitive humidity sensor which has a mass of less than 0.01 pounds (about 2 grams).

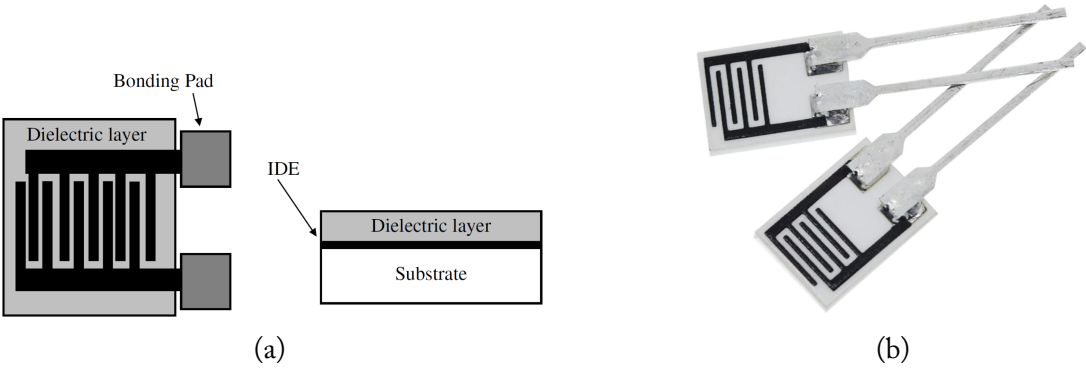


Figure 2.20. a) Diagram illustrating a capacitive humidity sensor (reprinted from Lee and Lee, 2005), b) example of a commercial capacitive humidity sensor (source: TZT Teng store).

**ii) Resistive Humidity Sensors**

The resistive humidity sensors have a relatively simple structure and are easier to make. These sensors use a thin layer of composite polymer or ceramic, which are sensitive to humidity because their electric resistivity changes as the humidity changes near the sensor. The resistive sensor structure looks similar to a capacitive humidity sensor with one difference: the thin dielectric layer is replaced by the conductive moisture-sensitive polymer or ceramic layer.

## 3. Cable-Stayed Bridge Structural Health Monitoring: A Literature Review

When it comes to designing a bridge health monitoring system, there are various choices and challenges to consider. To better organize these considerations, we can divide them into two main categories: (1) available approaches for instrumentation and state-of-the-art sensing technologies and data acquisition and (2) methodologies for post-processing the recorded data and detecting anomalies. The first category addresses questions regarding the sensing aspect of bridge monitoring, such as which parameters should be measured, what type of sensors should be deployed, whether a wireless or wired network should be used, and what data acquisition system and strategy should be employed. The second category focuses on the analysis of the collected data, using algorithms and surrogate models to assess the health of critical elements. Extensive research and real-world applications exist for both categories, providing valuable insights. In this chapter, our review will primarily emphasize recent advancements in the first category, specifically instrumentation and sensing technologies for cable-stayed bridges. It is important to note that the main objective of this study is to present a practical and detailed framework for instrumenting our case-study bridge, placing less emphasis on the post-processing methodology. Therefore, Section 3.1 provides comprehensive information about similar cable-stayed bridges worldwide that have active health monitoring systems, along with insights into successful implementation practices for one particular cable-stayed bridge. Additionally, to ensure a comprehensive understanding, Section 3.2 offers a brief overview of peer-reviewed structural health monitoring methods for bridge monitoring.

### 3.1. Instrumentation Approaches and Sensing Technologies Used for Monitoring Cable-Stayed Bridges

Designing a bridge health monitoring (BHM) system can be a challenging task, as it involves various critical steps and decisions. These steps include identifying the critical elements of the bridge, determining the variables to be monitored on these elements, selecting the most suitable sensors for data sensing, transmission, and acquisition, considering the energy consumption and lifetime of the network, and more. This process may initially seem complex, as different approaches can lead to different monitoring outcomes.

It is important to recognize that there is no universally optimal BHM strategy applicable to all bridges. Therefore, our objective is to identify and recommend the most appropriate and practical instrumentation framework for our specific case-study bridge. Rather than embarking on numerous trial-and-error attempts for each step, we can leverage existing examples of successful full-scale BHM implementations for large-span cable-stayed bridges worldwide. By studying these implementations, we can gain valuable insights into their accomplishments, best practices, encountered challenges, and strategies for overcoming those challenges. This section will delve into several detailed examples of bridge health monitoring, providing a comprehensive

understanding of their methodologies. The aim is to extract the best practices from these examples and incorporate them into our framework for monitoring the Gerald Desmond Bridge.

### *3.1.1. Examples of Bridge Instrumentation and Monitoring in Cable-Stayed Bridges*

BHM sensing (i.e., instrumentation) techniques can be categorized as either *global* or *local* (Alamdari et al., 2019). In the case of global techniques, sensors are placed on elements that may not necessarily be under direct monitoring, while for local monitoring, the sensors are attached to elements that are being monitored. Here is a brief comparison between the two techniques. An example of a global technique is vibration-based monitoring, which involves measuring a response parameter, such as acceleration response, at multiple locations of a bridge to identify the global signature of the structure, such as modal parameters. This method is commonly used for monitoring bridges. However, a drawback of global techniques is that the global response parameters (e.g., modal frequencies) of a structure can be significantly influenced by various operational and environmental conditions, such as traffic, wind, or temperature. Consequently, inferring damage to a specific element (i.e., locally) based on these parameters requires considerable model calibration and analysis. The acceleration and velocity at various locations of a bridge are among the frequently measured global responses.

In contrast, local techniques focus on measuring changes in a specific element's response, such as cable forces or cable stresses. Local element response encompasses a range of parameters, such as strain, crack width, temperature, and tension forces, to name a few examples. When damage occurs, it leads to a redistribution of forces and stresses in the monitored element (e.g., stay cables). For instance, a decrease in tension force in a cable due to cross-sectional loss causes an increase in forces experienced by the adjacent cables due to load redistribution (Alamdari et al., 2019). The goal of these local measurements is to detect any anomaly in the data as compared with the same response during a healthy state of the bridge in service.

The successful implementation of BHM relies heavily on the cornerstone of sensing technologies. These technologies involve a wide array of sensor types and systems, encompassing vital aspects such as data acquisition, data processing, communication, and the effective management and storage of the acquired data (Fujino and Siringoringo, 2011). It is noteworthy that increasing the data-collection frequency and employing a larger number of sensors can substantially increase the size of the collected and transmitted data (Noel et al., 2017). On the other hand, a BHM system must include a well-tested and calibrated post-processing approach involving the utilization of optimization theories to derive expressions that estimate the probability of a diagnostic based on prior observations or compared with an analytical model's response. These efforts aid in the early detection of anomalies in real or near real time (He et al., 2022). In the meantime, there are security challenges to be considered with the architecture of a proposed BHM, such as cyber-security risks. Safeguarding the integrity and security of the monitoring system is crucial to ensuring reliable and accurate results.

A cable-stayed bridge becomes a superior choice when there is a need for a large span (e.g., over a channel), fast construction process, and stability and economy of the construction. There are several long-span cable-stayed bridges around the world. The new Gerald Desmond replacement bridge, although the largest cable-stayed bridge in California, does not fall among the top ten largest cable-stayed bridges in the world (Zhang et al., 2021). These observations provide valuable insights into the extensive instrumentation, monitoring, and maintenance efforts dedicated to cable-stayed bridges over the past few decades. In the subsequent paragraphs, we will explore some of the efforts made in instrumenting and monitoring cable-stayed bridges worldwide and will highlight some noteworthy best practices and lessons learned from them.

The methods employed to identify various structural degradations rely on the detection of stiffness loss, time-dependent and temperature-induced deformations, fatigue, corrosion, scour, and accidental impacts (Rizzo and Enshaeian, 2021). It is worth noting that scour does not pose an issue for the bridge under study. To ensure a robust and reliable monitoring effort for a large structure such as a long-span bridge, it is necessary to deploy a variety of sensor types. The use of diverse sensors enables comprehensive monitoring, capturing different aspects of the structure's response and ensuring a more complete understanding of its condition. By employing a combination of sensors, the monitoring system can provide a more accurate assessment, enhancing the reliability of the monitoring effort. Chapter 2 discusses sensors that can record external loads acting upon the structure, such as traffic load, earthquake ground acceleration, and wind speed. These sensors can also measure the resulting load effects, including strain, displacement, and acceleration. Furthermore, it is essential to monitor and record the thermal and humidity effects on the structural elements of a bridge.

When employing global monitoring techniques for bridge condition assessments, two common challenges, among others, that can undermine the robustness of the results are noisy data and the temperature effect. Noisy data can introduce uncertainties in estimating global characteristics such as modal frequencies and modal curvatures, while temperature variations directly impact the global and local response of the bridge and its elements, posing challenges to the assessment effort (Rizzo and Enshaeian, 2021).

In regard to the temperature effect, a study conducted by Catbas et al. (2008) found that the strains induced by temperature on the truss chords of the Commodore Barry Bridge, one of the longest cantilevered steel truss bridges in the United States, were significantly greater than the strain magnitude caused by traffic. The researchers concluded that accurately modeling and separating the temperature effect on the response of critical elements could be a very challenging task and could negatively impact the overall reliability of the monitoring effort. Some approaches to compensate for the effect of temperature on the response of critical elements are as follows. In a project investigated by Zhang et al. (2015), an autoregressive integrated moving average model (ARIMAX) was utilized to relate the strain gage recording to the atmospheric temperature. In addition, when a sensor circuit starts recording, the current in the circuit can heat up the sensor and impact its reading (Bischoff et al., 2009). Huang et al. (2020) also designed a temperature-

strain correlation model that establishes a thermal baseline for recorded strains. This model can be utilized further to filter out thermal noise from the recordings, for an enhanced monitoring effort. Similar approaches were used by Yarnold et al. (2012) in the Tacony-Palmyra Bridge in New Jersey.

Fatigue failure of critical elements in a bridge is a consistent source of defects that necessitates consideration in monitoring regimes, as emphasized by codes and guidelines. Fatigue cracks, for instance, can be exacerbated by various loads and environmental factors, such as excessive traffic, harsh conditions, and aging. While steel elements generally exhibit reliable and isotropic behavior, fatigue remains a common occurrence among them. A notable example of a critical element prone to fatigue failure is the bridge edge girder, which experiences complex loading from both the floor beams and the attached cables. Therefore, conducting an analysis of the fatigue potential in these fracture-critical elements, along with direct measurements of their response, can aid in early detection of fatigue cracks. Zhou (2006) introduced a procedure for evaluating the fatigue life of existing bridges using field-measured strain data. The author of the study reviewed an AASHTO fatigue evaluation method and assessed fatigue life by analyzing stress range histograms derived from the measured data under traffic load. In the case of the Tsing Ma Bridge in Hong Kong, which is one of the longest suspension bridges in the world, the maximum stress range was selected as an index to identify fatigue-critical locations of bridge components. Similarly, Ye et al. (2012) developed a fatigue life assessment method for the same bridge, utilizing strain data and converting it into stress-time histories which was further used in the rainflow counting algorithm, a method used to predict the fatigue life of an element.

The rainflow cycle counting method was utilized by O'Connor et al. (2010) to estimate the fatigue life of a long-span bridge. Each cycle corresponds to a closed hysteresis loop in the stress-strain response of the steel member under cyclic loading. Wireless sensors were employed to record strain data for this analysis. Instead of placing strain gauges on all critical elements, the authors focused on fracture-critical elements with the highest strain demands. This approach minimized the amount of recorded data. Furthermore, the authors proposed an innovative method where the rainflow cycle counting process was performed at the sensor nodes rather than at the base station. This significantly reduced the amount of data transmitted from the sensor nodes to the base station, resulting in a faster feedback response and much lower energy consumption within the system. It is worth noting that providing a long-term energy supply for a BHM system on a large structure is challenging and that reducing energy consumption can greatly enhance system performance and resilience for long-term monitoring. The study underscores the significance of designing sensor nodes with the capability to perform basic data analysis and data filtering on the spot before transmitting the data to a central station for further processing (O'Connor et al., 2010).

Jindo Bridges, a pair of cable-stayed bridges situated in South Korea, serve as an excellent example of a successful BHM system. These bridges consist of three continuous spans, similar to the new Gerald Desmond Bridge, featuring a central main span measuring 1,129 feet in length, along with two side spans of 230 feet each (Jang et al., 2010; Jo et al., 2013). The twin bridge is equipped with

a diverse range of sensor types, employing various data collection and transmission technologies. Herein, we will provide an overview of the key instruments utilized for BHM purposes on this bridge, while reserving the discussion on monitoring strategies and research findings for subsequent sections of this report. The bridge is instrumented with a range of sensors, including 15 thermometers, 15 strain gauges, four biaxial inclinometers, two laser displacement meters, 24 Fiber Bragg Grating sensors, 20 uniaxial capacitive accelerometers, two biaxial force balance-type accelerometers, and three triaxial seismic accelerometers. The custom-designed sensor nodes feature accelerometers with specific ranges, resolutions, and other relevant parameters for data acquisition. For wind measurement, a 3-D ultra-sonic anemometer has been integrated into the Wireless Sensor Network (WSN). These anemometers are durable and well-suited for harsh weather conditions. The bridge instrumentation was further enhanced to a total of 669 channels, including 113 sensor nodes (Jo et al., 2013). Considering the challenges associated with battery replacement, the use of solar panels for energy harvesting could be beneficial in powering the sensor nodes. This important topic is further discussed in the following sections of this report.

He et al. (2022) conducted a comprehensive review focusing on the latest sensing technologies employed in the monitoring of cable-stayed and suspension bridges. The review article encompasses various sensing technologies including fiber optic sensors, piezoelectric sensors, GPS, and others, as well as wired and wireless data transmission methods. By compiling more than 180 articles, the authors aimed to examine the advantages and limitations of the latest smart sensors in bridge health monitoring, comparing them with conventional sensors like resistance strain gauges and wired accelerometers. The findings highlighted the effectiveness and suitability of FBG sensors in terms of measurement accuracy and durability, as supported by previous studies (Sheng and De, 2008; Qiu et al., 2013).

The second Wuhan Bridge, a cable-stayed bridge spanning the Yangtze River in China, has undergone extensive instrumentation for monitoring purposes. In their review, Shengchun and Desheng (2008) focused on the utilization of optical fiber sensing technology in the bridge's structural health monitoring. The instrumentation included a wide range of sensors, comprising 108 FBG strain gauges installed on beams and towers, 26 FBG vibration sensors placed on cables, and 20 FBG strain gauges for overweight vehicle detection. Additionally, a significant number of temperature sensors (57 sensors) were incorporated into the monitoring system. The authors highlighted the sensitivity of FBG sensors to temperature changes and stressed the importance of recording temperature data alongside to compensate for its impact on the measured strain. Furthermore, they emphasized the favorable advantages of optical fiber sensors over traditional electromagnetic-based sensors. Figure 3.1 provides a visualization of the sensor layout employed in monitoring the Wuhan Bridge (Shengchun and Desheng, 2008).

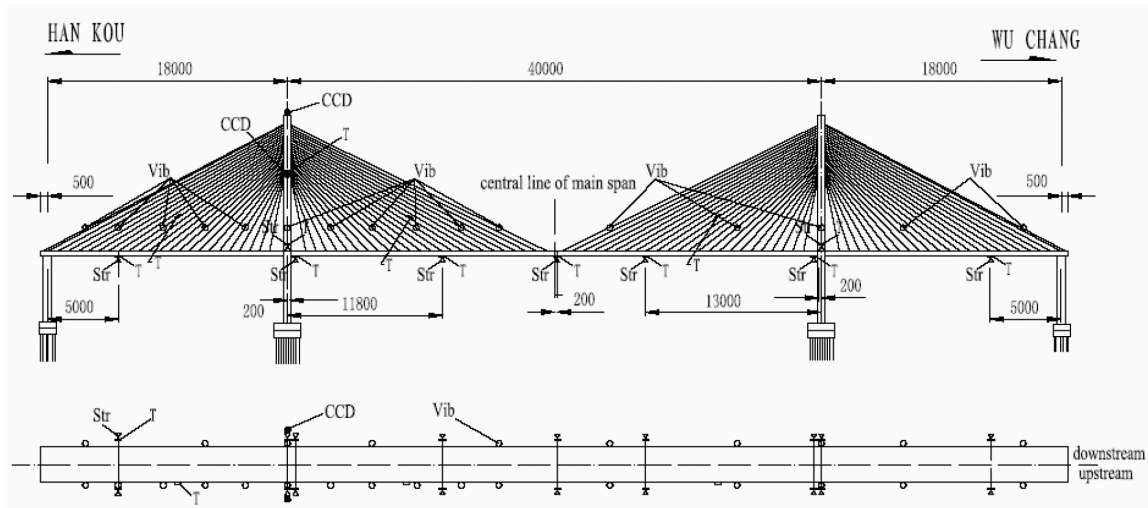


Figure 3.1. Sensor layout for Wuhan Bridge (No.2). Str: strain gauges; T: temperature sensors; Vib: vibration sensors; CCD: displacement monitoring system.  
Reprinted from Shengchun and Desheng (2008).

The Tsing Ma Bridge, a suspension bridge located in Hong Kong, stands as another significant example of BHM efforts in a large bridge structure. The bridge's monitoring system incorporates a total of 283 sensors, comprising various types such as anemometers, servo-type accelerometers, temperature sensors, strain gauges, global positioning systems (GPS), and displacement transducers (Ye et al., 2012). To facilitate data acquisition and transmission, the system utilizes on-structure data acquisition units and an optical fiber cabling network for signal conversion and transmission. Moreover, 110 weldable foil-type strain gauges were strategically installed to measure the strain levels of critical members. Given the potential fatigue risks faced by fracture-critical steel elements, the majority of these strain gauges were attached to the fatigue-prone sections of beams and girders, typically at the bottom flange of the beams. To assess the fatigue life of these critical elements, the rainflow cycle counting method was employed. The comprehensive monitoring approach implemented in the Tsing Ma Bridge showcases the importance of capturing various parameters for further BHM analysis and condition assessment. Figure 3.2 demonstrates the bridge elevation and strain gauge layout.

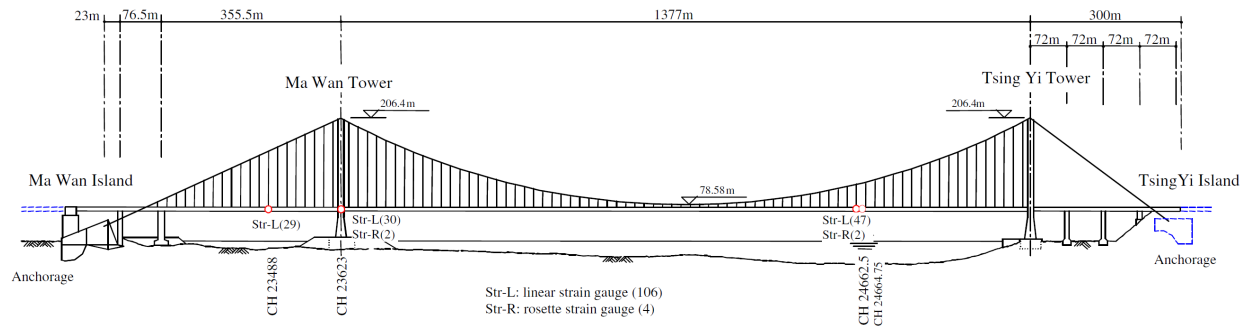


Figure 3.2. Strain gauge sensors layout for Tsing Ma Bridge. Reprinted from Ye et al. (2012).

Corrosion poses another significant risk to the steel elements of a bridge, as it can diminish the effective cross-sectional area of critical elements and lead to failure. In marine environments with higher humidity levels, such as the harbor zone of a port, corrosion can occur in various metallic components of the bridge, including cables, reinforcements, connections, beams, and box girders, resulting in performance degradation. Therefore, monitoring corrosion is crucial to detecting and addressing degradation, particularly in the case of stay cables. One approach to monitoring corrosion involves tracking the environmental conditions, such as humidity, in the proximity of the cables, which can provide insights into the interior environment of the cable (Rizzo and Enshaiean, 2021). Sloane et al. (2013) presented a strategy for indirectly assessing the corrosion rate of steel wires by utilizing a mock-up cable in the lab. In their study, they installed humidity, temperature, and corrosion sensors within the cable and discovered a significant correlation between relative humidity and the corrosion rate of the cable. The researchers further applied this method to a full-scale implementation on the Manhattan Bridge, where they observed that elevated humidity levels corresponded to increased levels of corrosion.

The presence of a protective sleeve on bridge cables poses a challenge for visual inspections. Typically, if any damage is observed on the sleeve, a more thorough inspection of the cable is conducted. It is worth noting that instances of corroded and fractured wires have been observed in relatively new bridges (less than six years old) in Japan (Son et al., 2021). Therefore, it is crucial to monitor and detect corrosion-induced damage either directly through sensors embedded within or attached to the wires and their anchorage, or indirectly by analyzing the vibrational response of the cables and comparing them with their counterparts on the same bridge. Additional preventive measures, such as reducing internal moisture and condensation inside cable sleeves (commonly known as dehumidification), can be implemented to slow down the corrosion rate, as suggested by Betti et al. (2016).

Indirect estimation of cable force can be achieved through the analysis of its recorded lateral vibration (Kim and Park, 2007). The calculated vibrational frequency of a cable exhibits a direct correlation with its axial tension. In their study, Kim and Park (2007) conducted wind excitation measurements on a laboratory cable setup using piezoelectric-type accelerometers. They

subsequently utilized their modified formula to estimate the cable tension. A comparison of the estimated cable forces demonstrated a high level of agreement with the direct force measured at the cables in the laboratory. The authors attributed this agreement to the small sag and low bending stiffness of the tested cable, influenced by the high-tension force. Cable sag and flexural rigidity are among the parameters that could impact the cable tension force estimate. To establish the relationship between cable force and vibrational frequencies, several formulas have been proposed by other researchers. These formulas take into account various variables, including cable length (whether short or mid-sized), cable sag, density, flexural rigidity, and cross-section (Zui et al., 1996; Geier et al., 2006). The measured vibration refers to acceleration or velocity recorded at one or more locations on the cable.

A cable-stayed bridge located in New South Wales, Australia, has undergone extensive instrumentation, including the installation of accelerometers, strain gauges, and environmental sensors. Alamdari et al. (2019) proposed an algorithm for data analysis that extracts features from the recorded vibration response of the cables and detects anomalies in the response of the bridge (i.e., damage). To validate their algorithm and the estimated cable forces, the authors conducted field tests involving 15 different damage scenarios. The objective was to observe the redistribution of cable forces in the event of cable damage, resulting in deviations from the baseline tension force. To simulate cable damage on the full-scale bridge, a common technique involving the placement of a lumped mass at various locations on the bridge deck was utilized. This concentrated mass altered the dynamic response of the bridge and its cables, creating a damaging event for evaluation purposes. Behmanesh and Moaveni (2015) and Lederman et al. (2014) employed a similar technique to induce artificial damage on a footbridge and a mock-up bridge, respectively. They achieved this by placing a lumped mass block at various locations on the bridge deck and subsequently attempting to detect the severity and location of the damage. These studies underscore the significance of validating Bridge Health Monitoring (BHM) systems (sensing and methodology) through field testing and measurements.

The selection of sensors for long-term BHM requires careful consideration of durability. The Wuhan cable-stayed bridge, another example of a long-span bridge, has been equipped with a variety of sensors, including a significant number of fiber-optic sensors. Specifically, fiber-optic strain gauges have been installed on critical elements to analyze stress distribution and monitor their responses (Liu and Jiang, 2008). The objective was to improve the estimation of element strength and identify potential degradation more effectively over a long monitoring period.

Another example of an extensively instrumented cable-stayed bridge is the Third Bridge over the Panama Canal. This impressive bridge stands tall with a vertical clearance of 246 feet, surpassing the height of the new Gerald Desmond Bridge, which has a clearance of 205 feet. The Third Bridge in Panama spans a total length of 3,445 feet, with its main span extending over 1,739 feet. It serves as a great example for various types of BHM sensors carefully chosen to meet the monitoring objectives of the project, which can potentially be applied to other cable-stayed bridges. The instrumentation plan for this bridge, proposed by Arlin and Melendez (2017), includes a

range of sensor types. Optical FBG temperature sensors were strategically placed on the box girder and pylons (towers) to monitor temperature variations. Temperature monitoring is essential for correcting the readings of the strain gauges. For corrosion monitoring, a selected pylon was equipped with sets of corrosion monitoring sensors at a designated section. The cables' anchorage zone will be instrumented with 10 sets of corrosion sensors. To capture the weight and speed of vehicles, weigh-in-motion sensors were proposed to be embedded in the pavement. Stay cables were instrumented with 44 triaxial force-balance accelerometers, while the deck and pylons were equipped with 20 biaxial piezoelectric accelerometers. Moreover, to monitor the bridge's global movement, six GPS receivers were installed on the top of both pylons, the middle of the main span, and both ends of the main bridge. Additionally, strain gauges and tiltmeters were strategically placed on the bridge towers, beams, and girders to gather essential data. Figure 3.3 shows a schematic view of all proposed sensors and sensing technologies for the Third Bridge at the Panama Canal.

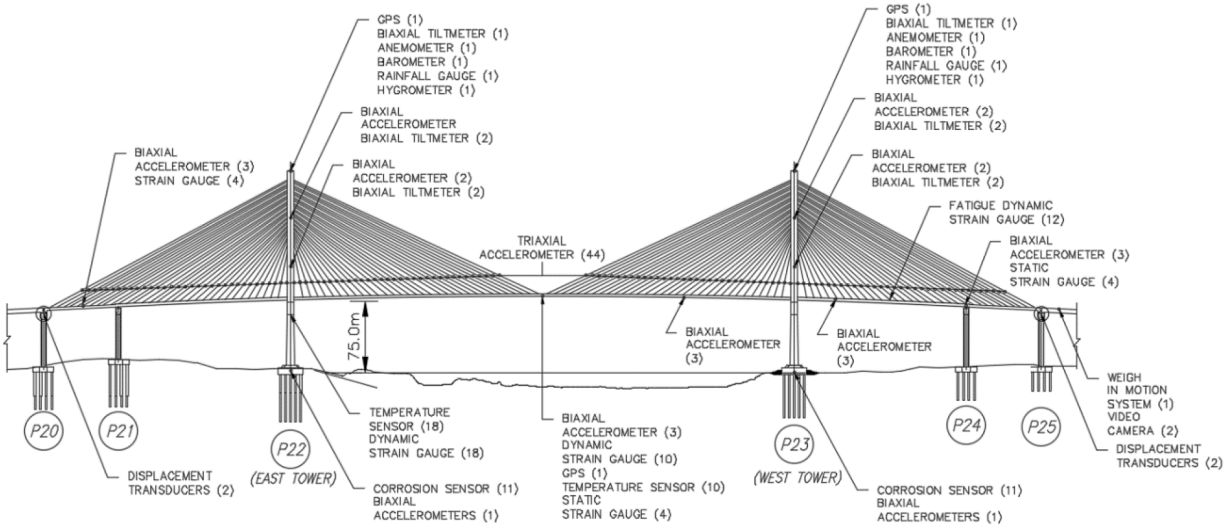


Figure 3.3. Sensor types and layout for Third Bridge at Panama Canal. Reprinted from Arlin and Melendez (2017).

As highlighted in the review article by He et al. (2022), accurately measuring the global displacement of a bridge deck or its tower is a significant challenge. Traditional displacement sensors or double-integration of the acceleration signal may yield inaccurate displacement estimates if the reference point for the deck displacement is not correctly identified. Additionally, the combination of semi-static displacement and dynamic response of the bridge deck makes it even more difficult to estimate lateral displacement using acceleration data alone (Kaloop and Hu, 2016). Geodetic techniques such as the Global Positioning System (GPS) offer a promising solution for measuring the global displacement of bridges (He et al., 2022). Increasing the sampling frequency of recorded GPS data can also aid in identifying the dynamic characteristics of the bridge (Moschas and Stiros, 2011). Typically, GPS recorders are placed on top of the towers

and the bridge deck, while a base station (i.e., a reference) is positioned near the structure (Kaloop and Hu, 2016).

After the collapse of the Tacoma Narrows Bridge in 1940, bridge engineers have given significant attention to wind load and wind-induced vibration (Fujino and Siringoringo, 2010). This is especially crucial for long-span bridges where the measurement of wind speed and its correlation with observed vibration and load effects are necessary. The objective is to distinguish wind-induced vibration from other sources of stress in bridge elements, such as traffic, temperature, and defects. According to Jo et al. (2011), a set of ultrasonic anemometers were employed to obtain precise wind speed measurements at the cable-stayed Jindo Bridge in South Korea.

As outlined in this section, the monitoring strategies, objectives, and sensing technologies employed in different cable-stayed bridges can vary significantly. A crucial decision in choosing a technology for bridge health monitoring is choosing between wired and wireless sensing technologies, including wireless sensors and data acquisition systems, or the conventional wired sensing equipment. The utilization of wireless sensor networks has emerged as a more recent approach that has gained recognition for monitoring large structures, such as long-span bridges, worldwide. This technology offers its own set of advantages and limitations, which will be explored further in the subsequent section of this chapter.

### *3.1.2. Wired Monitoring Systems vs. Wireless Sensor Network: A Comparison*

Wired sensors and data acquisition systems have been used by engineers and scientists for over four decades. These systems consist of sensor channels, which have continuously improved over time as discussed in Chapter 2, connected to a data acquisition system and a data storage unit using wires. Wired systems are highly popular and commonly employed for monitoring applications in buildings, laboratories, and short and mid-span bridges. On the other hand, Wireless Sensor Networks (WSNs) have proven to be particularly advantageous for large structures where deployment of a large number of sensors is necessary. As the name implies, WSNs enable wireless transmission of recorded data to other sensing nodes or to a central data acquisition node, eliminating the need for wiring within the structure.

To gain a complete understanding of the benefits and drawbacks of wired and wireless sensing technologies, a comprehensive review and comparison was conducted by Noel et al. (2017). In their study, the researchers presented a detailed analysis of the strengths and weaknesses of both systems. The researchers conducted a side-by-side analysis, exploring various aspects of monitoring systems in bridges as they relate to the network's reliability, practicality, and cost. Table 3.1 outlines key metrics used to evaluate and compare the two systems.

Table 3.1. A comparison between wired and wireless sensor networks for use in bridge health monitoring, adopted from Noel et al. (2017).

Comparison Criteria	Wired Sensor Network	Wireless Sensor Network
Average cost of a sensor (including data transfer)	High with examples ranging from \$10K to \$25K	Low with examples showing less than \$500
Time for deployment of one sensor	Long, ranging over several days due to wiring needs	Short, in a few hours
Lifespan or resiliency of the system	Long, only limited by hardware life	Short, limited by sensor node's battery life and hardware life
Connection bandwidth	High bandwidth and stable connection, due to use of wire	Limited bandwidth and relatively unreliable connection
Recorded signal synchronization	High synchronicity due to wired connection	Average to low synchronicity due to wireless connection

Table 3.1 presents several key factors involved in the selection and maintenance of a monitoring system, such as network cost, lifespan or resiliency, data transmission bandwidth, recorded signal synchronization, and overall cost (Noel et al., 2017). It is evident that neither system is advantageous across all metrics, as both have their own strengths and limitations. For instance, wireless networks generally have a shorter lifespan or resiliency compared to wired systems due to their reliance on batteries. In fact, power management was named as one of the main challenges faced by wireless sensor networks (Jang et al., 2010). To address this limitation, innovative approaches have been explored to harvest energy at wireless sensor nodes, enhancing the system's resiliency for continuous monitoring.

Furthermore, achieving signal synchronicity is crucial for most health monitoring techniques. Synchronized signals refer to signals with timestamps based on a common clock and triggered start time (e.g., zero). Smart wireless sensors within a network operate with independent local clocks, which may not be synchronized with the clocks of other sensors, resulting in potentially unsynchronized signals (Rizzo and Enshaeian, 2021). *Clock drift* is another factor contributing to unsynchronized recorded signals. This phenomenon occurs when time readings deviate from the actual time due to temperature increases during monitoring, such as from exposure to sunlight or heat emitted from the sensor's processor. Ensuring signal synchronicity in wireless connections poses challenges, often necessitating additional on-site pre-processing to correct any potential time-shifts in the signals (Rizzo and Enshaeian, 2021; Alamdari et al., 2018; Jang et al., 2010).

Noel et al. (2017) also presented a flowchart illustrating the components of a wireless sensor network, as depicted in Figure 3.4. The system consists of sensor modules, representing individual sensors like strain gauges, sensor nodes responsible for collecting and potentially pre-processing the raw data and a base station that receives the recorded data from either a segment or the entire network. The flowchart highlights the importance of synchronization coordination in two instances: between sensor nodes and between nodes and the base station. This emphasis on

synchronization is crucial to addressing the limitations associated with wireless sensor networks, as mentioned earlier.

On the other hand, one major advantage of a wireless sensor network over wired systems is its overall deployment cost. As indicated in Table 3.1, the cost of a wireless sensor for a large structure is often significantly lower than that of a wired sensor and its associated wiring requirements (Noel et al., 2017). Additionally, a wireless sensor node can be swiftly installed at any location on a bridge, whereas traditional wired sensors may necessitate several days for wiring, thereby reducing labor costs associated with wireless network deployment. The small size of the equipment and the ease of installation provides flexibility in designing the sensor placements and topology (Rizzo and Enshaeian, 2021). The comparatively lower costs of sensors and labor in wireless sensor networks can facilitate the deployment of a greater number of sensors, resulting in a denser sensor network configuration. A denser network could shore up the monitoring system’s reliability.

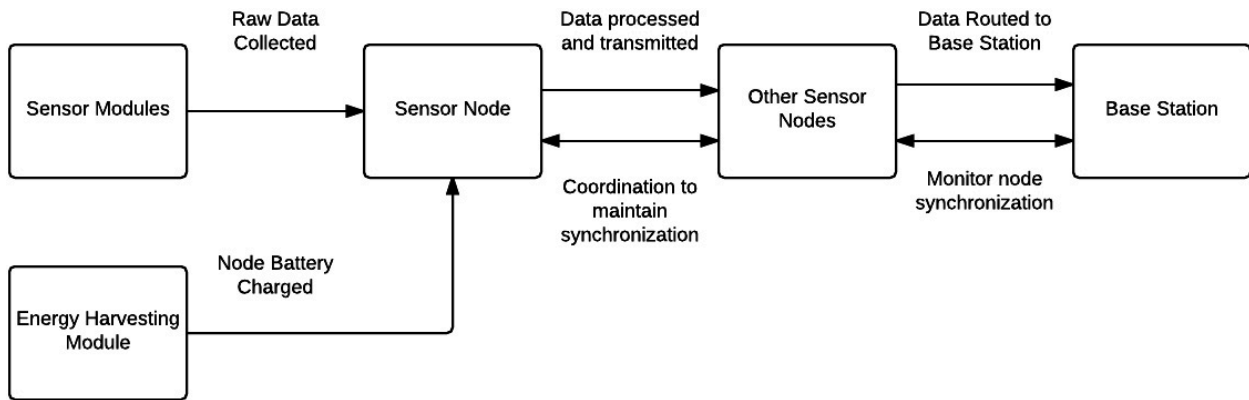


Figure 3.4. Flowchart of a wireless sensor network (WSN) components and communication order for bridge health monitoring. Reprinted from Noel et al. (2017).

The Golden Gate Bridge stands as one of the pioneering bridge health monitoring projects in California, employing a wireless sensor network (WSN) (Kim et al., 2007). A total of 64 wireless sensor nodes, along with a base station, were installed on the bridge, marking it as one of the most extensive WSN projects in the United States. The WSN system operated under a centralized approach, with all sensors transmitting their data to the central base station. The system's lifespan was approximately 10 weeks, as reported by Noel et al. (2017). Furthermore, the project faced the challenge of managing a large volume of collected and transmitted data, which is a common issue encountered with centralized data collection techniques.

One recent development in the arena of wireless sensing technology is the wireless smart sensor network (WSSN), which adds the capability of embedded data analysis at the sensor nodes, prior to transmission of data to a base station (O'Connor et al., 2010). The smart sensor nodes include an on-board CPU and a memory which enables the small device to act like a standalone

computation node. The pre-processing of data at the smart sensor will significantly reduce the volume of transmitted data, consequently helping the bandwidth limitations of a wireless network monitoring system. It also reduces the power consumption of the entire network, which is considered one of the challenges faced by wireless networks. It is noteworthy that in-network data processing methodologies should be developed, tested, and calibrated to achieve these benefits.

Jindo Bridge, as mentioned in the previous section, serves as another notable case of an advanced deployment of a wireless sensor network. This testbed structure is exposed to strong winds and typhoons, making it susceptible to significant movements and potential damage. Researchers have undertaken monitoring of the bridge using WSN, focusing on various aspects of the wireless monitoring system to overcome limitations and challenges related to system reliability and durability (Jang et al., 2010; Jo et al., 2013). One specific challenge investigated and addressed by Jo et al. (2013) was the difficulty faced by wireless sensors in accurately measuring low-amplitude ambient motions or strains. This challenge was caused by limitations in the analog-to-digital converter resolution and the presence of inherent circuit noise. To tackle this issue, the authors developed a novel high-precision sensor board. The Jindo Bridge stands as an excellent example of a successful WSN implementation. In the following section, we will dive into the instrumentation configuration of the bridge and explore innovative solutions and ideas aimed at enhancing the reliability of the recorded data and the durability of the network.

Sensing technologies utilizing the Global Positioning System (GPS) and Global Navigation Satellite System (GNSS) have gained significant interest in bridge health monitoring, particularly for monitoring bridge movement and displacement, as mentioned earlier. The GNSS offers notable advantages, such as relatively high accuracy and precision, making it an attractive wireless system for bridge monitoring (Kaloop and Hu, 2016; He et al., 2022). An example of GPS application in monitoring bridge tower response is the Yonghe Bridge in China, which connects Tianjin and Hangu (Kaloop and Hu, 2016). This cable-stayed bridge has undergone extensive instrumentation for health monitoring, including the deployment of three GPS sensors on the bridge towers, as shown in Figure 3.5. Additionally, a total of 176 sensors, including strain gauges, accelerometers, temperature and weight-in-motion sensors, and anemometers, were installed on the bridge. The authors acknowledge that GPS sensors may introduce measurement errors, necessitating cross-checks for data validation. One approach to enhance GPS recorded data is to pair them with adjacent accelerometers to validate their response. Moreover, a higher sampling rate can be advantageous for extracting dynamic characteristics, particularly for vibration analysis at the element level (Kaloop and Hu, 2016).

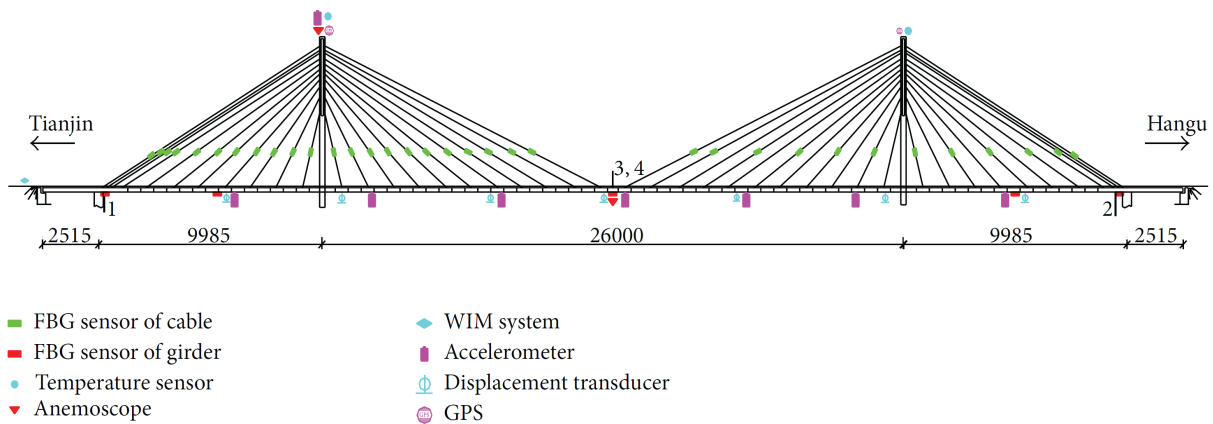


Figure 3.5. Sensor types and layout for the Yonghe Bridge. Reprinted from Kaloop and Hu (2016).

An example of a smaller-scale wireless sensor application is the Keraesjokk Bridge, a steel truss railway bridge located in Sweden (Bischoff et al., 2009). This bridge houses a wireless sensor network (WSN) system for its continuous monitoring purposes. Specifically, the WSN system was used to monitor strains on critical elements of the bridge, allowing for accurate measurement of loading during the passage of heavy freight trains. The monitoring system consisted of eight sensor nodes equipped with resistance-type strain gauges, with the root node connected to a base station powered by a rechargeable battery utilizing solar energy. Authors used very efficient MEMS accelerometers to save on the system's energy consumption.

One of the challenges encountered in WSNs is *sensor drift* (Rizzo and Enshaeian, 2021). This phenomenon refers to the degradation of measurement accuracy in wireless sensors over time, which can result in inaccurate measurements or even false positive detections. Fujino and Siringoringo (2011) further highlight the significance of the durability and reliability of sensors for continuous measurement in a dense network. To mitigate this issue, one approach is to create multiple clusters of wireless sensors that cover different areas of a structure and have overlapping measurements. This overlap allows for the detection of anomalies or malfunctions in a recording sensor node. If the data from one region differs significantly from its overlapping region, calibration of the sensors may be necessary, and the trigger threshold for the malfunctioning region may be temporarily disregarded to avoid false positives.

### 3.1.3. Wireless Sensors Network for Long-Span Cable-Stayed Bridges: A Successful Example

The new Jindo Bridge, a cable-stayed bridge located in South Korea, has been a testbed for deployment of a successful wireless smart sensor network (WSSN). The bridge has a main span of 1129 feet and side spans of 230 feet, very similar in length to the new Gerald Desmond Bridge. The bridge houses the largest WSSN for bridge health monitoring in the world. In this section, we aim to dissect the WSSN health monitoring system at the Jindo Bridge and learn from their research team's challenges, innovative solutions, and recommendations towards the proposed

framework for the Gerald Desmond Bridge. The information summarized and discussed in this section is mostly extracted from articles by Joe et al. (2011, 2013), Jang et al. (2010), and Cho et al. (2010). After a brief discussion on the Jindo Bridge’s network topology and sensor types, we highlight the major steps that improved the system’s reliability and durability.

The bridge was instrumented with a network comprising 113 individual sensor nodes and about 669 recording data channels, making it one of the most extensively instrumented bridges in the world. Figure 3.6 shows the bridge and its instrumentation layout. The system gets triggered by large load effects, likely caused by strong wind (Jang et al., 2010).

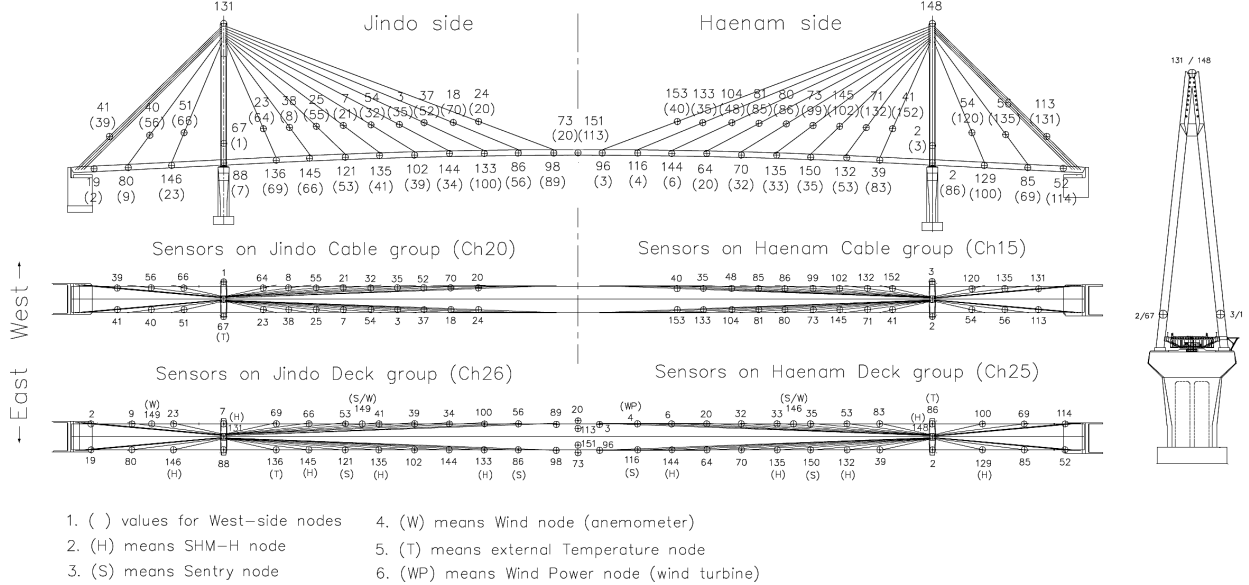


Figure 3.6. Sensor types and layout for the new Jindo Bridge. Reprinted from Joe et al. (2011).

The WSSN in the new Jindo Bridge is designed to be a hybrid system owing to its utilization of alternative power sources, charging of the onboard batteries, as well as its innovative data transmission design across sensor nodes, which further improves its resiliency. Using solar panels and wind turbines, energy harvesting capabilities were added to all sensor nodes on the bridge. This plays a critical role in the durability of the system’s continuous monitoring, further discussed in the next section of this chapter.

Moreover, the resiliency and scalability of the WSSN was improved by an innovative design to decentralize the data aggregation and acquisition effort. The counterpart centralized effort for the Golden Gate Bridge, as discussed earlier, posed some challenges with data transmission bandwidth and acquisition. The bandwidth limitation of a wireless network could prevent future expansion of the network in order to achieve a denser network in the future. The de-centralization of data aggregation has the benefit of reducing the transmitted data within the network, placing less stress on the network and helping with its future scalability. The main difference between a centralized and a decentralized data acquisition approach is that in a centralized data acquisition approach,

the raw data is directly transmitted to the base station, while a decentralized system pre-processes the raw data, compresses the data into smaller sized files, and transmits them. This puts less pressure on network bandwidth and reduces in-network energy consumption. The smart sensor platform used for the Jindo Bridge is Imote2, from the MEMSIC, which has a number of advantages over its older versions including a much faster processor (which improves at-node data processing) and the capability to accept an onboard memory, further enhancing the system for extensive at-node data processing. The condensed data can be saved on the onboard flash memory and retrieved later if needed, an assurance to the system's reliability. The system is operated using software developed by the Illinois Structural Health Monitoring Project (ISHMP), namely *ISHMP Service Toolsuite* (Joe et al., 2011).

A decentralized WSSN requires a hierarchical process for coordinating aggregated data and communication with the base station. For the Jindo Bridge network, a *cluster* topology approach was proposed for the de-centralized data coordination (Joe et al., 2011). Figure 3.7 illustrates the network topology and the coordination between three main types of wireless nodes, including local sensor nodes (i.e., Leaf nodes), the cluster head, and the Gateway node. The Gateway wireless node is at the base station. At the base station, the received data from the WSSN can be further processed using a powerful PC and the processed data can be sent to a remote station via the internet. Hence, the base station needs to have access to an uninterrupted internet connection at all times.

The pre-processing capability in the decentralized network exists at the cluster head and the leaf nodes. For instance, to monitor the cables' tension and any anomaly in their pattern, the Leaf nodes (end nodes) perform processing of recorded data locally by analyzing the acceleration data to find the natural frequency of vibration for the cable and infer the cable tension indirectly, as discussed earlier. Only the maximum cable tension force is being communicated with the cluster head rather than the entire time-history of recorded acceleration response. This reduces the magnitude of transmitted data to the gateway node (at the base station) significantly.

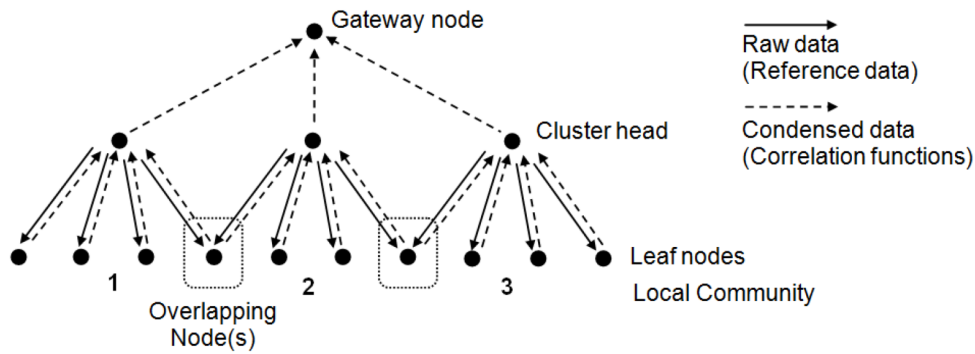


Figure 3.7. Hierarchical data coordination in a cluster-based topology. Reprinted from Joe et al. (2011).

At-node data processing and coordination will require a set of proprietary software applications. For the Jindo Bridge specifically, a set of applications were developed which were all housed under the software *ISHMP Service Toolsuite*. The applications perform various tasks related to the health monitoring goals, including at-node data analysis and condition assessments, battery charging, activation of the system, and more. For instance, the application *CableTensionEstimation* is used to estimate the cables' tension force using the recorded acceleration response; the application *ChargerControl* is used to charge the battery of a node when the system is awake, based on the battery's voltage level; the application *SnoozeAlarm* puts the leaf nodes in sleep and wakes them up periodically for sensor-status and battery-status checks; and the application *ThresholdSentry* is used to wake up the entire system for continuous monitoring for a set period if any of the event triggering thresholds (strain, cable force, displacement, etc.) are breached. All the applications, which are essential to the operation of the system, are managed under the *ISHMP Service Toolsuite*. The Jindo Bridge instrumentation includes a large number of environmental sensors. These sensors, as shown in Figure 3.7, are deployed to monitor wind speed, temperature, and humidity near critical elements.

The many sensors deployed on the Jindo Bridge were clustered into four subnetworks. The subnetworks were chosen according to the type of monitored elements, their locations, size of cluster, and the communication protocol to the base stations. All the clusters share the same software applications discussed earlier. The four subnetworks include the deck sensors and the cable sensors on the Haenam side (forming two subnetworks) and the deck and cables sensors on the Jindo side. Each group of sensors under each cluster communicates with their own gateway node. The gateway nodes transfer the data to the base station. Hence, the base station becomes an essential part of the monitoring system and subsequently must be of superior durability against the harsh environment, as well as being able to process large volumes of data and transmit them to a base station using relatively high-speed internet connection (Joe et al., 2011; Cho et al., 2010). To verify the accuracy of recorded responses by the WSSN, authors have compared acquired ambient (i.e., service) vibration data with those recorded by a few wired sensors, which were found to be in

great agreement. The presence of some wired sensors within the network could help with the validation and calibration of a WSSN.

One main reason behind creating the subnetworks (clusters) is the limited reception rate for wireless sensors at large distances. Jang et al. (2010) have performed a test on the reception rate of 73 sensors (referred to as “leaf nodes”) located at varying distances from the gateway node. The distance has been increased gradually, with the gateway being placed at the tower and the sensors being moved towards the midspan of the bridge. Then, the number of responsive sensor nodes were counted at each station. Figure 3.8 shows the number of responsive sensors given their distance from the gateway node. Only 23 sensors (out of 73) were found to be responsive at the midspan (a distance of about 564 feet). This finding emphasizes the importance of the clustering topography depicted in Figure 3.7 to ensure all sensor nodes and their respective cluster head node are fully connected to the gateway.

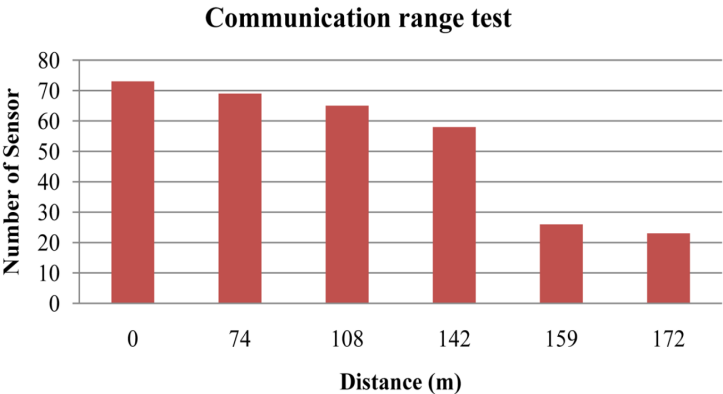


Figure 3.8. Number of responsive wireless sensors as a function of their distance from the gateway node. Reprinted from Jang et al. (2010).

Communication wait time is another important factor when designing the topography of a WSSN. Specially, when the system is designed for real-time monitoring, the time lag from the communication should be accounted for. The performance of a BHM system is directly impacted by the required response time from the network, which is a function of the communication wait time for the wireless network (Jang et al., 2010). In the study by Jang et al. (2010), they found that the wait time increases linearly with the acquired data points at the gateway. They found that the communication wait time for downloading 30,000 data points from 46 accelerometers in the network took about 30 minutes. For accelerometers that record with a sampling frequency of 25Hz, this translates to about 27 seconds of continuous acceleration time-history recording, which one may consider a very short time span. As a result, at-node pre-processing and condensation of data is essential for monitoring the structure over a longer period and acquiring data in real time or near real time.

In the BHM design at the Jindo Bridge, special consideration was given to the type of sensor board to enable accurate measurement of low-amplitude vibration. Basic wireless sensor boards are

unable to record very small strain amplitudes of only a few micro-units strain. This is particularly important as the majority of the at-service vibration at a bridge has relatively small amplitude or can be considered as the ambient vibration. Therefore, a high-precision sensor board was designed to precisely measure the ambient vibrations. A high-precision wireless sensor board should be able to amplify the signal up to 2,500 folds (Jo et al., 2013). In addition, the sensor board should have the capability to compensate for the recorded strain from thermal effects, which could be significant.

Relatively fast installation of wireless sensors on a bridge makes them a compelling choice. Sokki Kenkyujo Co. has come up with a frictional strain gauge that is housed in a metallic cylinder equipped with a magnet at one end. The wireless sensor can be easily attached to the bottom flange of a steel girder. An adhesive can be applied to the flange surface to avoid sensor slippage. This approach eliminates the need for removing paint or applying welding to attach the strain gauge. Figure 3.9 illustrates this type of sensor and its attachment to a bridge girder at the Jindo Bridge (Jo et al., 2013). Using a lead wire, the strain gauge is connected to a sensor node box as shown in the figure.

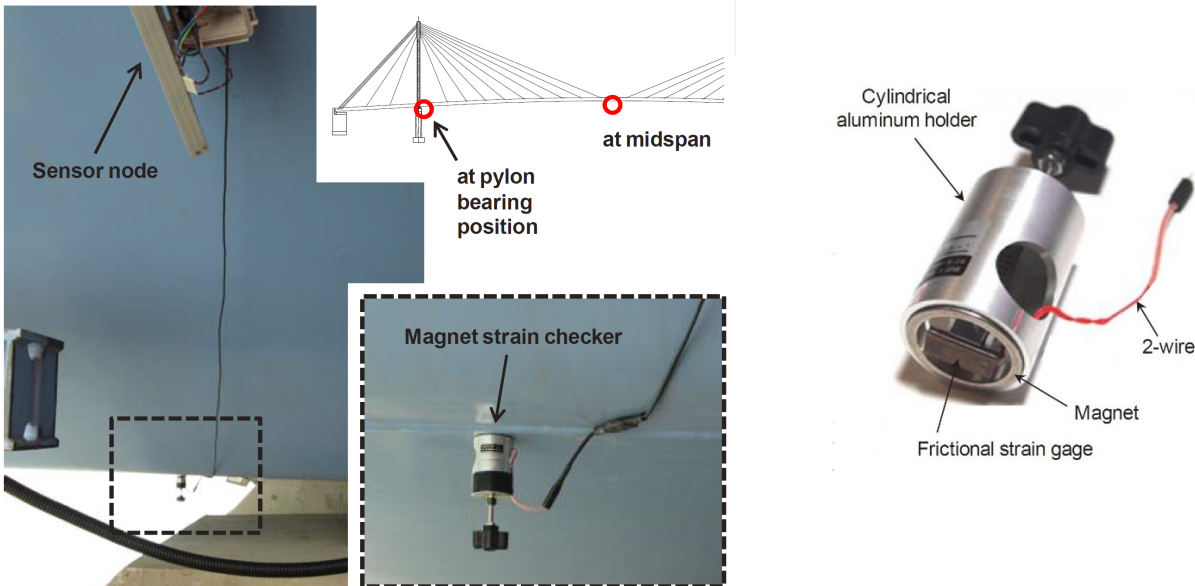


Figure 3.9. Application of a magnetic frictional strain gauge produced by Sokki Kenkyujo Co (right) attached to the bottom flange of the Jindo Bridge (left). Reprinted from Jo et al. (2013).

### *3.1.4. Energy Harvesting and Monitoring System's Resiliency*

In the effort of monitoring the Jindo Bridge, Cho et al. (2010) note three major challenges every wireless sensor network with a large number of sensors faces. These challenges, which must be addressed during the design of a network, include (1) reducing the network's energy consumption, (2) handling the network's data overflow, and (3) providing continuous operation anytime needed. Interestingly, the first challenge impacts the other two since transmitting more data requires more energy, and in the event that a battery's voltage is excessively low, continuous monitoring will not be possible. This underscores the importance of energy saving and energy harvesting in a WSN to ensure that the maximum benefits of the system are achieved. It is critical to deploy a rechargeable battery at the sensor nodes and design applications to monitor the battery voltage of each node. If the battery voltage drops below a certain threshold, the battery should be recharged using solar or wind energy. It is noteworthy that techniques such as putting the system in sleep periodically and compressing acquired data could significantly reduce energy consumption in the network, as discussed earlier.

At the Jindo Bridge, the sensor nodes were augmented by a small solar panel. Given the location of the Jindo Bridge, a small wind turbine could be a great alternative source of energy generation during seasons when sun exposure is low. Figure 3.10 shows utilization of solar panels at cable nodes and a wind turbine at the beam/girder where the sun exposure is low. Cho et al. (2010) found that a brand-new battery with a voltage of about 4.6V can last about two months with an efficient monitoring protocol (e.g., including sleep mode and threshold trigger applications). When the voltage dips below 3.6V, the node will not be able to sense anymore. On the other hand, a rechargeable battery could well keep its voltage level above 4V during the monitoring period. Figure 3.11 illustrates voltage level for multiple nodes at the Jindo Bridge with a solar-based rechargeable battery. The only node with a declining battery level is the one installed under the bridge deck where sun exposure is minimal (Cho et al., 2010). Hence, for sensor nodes located under the bridge deck, a solar panel should be installed on the side of the bridge, facing up, and connected via a lead wire to the sensor node.

Although energy harvesting using solar panels is essential for ensuring continuous functionality of the network, from time to time, the need for replacing defective batteries may arise. Therefore, sensor nodes should be placed at locations where they can be accessed easily by the maintenance team. For instance, sensor nodes installed on the cables should be at a height less than 10 feet (3m) so that one could replace their batteries or any defective hardware using a step ladder.

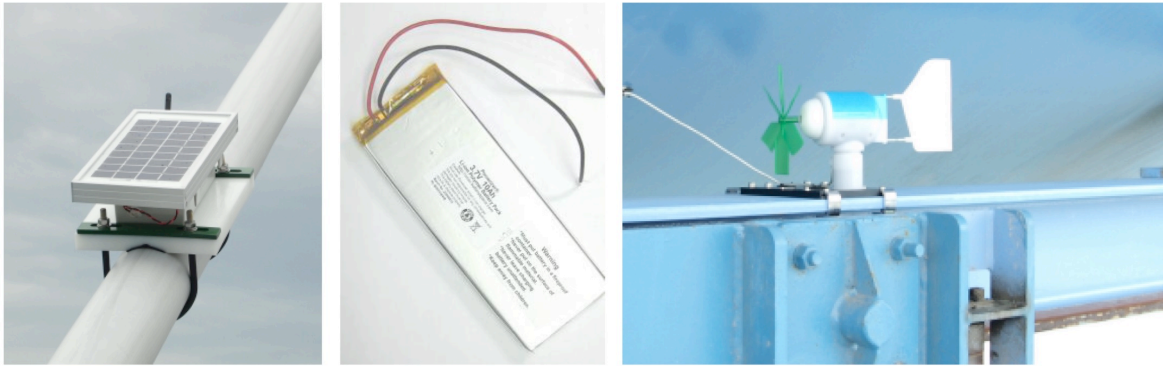


Figure 3.10. Use of solar panel for energy harvesting at the cable node (left), rechargeable battery (middle), use of wind turbine at girder's bottom flange. Reprinted from Jo et al. (2011).

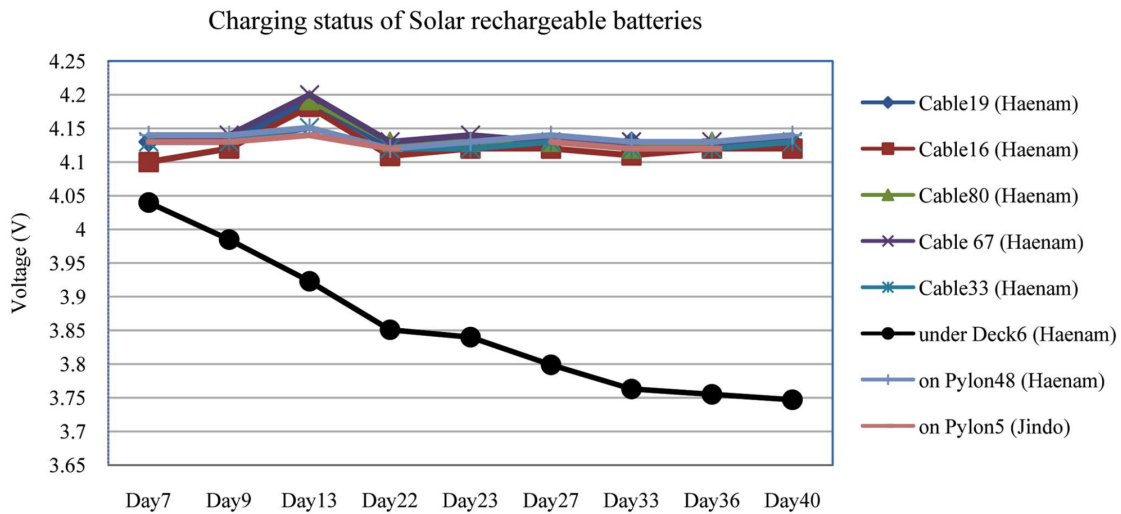


Figure 3.11. Status of sensor node solar rechargeable battery voltage over time. The black curve belongs to a solar battery installed under the deck. Reprinted from Jo et al. (2011).

In summary, energy harvesting and maintaining the sensor nodes' battery levels are essential for a WSSN's continuous monitoring and its resiliency for condition assessment at all times. As discussed in previous sections, other techniques for data management and assessment that utilize the smart sensors' computation power locally can help save energy in the network. For instance, at-node analysis of cable forces and communicating only beyond-threshold values with the base station could significantly reduce the transmitted data and energy consumption of the network. For fracture-critical elements, techniques such as at-node analysis of strain data, rainflow counting, and communicating updates on the fatigue life of the girder or other fracture-critical elements in a bridge could help reduce need for transmitting large amounts of data to the base station (O'Connor et al. 2010). Moreover, sensors with low energy consumption could help with the resiliency of the network. For example, Bischoff et al. (2009) utilized an ultra-low power MEMS sensor to measure acceleration at a railway truss bridge. An event-triggered monitoring system will

require sensors that continuously measure certain response parameters; hence, use of such low-power sensors may be necessary to allow for such continuous monitoring.

### 3.2. A review of bridge health monitoring methodologies: The Post-Processing Attempt

Over the past five decades, researchers worldwide have dedicated their efforts to developing various methodologies for identifying and detecting damage in both small laboratory-scale and full-scale bridges using sensory data. The primary focus has been on enhancing the accuracy and practicality of data-based structural health monitoring (SHM) techniques while also reducing the time required for analysis. Most of these proposed SHM methods rely on data acquired from a sensing network on the bridge. Data used for post-processing methods ranges from small-amplitude ambient vibration data to post-event data after larger earthquake events. This section focuses primarily on the methodology part of a bridge health monitoring (BHM) system, as depicted in Figure 1.2, and provides a brief overview of some of the methods and research conducted in this field.

In their study, Seo et al. (2015) extensively reviewed prior research on damage detection, bridge capacity evaluation, and remaining life estimation. Their findings indicated that vibration-based and strain-based structural health monitoring (SHM) systems have demonstrated their effectiveness in detecting alterations in dynamic characteristics over time. These two SHM approaches have been integrated into various methodologies developed for bridge damage detection throughout the past four decades.

In their research, Ntotsios et al. (2008) investigated the application of vibration-based SHM on both a full-scale bridge—Polymylos—in Greece and a small-scale laboratory bridge section constructed from steel. Their approach involved utilizing a modal identification algorithm and a graphical user interface (GUI) to analyze and compare variations in dynamic structural parameters, including mode shapes and modal frequencies, before and after damage occurred. The objective was to assess the extent of damage by observing changes in these parameters. To identify the specific locations of damage, the researchers compared elemental-stiffness values and measured reductions in stiffness. The study presented findings for two different damage scenarios, indicating that the method's accuracy in detecting minor damage was not satisfactory. It is worth noting that modal frequencies of vibration reflect overall characteristics of a structure, making it challenging to precisely pinpoint the exact location of damage within the structure.

Zhou et al. (2007) introduced a vibration-based damage detection (VBDD) method that centered on analyzing variations in mode shape curvature, uniform flexibility curvature, and overall structural flexibility. The researchers evaluated the effectiveness of their method by employing five different variants and assessing their performance in detecting and localizing damage. The findings revealed that the accuracy of the method was strongly influenced by the number and placement of sensors. In particular, using a low-density sensor array resulted in subpar damage-detection performance. This highlights the importance of having an adequate number of sensors distributed

strategically throughout the structure for a method or BHM algorithm to achieve successful outcomes.

In summary, vibration-based structural health monitoring (SHM) methodologies have typically involved selecting a set of critical structural characteristic parameters and comparing their changes before and after the introduction of damage. In their study, Soyoz et al. (2009) conducted a parameter-identification analysis on a large-scale shake table test of a three-bent concrete bridge model. Initially, a set of structural parameters was generated using nonlinear time history analysis and a Monte Carlo simulation. The researchers then employed a *Bayesian* update process to adjust the structural parameters and estimate the reliability of the bridge elements after significant shaking. The results indicated that the residual reliability of the damaged elements, as estimated by the Bayesian-updated model, was lower compared to the non-updated model. This highlights the importance of incorporating parameter updates in accurately assessing the reliability of structural elements following damage.

Costa et al. (2014) conducted a case study on the Luiz I Bridge in Portugal, highlighting the effectiveness of modal analysis as an SHM technique. They utilized this method to evaluate the impact of a rehabilitation project on the bridge by comparing data collected before and after the retrofit. The study focused on dynamic parameters such as mode shape, natural frequencies, and lateral stiffness. Similarly, Hsieh et al. (2008) employed frequency response functions and ERA-OKID (Eigen-system Realization Algorithm with Observer Kalman Filter Identification) for modal parameter identification and stiffness matrix optimization. They successfully applied this SHM approach to a six-span highway bridge subjected to various excitations, demonstrating its capability in detecting damage. In another investigation, Catbas and Aktan (2000) utilized experimental modal analysis to assess the damage conditions of a three-span steel-stringer bridge. Their results indicated that valuable information about the structural condition can be obtained from a well-designed dynamic test.

Iranmanesh and Ansari (2014) proposed a damage-assessment methodology based on energy dissipation and applied it to a reinforced concrete bridge column. The primary aim of this methodology was to quantitatively evaluate minor to moderate damage caused by seismic shaking, which can be difficult to detect through visual inspection alone. The experimental investigation involved analyzing a scaled two-span reinforced concrete bridge with circular cross-sectional columns using a hybrid simulation program. To assess the damage, the researchers utilized the height of the plastic hinge and average curvature to calculate the energy dissipation in the column. Furthermore, they employed a dissipated-energy index to determine the level of structural damage. The study concluded that their SHM method was effective in detecting and quantifying minor and moderate damage that may not be readily identifiable through visual inspection alone.

To enhance the accuracy of SHM systems, researchers have explored the combination of multiple methods. A study conducted by Noman et al. (2013) focused on integrating statistical pattern recognition with vibration-based methods. This combination aimed to improve the system's

performance in dealing with noisy data and environmental effects, as the statistical pattern-recognition approach exhibited greater tolerance under such challenging conditions. Another research work by Huang et al. (2011) incorporated non-destructive tests into a probabilistic framework for monitoring bridge health conditions. By integrating probabilistic models and non-destructive testing techniques, this approach enabled a comprehensive assessment of the bridge's health, providing a more holistic view of its condition. As a result, the combined approach facilitated more accurate and more reliable monitoring of the bridge's health status.

The presence of a well-designed and efficient SHM algorithm is essential for processing and analyzing the collected data. It enables the utilization of the acquired information to generate reliable results that effectively detect any possible damage or abnormalities in the structure. The combination of dependable data collection and sophisticated analysis algorithms is vital for the overall success of an SHM system.

## 4. The Case-Study Cable-Stayed Bridge: Description and Dynamic Response

In this chapter, we focus on the unique structural system of the newly constructed Gerald Desmond Bridge, which has been specially designed to withstand seismic events due to its proximity to active earthquake faults in the region. Our discussion centers on the different structural components of the bridge and the design considerations that adhere to relevant design codes. Through this analysis, we identify the critical elements of the bridge that should be monitored using the proposed framework in this study.

The California Geological Survey (CGS) has already installed a series of accelerometers on various parts of the bridge, including the deck, tower, and foundation. These accelerometers enable the measurement of the bridge's acceleration response during seismic events. Notably, in 2022, the bridge experienced an earthquake, providing valuable data for assessing its dynamic behavior. In this chapter, we thoroughly examine the current instrumentation setup of the bridge and evaluate its response in both the time domain and frequency domain, specifically focusing on the recorded acceleration data during the 2022 earthquake.

Section 4.1 provides an in-depth description of the critical components of the bridge, highlighting their significance in the overall structural system. Subsequently, we discuss the general code regulations that govern the design of bridges, ensuring compliance with safety standards. Finally, in Section 4.3, we present the existing layout of the bridge instrumentation, detailing its dynamic response as captured by the recorded data.

### 4.1. Bridge Structural System, Design Considerations, and its Critical Elements

Gerald Desmond Bridge is the first large-span cable-stayed bridge in California and opened in 2020. The six-lane bridge consists of a signature 2,000-foot-long cable-stayed segment, with a 1,000-foot main span over the channel and two 500-foot back spans along the east and west approaches. Figure 4.1 shows a rendering of the new bridge. The cable-stayed span is supported by two 515-foot super tall reinforced concrete towers. There is a total of 80 stay cables, 40 at each tower, that connect the deck's edge girders to the towers. Figure 4.2 shows a side-rendering of the main span, towers, and stay-cables arrangement. In addition, because of its location in the highly seismic zone of southern California as well as its proximity to two local, active faults, the bridge required a special seismic design to ensure immediate serviceability during small- to moderate-level earthquakes and resiliency during large regional events. Flexibility of cable-stayed bridges are to their advantage during seismic events; however, controlling the large displacements of the bridge during wind or earthquake events was a design challenge. To accommodate large displacements, horizontal and vertical viscous dampers (i.e., shock-absorbers) as well as an innovative swivel end-joint were deployed between the deck and towers and at the end-bents, respectively. The

dampers are designed to activate only during large motions, when they will contribute to the dissipation of energy and reduce the peak displacement demand of the deck.



Figure 4.1. A rendering of the completed Gerald Desmond Bridge (Source: Port of Long Beach).

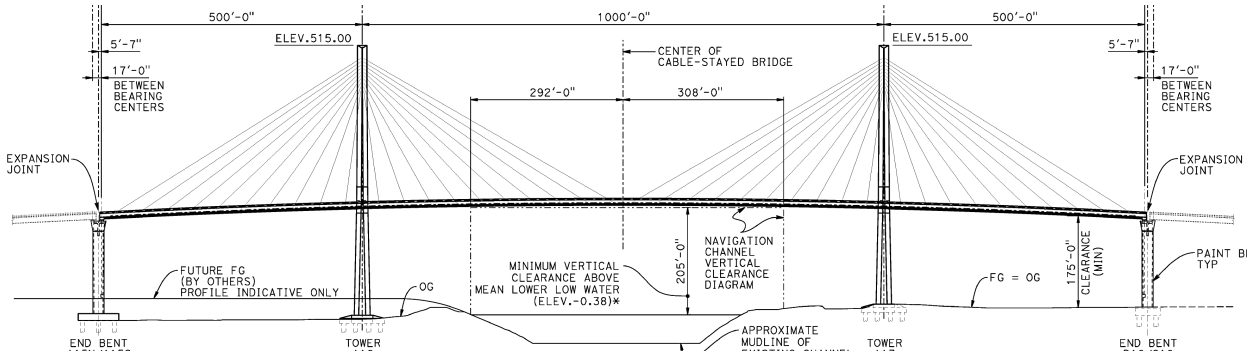


Figure 4.2. The main span, towers, and stay cables arrangement (Source: structural drawings supplied by the Caltrans).

The main span of the Gerald Desmond Bridge features an intermediate support system for the superstructure, consisting of two cable planes that extend outward from each tower and connect to the superstructure at 50-foot intervals. The lengths of the stay cables vary between approximately 235 feet to 572 feet, and the number of strands per cable ranges from 37 to 109. The stressing of the mono-strand stays is performed from the outboard side of the edge girders.

Each tower of the bridge is supported by a total of twelve Cast-In-Drilled-Hole piles with a diameter of 8'-2½" and a length of approximately 180 feet. The pile foundations were designed for the exact soil conditions at their specific location. The site does contain liquefiable soils; therefore, the depth of the piles was extended beyond the liquefaction zone. The towers have a variable cross-section, starting with an octagonal shape at the base and tapering to a diamond shape in the upper part. The connection between the stay cables and the tower is achieved through either anchor boxes or reinforced concrete corbels. The lower two sets of stay cables are nearly vertical, allowing them to rest on reinforced concrete corbels, while the upper eight sets of stay cables are connected to fabricated steel anchor boxes that are integrated with the tower. Figure 4.3 presents a visual representation of this configuration.

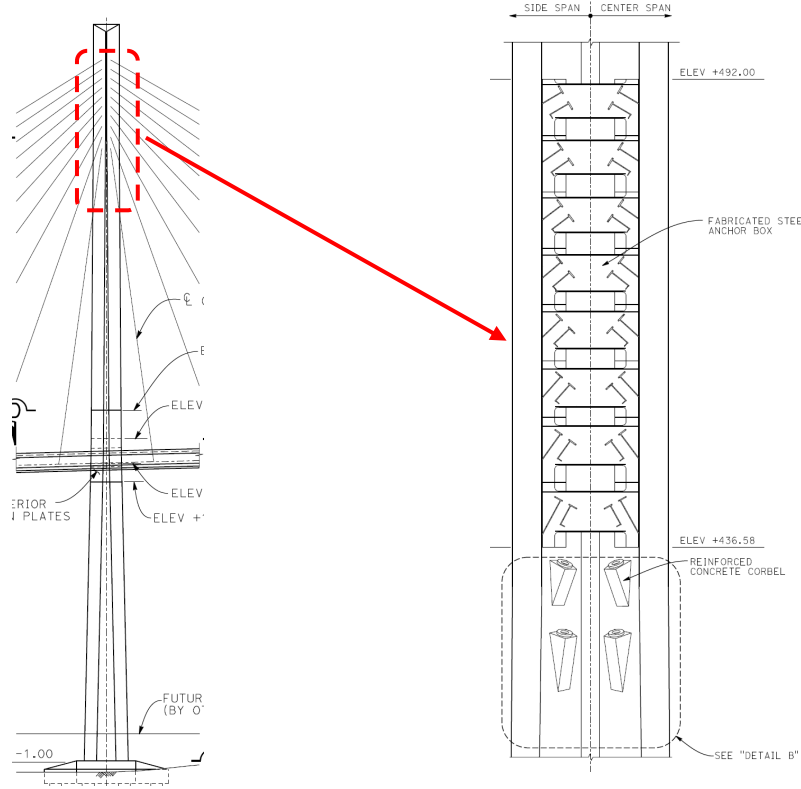


Figure 4.3. Stay cables' connection to the tower (left) and a close view of steel anchor boxes and concrete corbels (right) (Source: structural drawings supplied by the Caltrans).

The superstructure of the Gerald Desmond Bridge features a structural steel-floor system. This system comprises two lines of longitudinal box-shaped edge girders, which are connected to variable-depth transverse floor beams. The floor beams frame into the edge girders, providing

support to the deck. Additionally, four lines of longitudinal steel stringers span between the floor beams, further reinforcing the overall system. The floor system supports 10"-thick precast concrete deck panels, positioned on top of the floor system, which serve as the bridge's deck pavement. To enhance the longitudinal strength and stability of the deck, it is post-tensioned using bonded internal tendons. The combination of the structural steel-floor system, longitudinal box-shaped edge girders, transverse floor beams, longitudinal stringers, and precast concrete deck panels with post-tensioning creates a robust and resilient superstructure for the bridge. Figure 4.4 shows an aerial view of the bridge deck during construction where all the noted members are exposed.

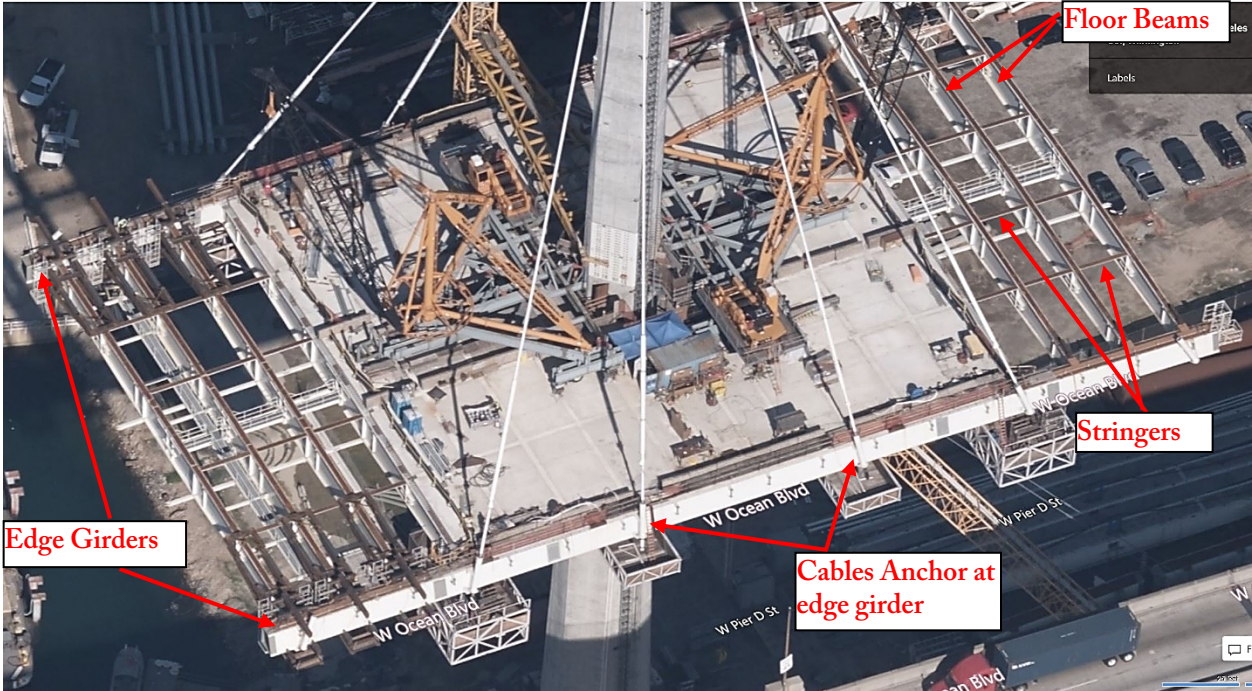


Figure 4.4. Aerial view of the bridge deck framing including girders, floor beams, stringers, and cable anchorage (Source: Bing map bird's-eye view).

At the end-bents of the bridge, a custom-designed expansion joint was incorporated to accommodate the significant movement that occurs during large-amplitude earthquakes. The expansion joints, also referred to as *swivel* joints, are capable of accommodating displacements of up to 70+ inches in the transverse direction and 62+ inches in the longitudinal direction. During large motions, sacrificial shear keys at the expansion joints will be activated. Furthermore, measures have been taken to control and dampen the extensive lateral sway of the bridge during a major earthquake. This is achieved through the use of six longitudinal and three transverse viscous dampers at each tower, as well as two longitudinal and two transverse dampers at each end-bent, as depicted in the instrumentation drawings in Chapter 5. These dampers play a vital role in dissipating seismic energy and reducing peak-displacement motion of the bridge in both longitudinal and transverse directions. It is important to note that the viscous dampers remain

inactive until a significant earthquake occurs, maintaining a rigid connection between the deck, towers, and bent joints during smaller motions caused by loads such as traffic loads and wind.

The overall health of the bridge relies heavily on the condition of its critical elements, as described above, which are responsible for transferring loads from the superstructure to the foundation. Here is a simplified description of the bridge load-path: The dead loads of the bridge deck, as well as the loads from traffic, wind, temperature, etc., are transmitted from the reinforced concrete pavements to the steel stringers and then to the floor beams. These floor beams, in turn, transfer the loads to two parallel steel edge girders that run along the bridge on the north and south sides. The vertical load effects on the edge girders are supported by the stay cables, which are connected to the side of the girders at equal intervals as depicted in Figure 4.2. The stay cables are further connected to the reinforced concrete towers through steel anchorage boxes and corbels that are embedded within the hollow towers. The vertical and lateral loads exerted on the cantilevered towers by the stay cables are then transmitted to the deep foundations of the towers. Figure 4.4 provides a closer look at the deck, girders, floor beams, and cables. The monitoring strategy presented in this study will target these critical elements along the load path and aims at utilizing the existing wired accelerometers installed on the bridge by CGS.

## 4.2. Codes and Guidelines for the Design of Bridges and Their Maintenance

This section provides a brief overview of the main load types used in the analysis of bridge structures, as well as the LRFD design procedure, including design-limit states and the load-rating process for structural members. The information presented in this section is primarily sourced from two codes: the AASHTO LRFD Bridge Design Specifications (2020 edition) and the Reference Manual for Load and Resistance Factor Design (LRFD) for Highway Bridge Superstructures (FHWA-NHI, 2015). Additionally, there is a brief commentary on the design and maintenance practices of the Gerald Desmond Bridge in this section.

There are various types of loads that can affect a bridge structure. These loads are classified according to design codes into categories such as permanent loads, transient loads, wind loads, earthquake loads, and temperature loads. Permanent loads encompass the dead loads of the structure, including the weight of girders and slabs. On the other hand, transient loads consist of live loads and dynamic allowances, represented as a percentage of the design live-load, applied to the bridge. The transient load includes different truck models, such as HL-93 (AASHTO LRFD Design, 2020). The design of the bridge considers transient loads at three different levels: design loads, legal loads, and permit loads, each corresponding to a specific loading model.

Wind loads are taken into account for each exposed element of the bridge individually and for the bridge as a whole. These loads reflect the local wind conditions specific to the area where the bridge is designed. To ensure its stability, the design considers both horizontal and vertical wind forces (e.g., pressure or suction) acting on the structure. The uniqueness of the Gerald Desmond Bridge required a special wind-tunnel study to be performed. The testing was performed in three

aerodynamic study phases. The first phase focused on wind-tunnel testing of a sectional model and a wind-buffeting analysis. The second phase of testing was focused on the aeroelastic model, and in phase three, stay-cable wind-induced vibration and pedestrian comfort were investigated. The extensive wind-tunnel tests conducted on the bridge yielded valuable insights into the effects of wind-induced pressure and vibration. These tests helped to minimize uncertainties and improve design engineers' understanding of the bridge's response under different wind load scenarios.

According to the AASHTO bridge design code, the seismic performance goal of bridge structures aims for seismic resistance within the elastic range of the structural components, with minimal damage during small to moderate earthquakes. Specifically, bridges located in Zone 4, including southern California, are subjected to special seismic analysis, as stated in the AASHTO LRFD Bridge Design. The goal is to ensure that the bridge can withstand seismic forces and maintain its serviceability during small and moderate events, providing a safe passage for vehicles. The seismic load is considered the most important type of load for the design of the Gerald Desmond Bridge but achieving the performance goals noted earlier was a challenging task. This is because the bridge is situated in a region that is relatively close to two faults. The Palos Verdes fault zone is located approximately 3.1 miles west of the bridge, while the Newport-Inglewood fault zone is approximately 3.8 miles east of the bridge. The proximity of these faults to the bridge highlights the importance of considering large seismic activity in the design. The design engineers implemented a concept to seismically isolate the cable-stayed main span bridge from the east and west approach bridges. This approach involved the use of swivel joints, as explained earlier, along with the installation of longitudinal and transverse viscous dampers at the intersection of the deck and towers. Additionally, viscous dampers were employed at the joint connecting the end approaches (refer to Chapter 5 for a plan view of the dampers). These measures are aimed at enhancing energy dissipation during significant seismic events and minimizing the peak response amplitude, such as displacement, of the superstructure. Site-specific earthquake motions were simulated, and a finite element model of the bridge was created to analyze the nonlinear response of the bridge subject to those earthquake excitations. Large earthquake motions were used to assess the safety of the bridge in terms of the degree and location of its damage (Barzak, 2020). As noted above, most bridge elements sustain small to moderate damage during the rare case of a large earthquake event, while isolated areas, not critical to the stability of the bridge, may experience significant damage.

In addition to the loads mentioned earlier, there are several other loads considered in the design of a bridge structure. One such load is the pedestrian load, which accounts for the weight and movement of pedestrians on the bridge. This load is typically calculated based on the expected density of pedestrians and their anticipated actions while using the bridge. Temperature loads are also taken into account, including both uniform and gradient temperature loads. Uniform temperature load considers the thermal expansion and contraction of the bridge components due to changes in ambient temperature. Gradient temperature load accounts for the temperature differences across the bridge, which can cause thermal gradients and resulting stresses and moments. Bridges on the west coast of the US are more susceptible to temperature gradient load.

Moreover, the friction forces due to moving objects, such as vehicles or other dynamic loads, are also considered. These forces arise from the interaction between the bridge surface and the objects moving across it.

Once the load types and their intensities have been determined, structural analysis is performed to evaluate the load effects on various structural elements of the bridge. The Load and Resistance Factor Design (LRFD) procedure, specified by the American Association of State Highway and Transportation Officials (AASHTO), is commonly used for designing bridge elements. The LRFD procedure is based on the principle that the combination of factored loads, known as the *Limit States* in LRFD, must not exceed the capacity or resistance of the material multiplied by a resistance factor that is less than one. This approach ensures a sufficient level of safety by accounting for uncertainties in load estimation and material behavior.

The LRFD procedure incorporates various *limit states* (i.e., factored load combinations) to evaluate the performance of the bridge structure. These limit states include the Service Limit State, Fatigue and Fracture Limit State, Strength Limit State, and Extreme Event Limit State. Each limit state encompasses multiple load combinations specific to its respective requirements.

The Service Limit State, including four different load combinations, considers the long-term performance of the bridge under normal service conditions, ensuring that the structure remains functional and meets the specified serviceability criteria. The Fatigue and Fracture Limit State evaluates the potential for fatigue and fracture in the structural elements due to cyclic loading under relatively large stresses. According to AASHTO LRFD Article 3.6.1.4., “*For the fatigue and fracture limit state, failure means that crack growth under repetitive loads exceeds the limitations established by AASHTO to prevent fracture during the design life of the bridge.*”

The Strength Limit State verifies the structure’s capacity to resist the applied loads, ensuring that the elements have adequate strength and do not experience failure or excessive deformation under load combinations that are probable during the design life of the bridge. On the other hand, the Extreme Event Limit State addresses the behavior of the bridge under rare and severe events such as major earthquakes, collision by a vessel, or strong winds, ensuring that the structure can withstand extreme forces without loss of structural integrity. Bridge engineers assess the bridge design by checking and satisfying all the limit states and their corresponding load combinations specified in the LRFD procedure.

In addition to rigorous nonlinear analysis of the bridge model in a finite element software, a separate three-dimensional finite element model of the “as-built” structure was created by the design engineers for the purpose of evaluating the *load ratings* of bridge elements under various load combinations (i.e., limit states), as well as under extreme events. The load rating factors are calculated according to equations and multipliers outlined in the AASHTO Manual for Bridge Evaluation (MBE, 2018). A rating factor greater than one indicates an acceptable design. For the load rating calculation, the finite element software MIDAS Civil was employed. This software

provided the necessary tools and capabilities to perform accurate and comprehensive load-rating analyses. Specifically, the following structural elements were evaluated for their load rating of the bridge: (1) stay cable anchorage, (2) stay cables, (3) steel edge girders, (4) floor beams and PT deck slab, and (5) framing at the end bents. Detailed results for load ratings and corresponding analytical models were reported to stakeholders.

Detailed review of the analytical models, design goals, and load ratings are out of scope of this study. In this report, we focus on monitoring the response of the structure, as is, and aim to detect anomalies in its critical elements' response using our proposed instrumentation framework. It is noteworthy that documents such as structural drawings and members' load ratings were supplied by the project sponsor conditioned upon a non-disclosure agreement, which does not permit sharing detailed information about the analysis and design findings of the project. For this project, the as-built bridge is being considered for deploying the bridge health monitoring network. If the proposed framework in this study was to be considered for implementation on the physical structure, a detailed analysis of the digital-twin finite element model would be essential. The analyses would involve evaluating the model under all relevant load combinations (i.e., limit states).

### 4.3 Existing Monitoring System on the Bridge and Recorded Response During Carson's 2021 Earthquake

The California Strong Motion Instrumentation Program (CSMIP)<sup>2</sup> of the California Geological Survey (CGS) was established to collect, pre-process, and distribute earthquake ground motion and structural-response data. The data is collected by instruments that CSMIP deploys on select structures, such as buildings, dams, and bridges. Over 80 bridges have been instrumented by CSMIP, and their vibration data during local earthquake events are disseminated to engineers and seismologists. Acceleration data is the common type of response parameter collected by the agency and distributed to stakeholders and researchers.

The new Gerald Desmond Bridge was among the critical structures that has been instrumented by the CSMIP (Station No. 14703) in 2021. The instrumentation was funded via an interagency agreement between the California department of transportation (Caltrans) and the CGS. Sensors deployed on the structure include 62 accelerometers placed on the deck, towers, foundation cap, and part of the bridge's east approach. Also, 12 accelerometers were deployed at reference ground and borehole (i.e., underground) locations. Compared to other bridge instrumentation projects by the CSMIP, this is considered a relatively large number of accelerometers. It is noteworthy that the accelerometers are part of a *wired* monitoring network.

Figures 4.5 through 4.8 illustrate the placement and orientation of the sensors on the main span of the bridge. As shown in the figures, the majority of the accelerometers are placed at the deck level, adjacent to the edge girders, while other sensors were placed at the top of the towers and the

---

<sup>2</sup> <http://www.conservation.ca.gov/cgs/s mip>

foundations. The red arrows indicate the direction of measurement, and the number next to each arrow indicates the recorder channel number.

Just a few months after the installation of the accelerometers, the Carson earthquake of 2021 was recorded at this station. The agency only made available the processed data of 19 channels (out of 62), likely due to the very small amplitude of the recorded response. The provided channels are channel No. 44 through channel No. 62. These channels are mainly located at the east end of the main span and the east approach of the bridge. In this section, we will provide a brief overview of the recorded acceleration responses as well as their Fourier spectra for illustrating the modal characteristics of the bridge.

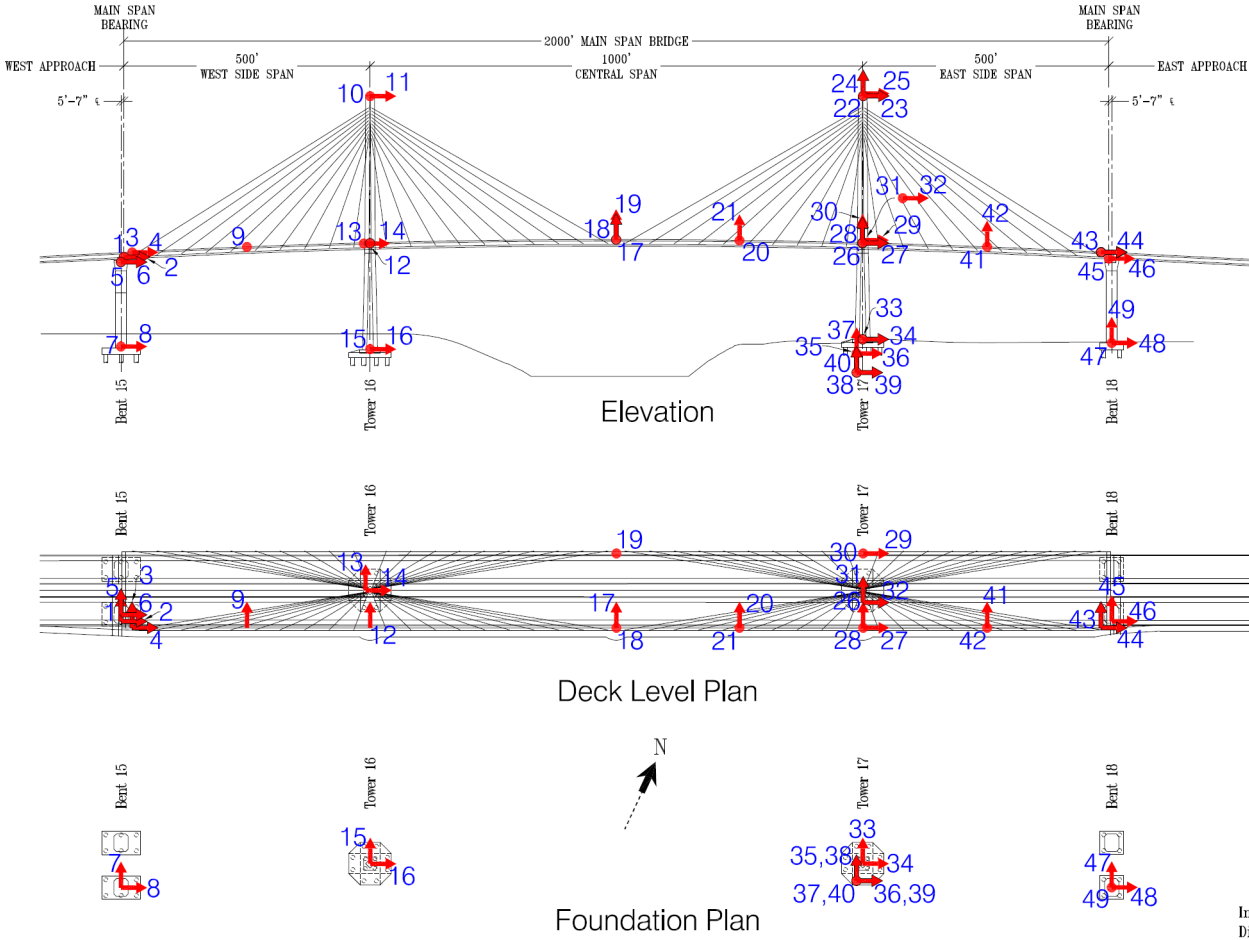


Figure 4.5. Existing Accelerometers layout on the main-span of the bridge – CSMIP station 14703 (source: <https://www.strongmotioncenter.org>).

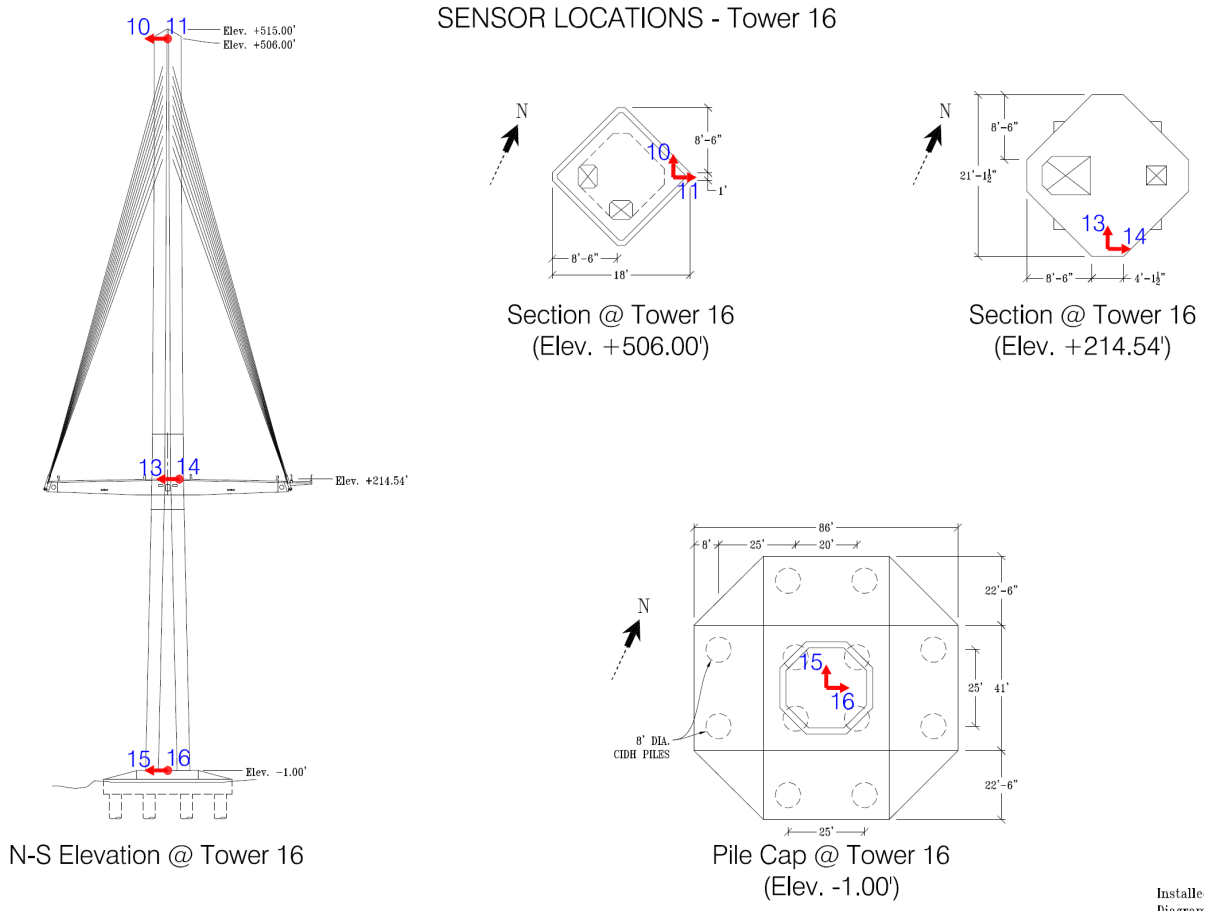


Figure 4.6. Placement of existing accelerometers on the West Tower – CSMIP station 14703 (source: <https://www.strongmotioncenter.org>).

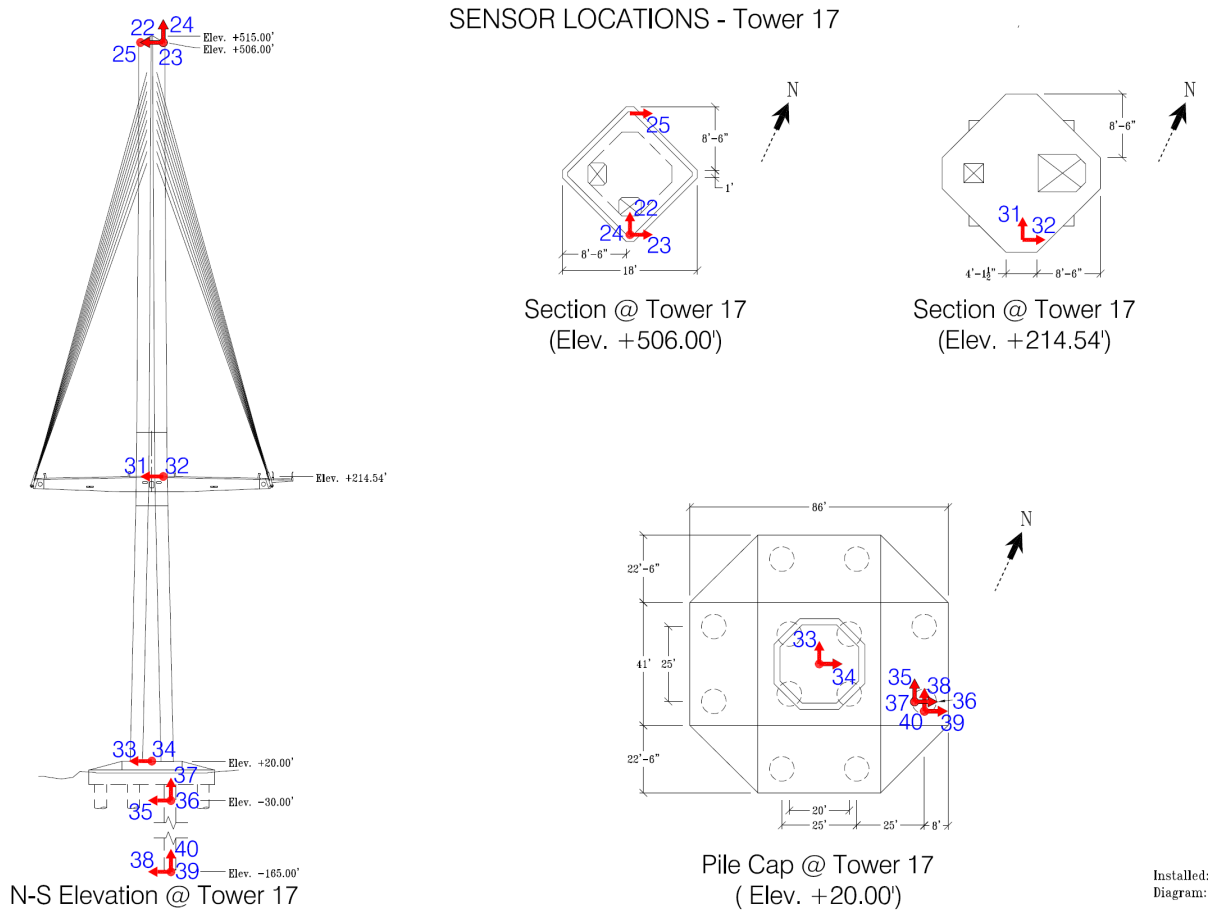


Figure 4.7. Placement of existing accelerometers on the East Tower – CSMIP station 14703 (source: <https://www.strongmotioncenter.org>).

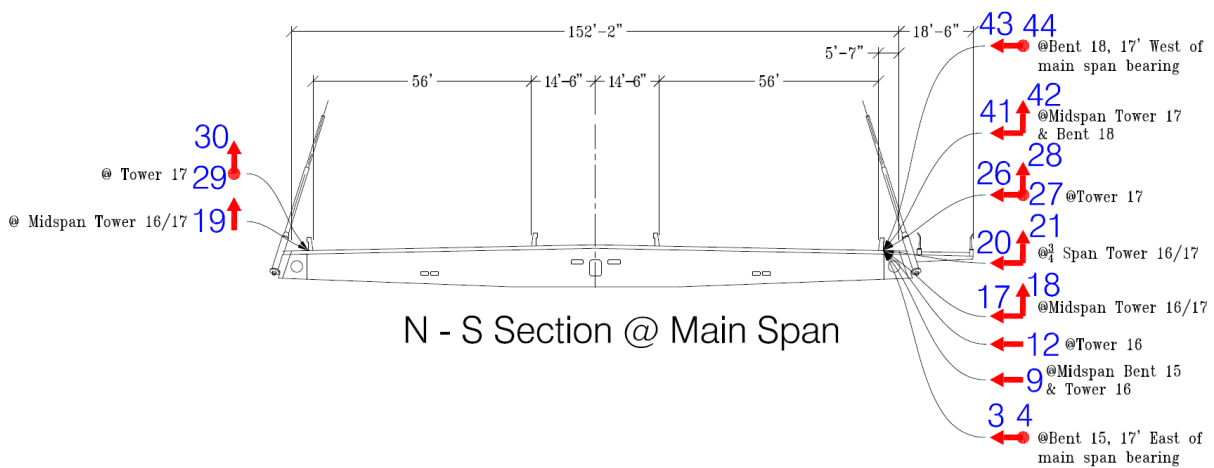


Figure 4.8. Cross-section view of the placement of existing accelerometers on the edge girders – CSMIP station 14703 (source: <https://www.strongmotioncenter.org>).

On September 17, 2021, a small earthquake event occurred in Carson, Los Angeles, with a magnitude of 4.3. Although not as powerful as some of the region's larger seismic events, the earthquake still shook structures in its proximity and triggered their monitoring systems, including the recorders installed on the Gerald Desmond Bridge. Figure 4.9a shows the epicenter of the earthquake on a ShakeMap generated by the California Geological Survey. The map has color contours indicating the shaking intensity in the vicinity of the earthquake epicenter. The Gerald Desmond Bridge is located about 8.4 km to the south of the epicenter, as depicted in Figure 4.9b.

Recordings for channels No. 44 through No. 62 were made available to the public by CSMIP. Among these channels, only channel No. 44 is located on the cable-stayed main span deck, recording acceleration in the longitudinal direction (along the bridge). Other sensors are located on the east approach deck, which is the adjoining box-girder reinforced concrete bridge to the east of the main span. Among them, channels No. 45, 46, and 50, located at the start of the east approach, are of interest for our review. In addition, there are accelerometers located on the foundation of the Bent 18 located at the joint between the main span and the east approach.

Figures 4.10 and 4.11 present recorded acceleration and estimated displacement response on the bridge deck and foundation level in longitudinal and transverse directions, respectively. Overall, the bridge acceleration and displacement response are very small (less than 5 millimeters displacement in each direction), indicative of the weakness of the shaking at the site. In addition, the plots for displacement show a larger movement of the bridge in the transverse direction compared to its longitudinal direction, indicating a higher rigidity in the longitudinal direction. The recorded response could provide valuable information about dynamic characteristics of the bridge, including its modal frequencies of vibration and its mode shapes. The former can be observed through investigating the bridge response in the frequency domain using the Fourier transform (FT).

Figure 4.12 illustrates the FT for the longitudinal deck response (top) and the foundation pile-cap response (bottom). To help identify the fundamental modes of vibrations, the power spectral density (PSD) for the same responses is presented in Figure 4.13. The PSD is a function of the square of the FT, which provides better emphasis as to where the potential modes of vibration are. Note that only channel No. 44 is located on the main span (i.e., the cable-stayed steel bridge). The small excitation amplitude of the bridge, its high longitudinal rigidity, along with multiple coupled modes of vibration, such as the vertical, longitudinal, transverse, and torsional motions, make it difficult to identify the modal frequencies for longitudinal motion. As shown by the red arrow in Figure 4.13, 2.3 Hz is one of the bridge's longitudinal modes of vibration. The FT and the PSD were calculated for the transverse response as well.

Figures 4.14 and 4.15 show the results. It can be seen that the transverse response provides a better indication of the modal frequencies in the transverse direction. A long period mode of vibration at  $f = 0.6$  Hz is evident in Figure 4.15. Other modes of vibration can be seen at 1 Hz and at 3.2 Hz, though it should be further investigated if these modes belong to transverse motion of the bridge

or are due to coupling effects from other motions such as vertical or torsional. This cursory review of a few channels provides valuable information about dynamic characteristics of the bridge. Data from more channels could help increase the certainty of the identification results and the accuracy of detecting changes to these global characteristics of the bridge. It is noteworthy that the example presented herein provides insight into the global response of the bridge, not its specific elements. In other words, the localization of anomalies remains a challenge to be addressed in the instrumentation framework discussed further in Chapter 5 of this report.

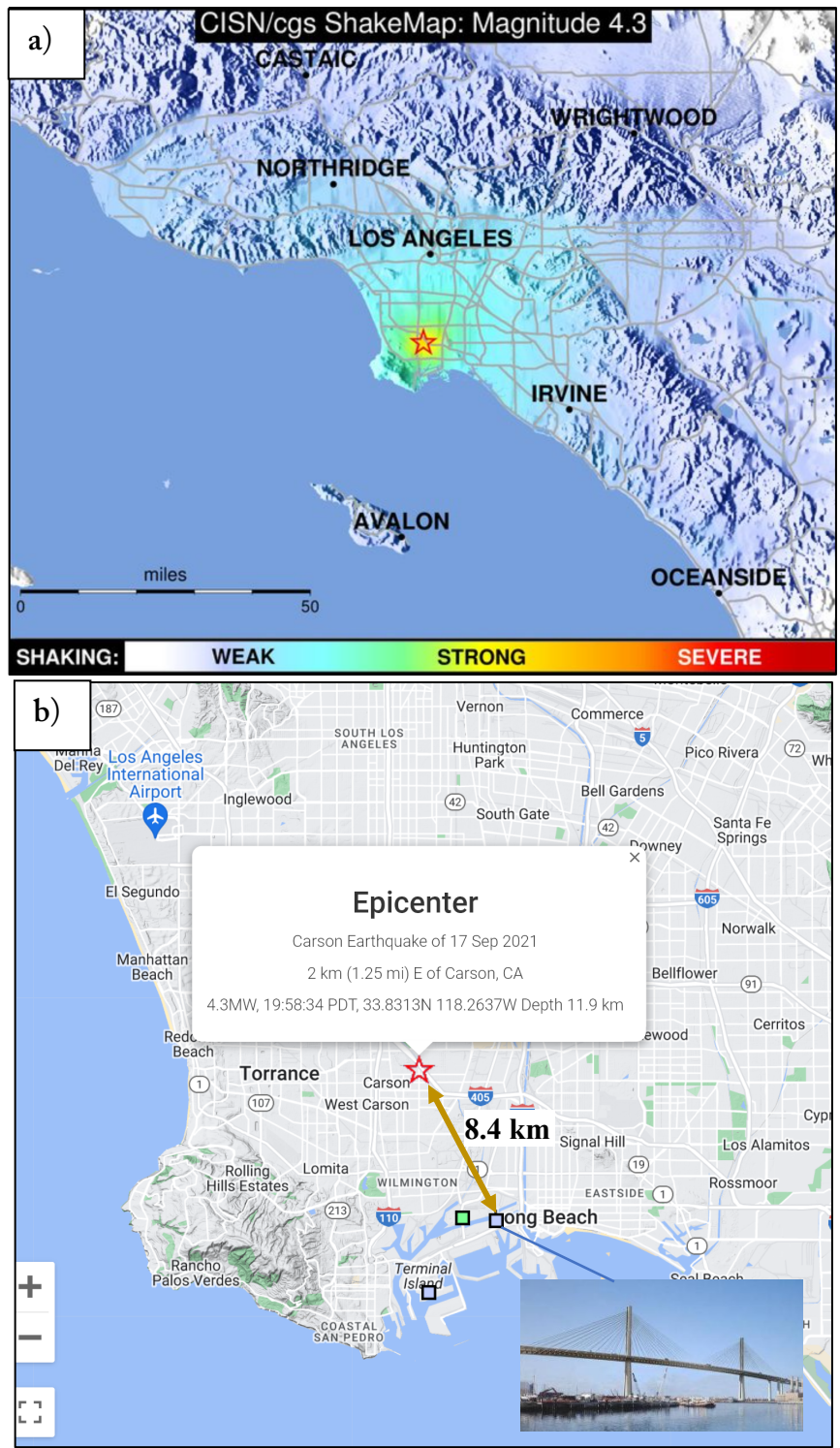


Figure 4.9. ShakeMap of the Carson 2021 earthquake and the shaking intensity contours a). Location of the earthquake epicenter relative to the bridge b). (source: <https://www.strongmotioncenter.org>).

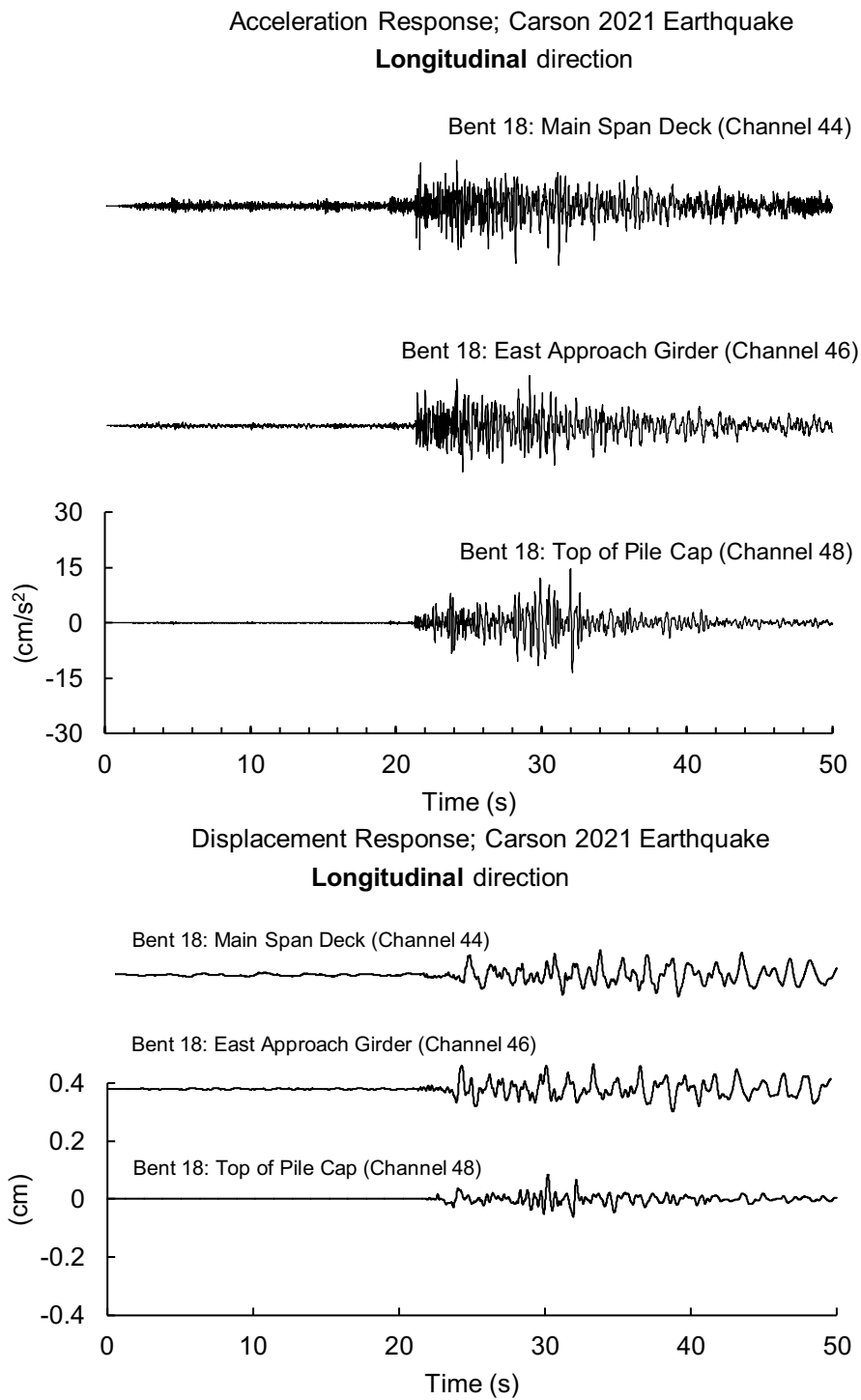


Figure 4.10. Recorded acceleration and estimated displacement response on the bridge deck and foundation level during Carson 2021 earthquake. The recorded motion is in longitudinal direction (i.e., along the bridge).

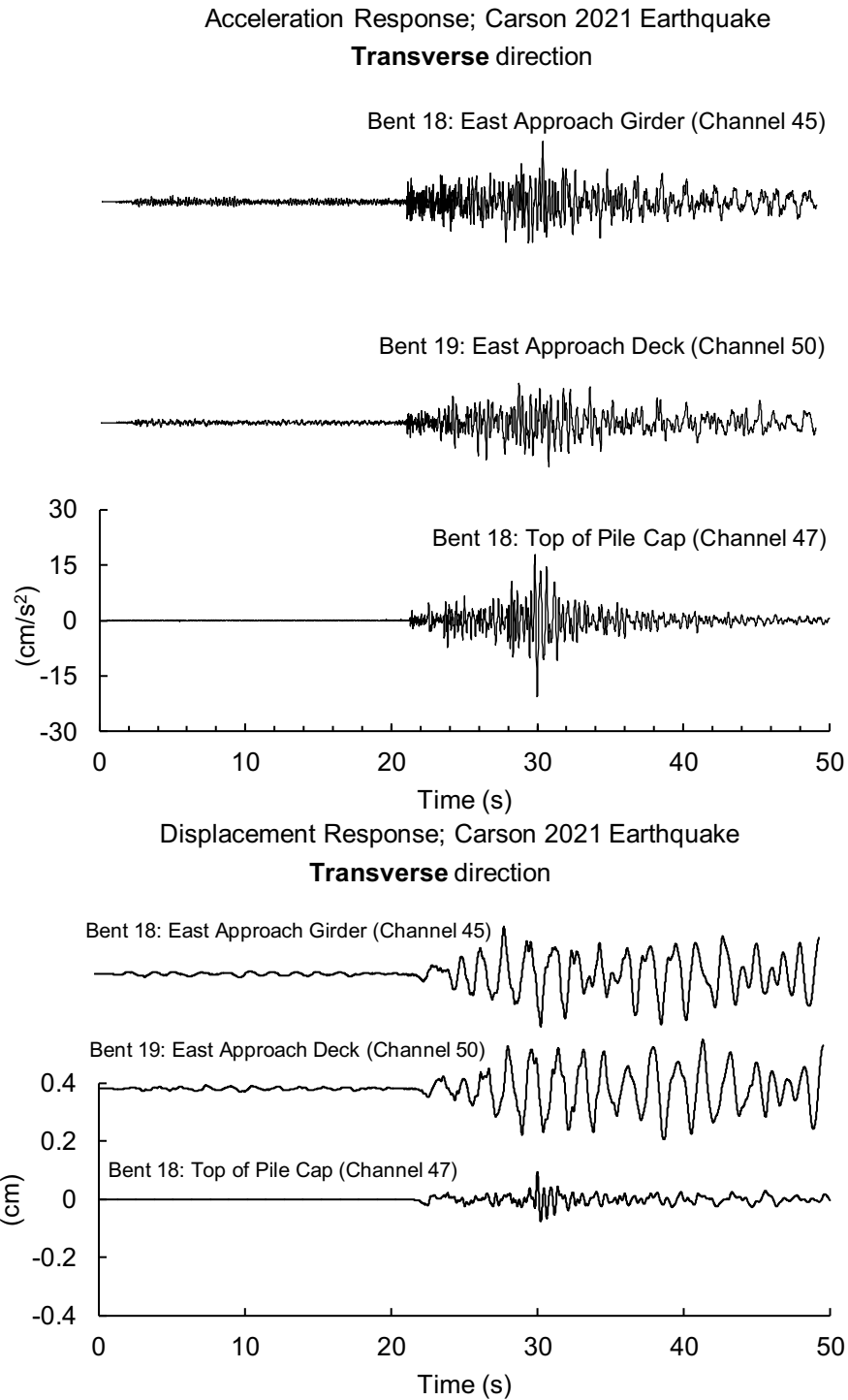


Figure 4.11. Recorded acceleration and estimated displacement response on the bridge deck and foundation level during Carson 2021 earthquake. The recorded motion is in transverse direction (i.e., perpendicular to the bridge).

Fourier Transform (FT) amplitudes of accelerations response  
Carson 2021 Earthquake

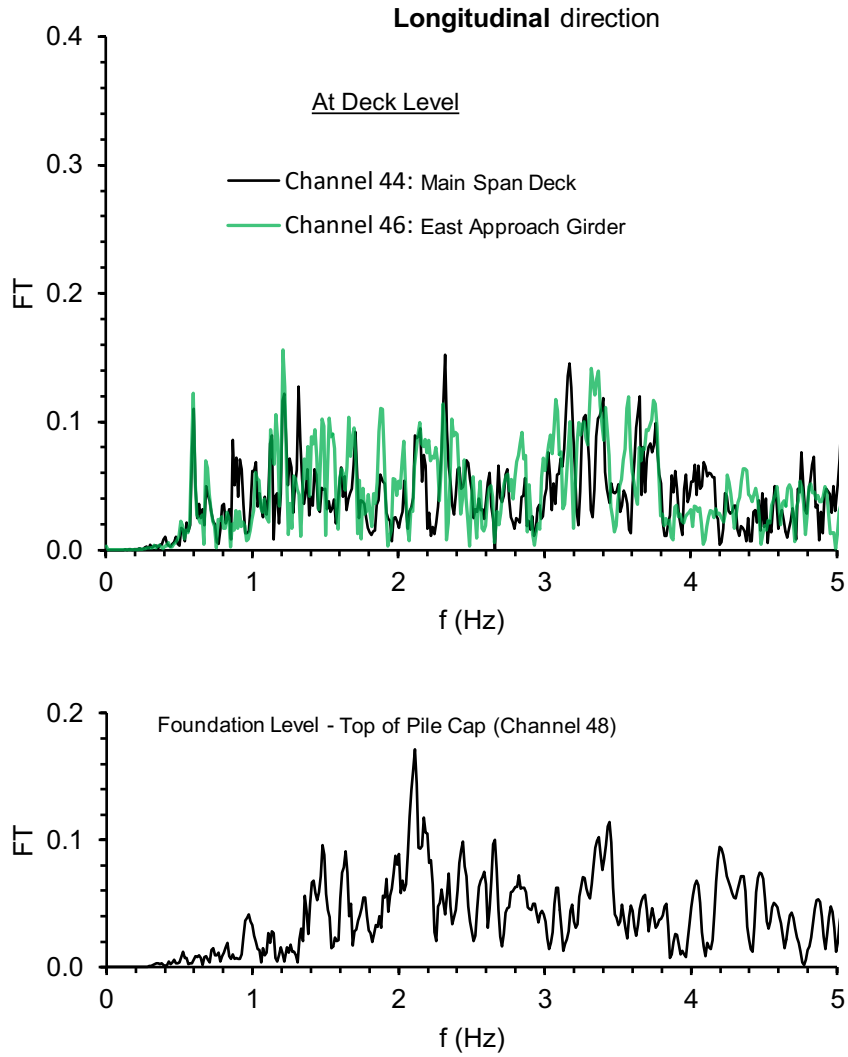


Figure 4.12. Fourier transform amplitudes (FT) of acceleration response at the deck level (top) and foundation level (bottom) along the longitudinal direction.

Power Spectral Density (PSD) of accelerations response  
Carson 2021 Earthquake

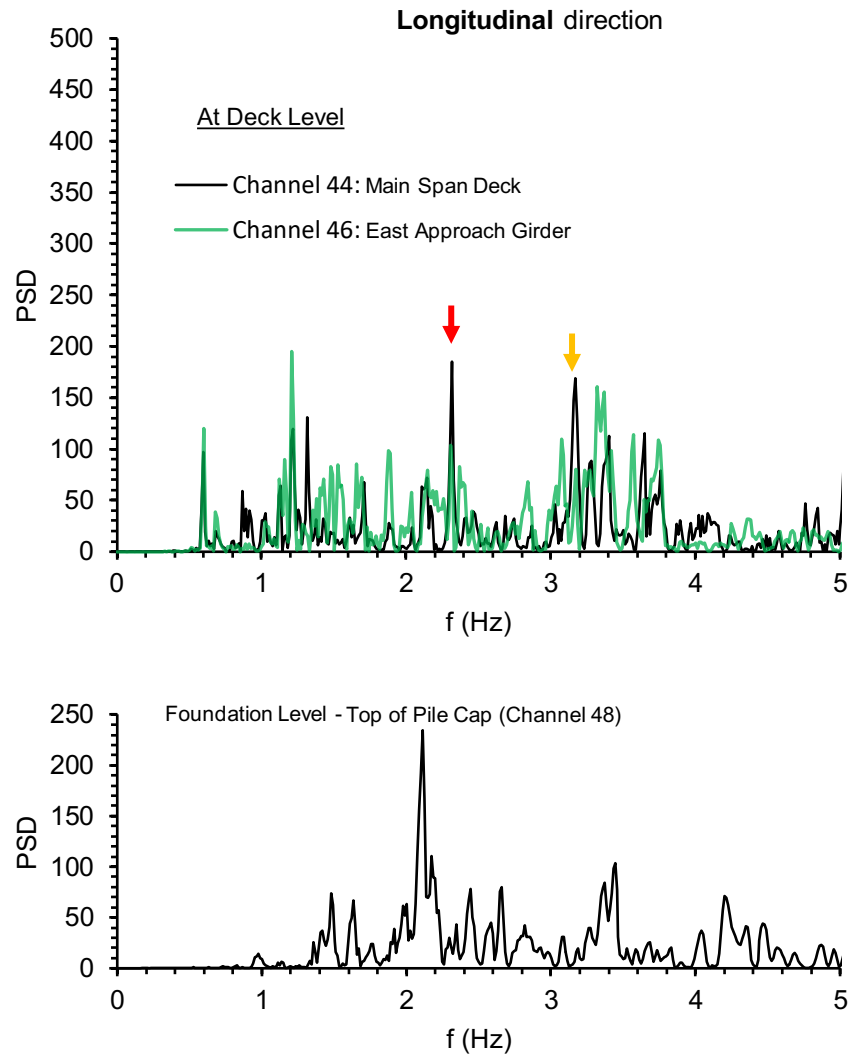


Figure 4.13. Power Spectral Density (PSD) of acceleration response at the deck level (top) and foundation level (bottom) along the longitudinal direction.

Fourier Transform (FT) amplitudes of accelerations response  
Carson 2021 Earthquake

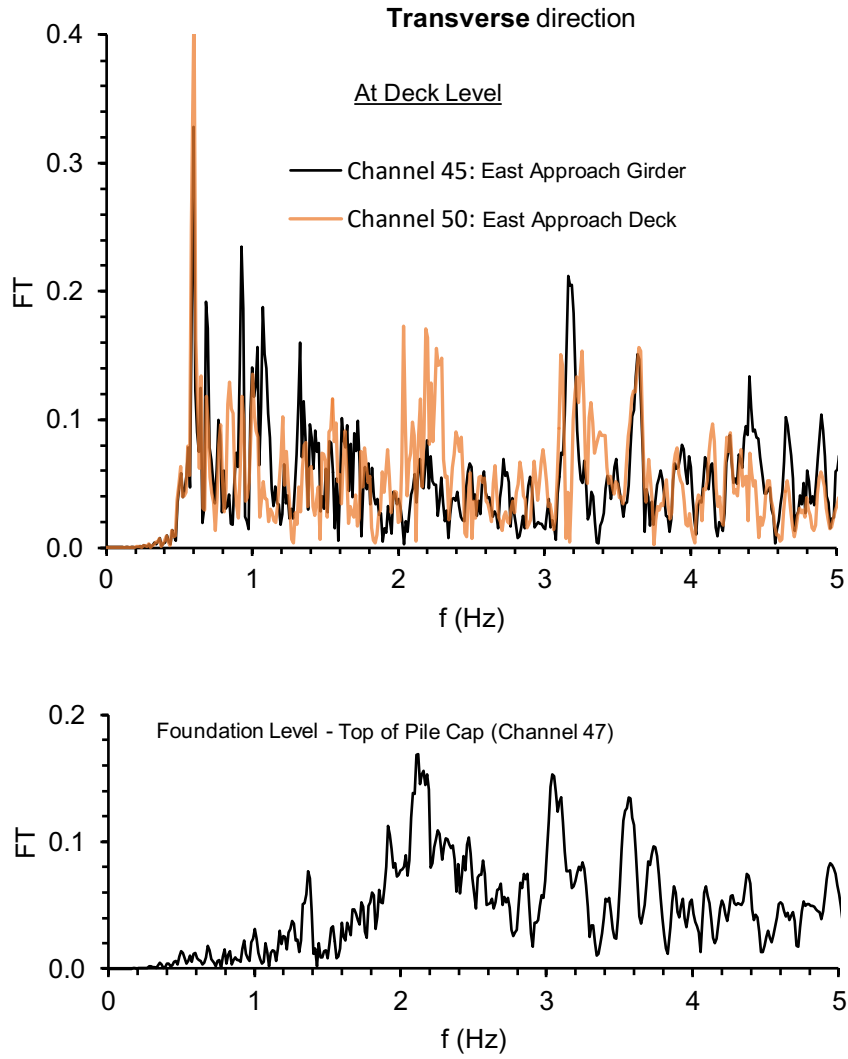


Figure 4.14. Fourier transform amplitudes (FT) of acceleration response at the deck level (top) and foundation level (bottom) along the transverse direction.

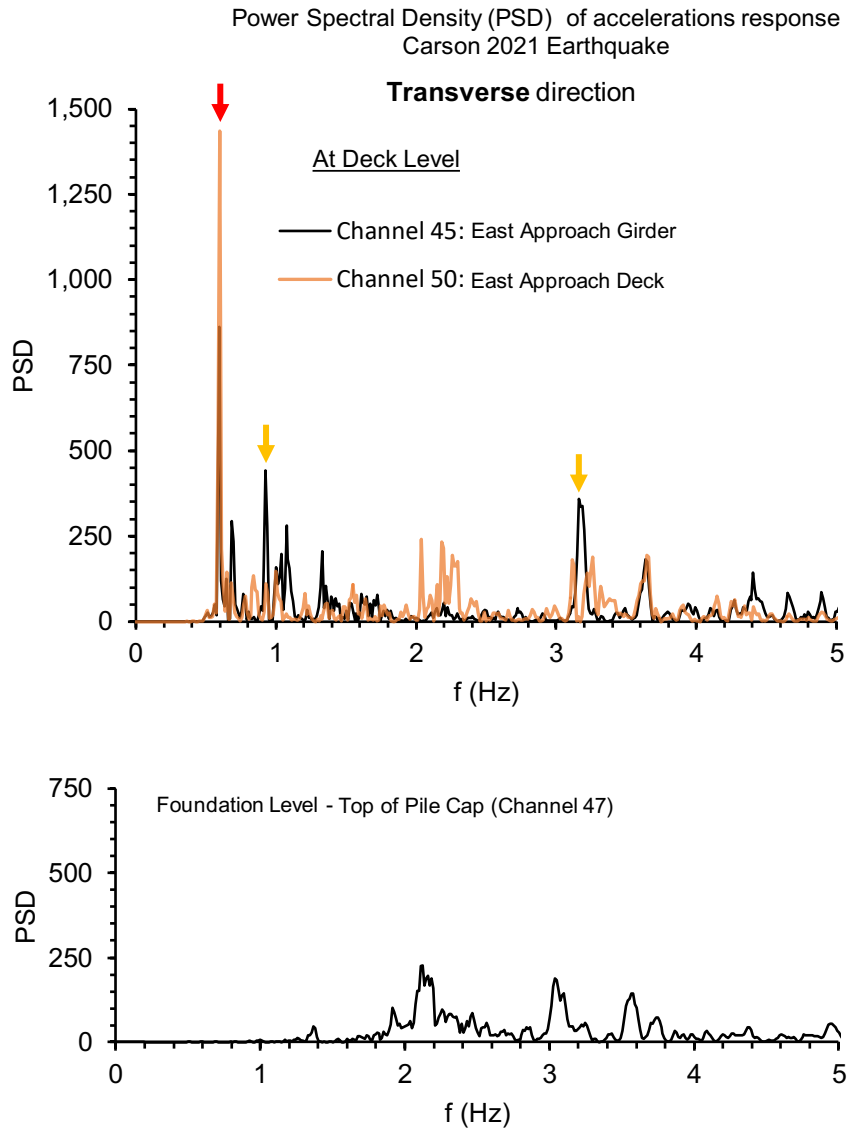


Figure 4.15. Power Spectral Density (PSD) of acceleration response at the deck level (top) and foundation level (bottom) along the transverse direction.

## 5. Proposed Instrumentation Framework for the Bridge

In prior chapters of this report, we extensively reviewed key factors in establishing a practical and reliable bridge health monitoring (BHM) system mostly through best practices and prior success examples. Some of these factors included identifying the critical elements of the bridge, determining the parameter of interest for the monitoring effort, selecting sensor types and acquisition equipment, durability of the network, and more. Moreover, for a long-span cable-stayed bridge, it is necessary to deploy a variety of sensor types in order to enable comprehensive monitoring, ensuring a more complete understanding of its condition. In this chapter, we begin by presenting a checklist encompassing all essential factors to be considered when designing a BHM system. Subsequently, we propose element-specific instrumentation for all critical components of the bridge.

### 5.1. Monitoring Strategy and Proposed Sensing Network

A health monitoring system for the new Gerald Desmond Bridge is proposed. Our strategy for design of the monitoring system stemmed from prior best practices and studies, design and analysis reports and drawings for the case-study bridge, as well as the latest monitoring technologies available for structural monitoring and condition assessment. In prior chapters, we provided a comprehensive review and discussion of different approaches, challenges, and solutions. In this chapter, we begin by presenting a brief checklist outlining the key requirements for establishing a reliable and resilient monitoring system for the long-span bridge. Next, we propose element-specific instrumentation and layout designs tailored to the critical elements of the bridge. These proposals aim to provide comprehensive monitoring coverage, though could also be implemented in stages. The essential requirements of the proposed system are as follows:

1) *Wireless Sensor Network*: Given the benefits of a wireless sensor network (WSN), particularly for large structures where deployment of a large number of sensors (i.e., a dense network) is necessary, a WSN is highly recommended. Other notable benefits include ease of installation and cost, as well as the flexibility to expand the network in the future. It is noteworthy that the bridge comprises a wired monitoring system, as discussed earlier, including over 60 accelerometers (refer to Section 4.3).

2) *Local Monitoring*: The sensing effort on the bridge could be either local (element-level response) or global (overall bridge response). The existing, relatively large, number of accelerometers on the bridge (Section 4.3) provide adequate information on the global dynamic characteristics of the bridge (e.g., modal frequencies). Hence, our proposed monitoring network primarily focuses on sensing the local response of the critical elements to complement the existing data. Local element response encompasses a range of parameters, such as strain, crack width, temperature, and tension forces.

3) *Dense and Scalable Network*: A dense instrumentation is essential for component level monitoring of the bridge, as it increases the reliability of inferred damages and provides data for inter-dependency analysis of adjacent elements and inference on damage-related anomalies as opposed to non-damage noises. In addition, the sensing network must be scalable such that it provides an option for adding more devices or replacing them in the future. It is noteworthy that dense networks could pose a challenge, as they produce large, collected data and increase the post-processing costs and consume energy due to large data transmission. This challenge is addressed by a decentralized sensing network as discussed further below.

4) *Network Security*: When designing a wireless network capable of transmitting data via the internet, cyber-security risks should be considered in the design of its data-management system. Approaches for ensuring security of the proposed sensing network are not discussed in this report but should be reviewed prior to the implementation of any real-time monitoring effort.

5) *Sensor Selection Considerations*: When selecting sensors for various sensing tasks, one should consider the sensors' technology (refer to Chapter 2), sensitivity, energy consumption, durability, noise level, ease of installation, and more. For instance, for strain measurement, FBG sensors offer favorable advantages in terms of measurement accuracy and durability. The sensor types included in the proposed network have been selected with careful consideration to maximize the system's effectiveness. It is important to note that in many bridge structures, invasive sensor installations involving pinning, welding, or bolting are not permitted. Therefore, the use of magnets or adhesives is recommended, which may influence the choice of sensors. Moreover, the need for battery replacements may arise frequently in a wireless sensing network. This need underscores the importance of accessibility and ease of installment of the selected sensors.

6) *Thermal Effect Compensation*: Temperature is a major challenge when it comes to recording and interpreting structural data. It can have an impact on the readings of sensors, necessitating the correction of data by simultaneously recording temperature data alongside the desired data, such as strain. Additionally, temperature variations can induce thermal stress on the structure, which complicates the recorded data and makes it challenging to identify anomalies in the structural elements.

7) *Fatigue Life Estimation*: The fatigue failure of crucial components in a steel bridge is a significant factor that must be taken into account in monitoring strategies. A key objective of the sensing network is to estimate the fatigue life of the fracture-critical element using strain data. To achieve this, strain gauges should be carefully attached to the sections of girders and anchor boxes that are susceptible to fatigue cracks. It is crucial to employ appropriate formulas, such as the rainflow cycle counting method discussed earlier, to estimate the fatigue life.

8) *Energy Saving and Harvesting*: Running out of battery power can be a major challenge for a wireless network. Therefore, both saving energy via reducing energy consumption and harvesting energy at the sensor nodes should be considered in the design of the network. Reducing energy

consumption could be done by (1) using low-consumption sensors, (2) designing event-triggered recording with sleep-mode capabilities, and (3) using at-node pre-processing and data condensation to reduce volume of transmitted data. On the other hand, harvesting energy using solar panels or small wind turbines at the sensor nodes could significantly help in recharging sensors' batteries and keeping their voltage at a desirable level. These measures greatly enhance system performance and resilience for long-term monitoring efforts.

9) *Corrosion Monitoring*: Corrosion is a substantial risk factor for steel members in bridges, particularly in marine environments characterized by higher humidity levels. To ensure comprehensive monitoring of the bridge, it is crucial to install corrosion and humidity sensors at specific steel elements.

10) *Cable Tension Monitoring*: The estimation of cable forces is a crucial aspect that should be addressed by the proposed sensing network. Due to the protection of cables with covers to prevent external impacts and vandalism, direct measurement of strain or forces on the elements is not feasible. Therefore, an indirect approach is required to estimate the tension of cables based on their vibrational response. The vibrational frequency of a cable can be used to calculate its axial tension, as there is a direct correlation between the two. Formulas for estimating cables' tension take into account various variables, including cable length, cable sag, density, flexural rigidity, and cross-section. It is important to note that longer cables have smaller load ratings (i.e., higher load demands) and should be prioritized for instrumentation and monitoring within the network.

11) *Deck and Towers' Displacement*: Accurately measuring the global displacement of a bridge deck or its towers presents a challenge but is essential for monitoring purposes. To address this, the use of Global Positioning Systems (GPS) can be employed. By installing a few GPS receivers on top of the towers and the bridge deck, the system can effectively monitor the global movement of the bridge, providing valuable data for a condition assessment of the bridge.

12) *Recording Ambient Vibration*: A suitable wireless sensor board, capable of accurately measuring low-amplitude ambient vibrations, should be used. This is crucial as ambient vibration data is valuable for periodic condition assessment and establishing baselines for monitored parameters.

13) *Wind Pressure and Induced Vibration*: Special attention should be given to wind load and wind-induced vibrations in the monitoring network design. To obtain precise measurements of wind speed, the use of ultrasonic anemometers is recommended. These sensors should be placed at the top of the towers, and ideally, at the deck level given the long span of the bridge.

14) *A Decentralized Data Acquisition*: Decentralized data acquisition and aggregation must be employed to improve the network's resiliency and lifetime. This decentralized system involves pre-processing the raw data and compressing it into smaller-sized files before transmission. By reducing the amount of data transmitted within the network, this approach conserves energy, thereby improving the monitoring system's lifetime and resiliency. Additionally, a decentralized

data-acquisition strategy allows for scalability, enabling the system to accommodate more sensors in the future.

15) *A Disaggregated Sensing Topology*: In order to effectively coordinate aggregated data from the entire network of sensors, and facilitate communication between individual sensors and the onsite base station, a hierarchical process is proposed. A cluster topology approach with decentralization at the cluster head and sensor nodes is proposed. In fact, the network is almost equally divided into four subnetworks (i.e., sensing clusters). Within each sensing cluster, the sensors communicate with their dedicated cluster-head sensor node, and further with a gateway node, which then transfers the data to the base station. The creation of subnetworks, or clusters, is motivated by the limited reception rate of wireless sensors over large distances, and this approach helps increase the number of responsive sensors. By implementing a hierarchical structure and utilizing cluster topologies, the coordination of data transmission and communication within the monitoring system is optimized, enhancing the overall performance of the network.

Figure 5.1 illustrates the proposed wireless sensor network for the Gerald Desmond Bridge. As discussed earlier, the network is divided into four sensing clusters. Each cluster encompasses a group of sensors attached to bridge elements and sending their data to a cluster head-node, located at the center of the cluster to maximize reception from the sensor nodes. The head nodes transfer the data to gateway nodes located at the deck level near the west and east towers. The gateway nodes transfer the data to two separate base stations located on the top of the pile caps (i.e., tower foundations). To enhance the resiliency of the system, it is recommended to employ two base stations. The base station plays a crucial role in the network, having two of them provides redundancy and improved reliability. It is important to locate these base stations in easily accessible and safe locations, ensuring they are free from excessive movement and vibration. This will enhance the overall stability and functionality of the monitoring network.

Table 5.1 summarizes the proposed sensor types for each critical element of the bridge. Additionally, in this chapter, we provide detailed information on the layout of sensors on various elements. This includes sensor-specific identification names for the entire sensing network, which helps in the proper identification and organization of sensor data.

Table 5.1. Recommended sensor types for monitoring the critical elements of the bridge

Critical Element	Proposed Sensor Types
Stay Cables	Accelerometer, humidity sensor
Edge Girders	Fiber Optic Strain Gauge, Accelerometer, Displacement Transducer, Tiltmeters
Towers	Accelerometer, Tiltmeter, Fiber Optic Temperature Sensor, Anemometer, GPS sensor
Anchor Boxes	Fiber Optic Strain Gauge, Fiber Optic Temperature Sensor, Corrosion Sensor, Humidity sensors,
Deck	Anemometer, GPS
Viscous Dampers	Displacement Transducer, Fiber Optic Temperature Sensors

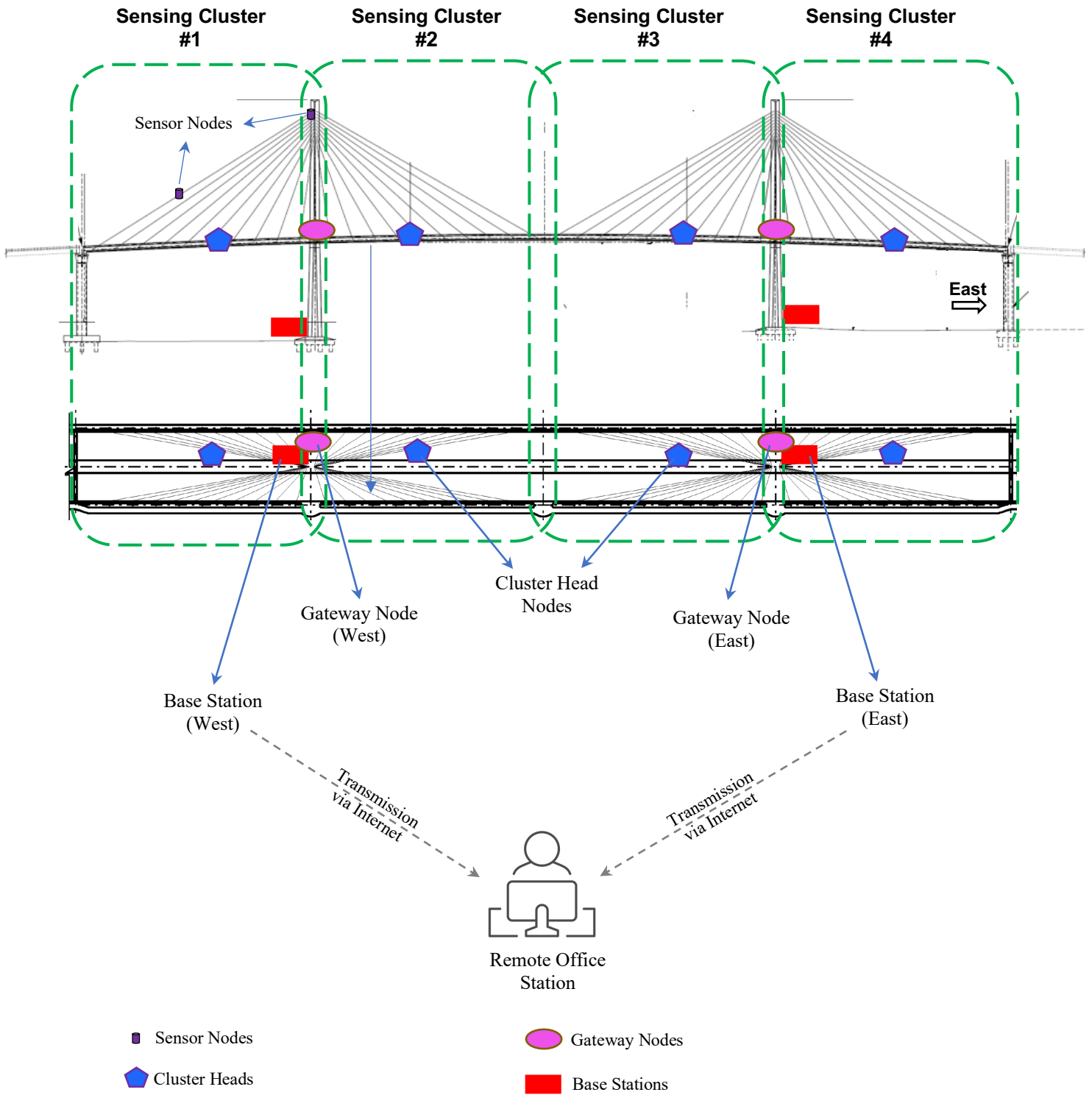


Figure 5.1. The proposed wireless sensors network topology for the Gerald Desmond Bridge.

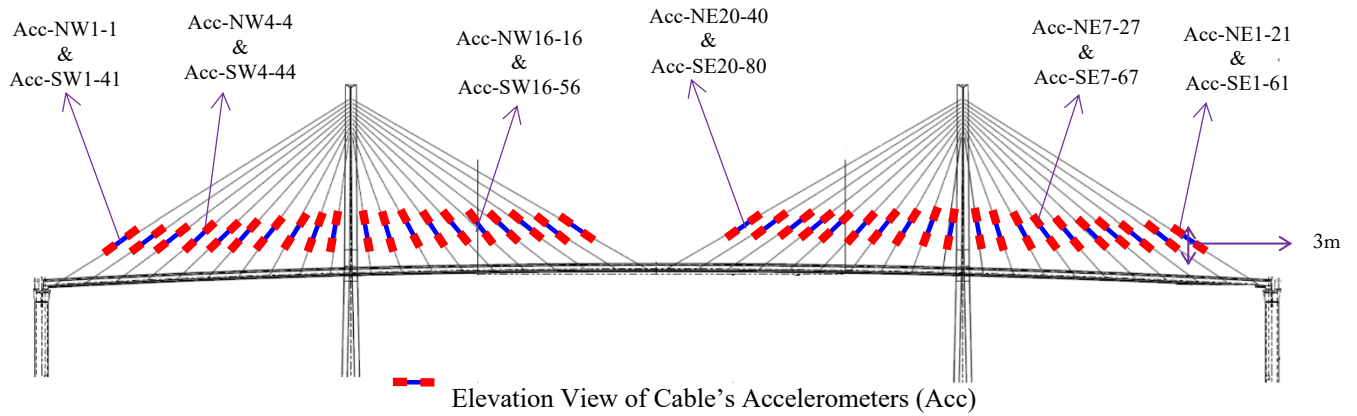
## 5.2. Recommended Sensor Types, Placements, and Naming Conventions

In this section, a detailed set of drawings are provided in order to illustrate the recommended sensor types and their placements on critical elements of the bridge. The choices were made according to the key factors for implementing a resilient and reliable monitoring network, as well as best practices discussed in previous chapters. The drawings also include naming conventions for each type of sensor and the critical element they sense (refer to Table 5.1). After all element specific layouts are presented, a comprehensive summary table including all recommended sensor types, sensor IDs, and their constituent subnetwork will be provided.

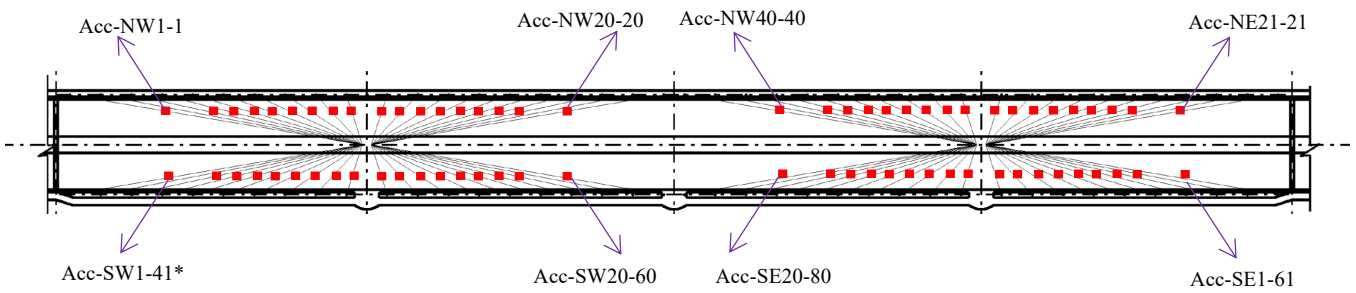
The drawings also incorporate naming conventions for each type of sensor and the critical element they are designed to monitor. Following the presentation of element-specific sensor layouts, a summary table will be provided. This table will include all recommended sensor types, their corresponding sensor IDs, and the respective subnetwork they belong to, serving as a comprehensive reference for the entire sensing network.

### 5.2.1. Stay Cables' Sensors and Sensors Placement

The cables in a cable-stayed bridge are among most critical elements of the structure, ensuring the structure's stability and integrity. In the recommended sensing network, all cables are included in the monitoring regime. There is a total of 80 stay cables on the bridge. The parameter of interest for cables' response is the cables' acceleration (i.e., vibration). Due to the use of covers to protect cables from external impacts and vandalism, direct measurement of strain or forces on the cables is not feasible. Therefore, an indirect approach is required to estimate cable tensions based on their vibrational response. Figure 5.2 shows placement of the accelerometers on the stay cables. The sensors should be placed at a height of about 10 feet (3 meters). This ensures ease of access for maintenance and replacement of batteries and parts, while keeping the sensors out of reach of pedestrians. The sensor names included in the drawing start with "Acc," which denotes an accelerometer, and are followed by the unique cables' ID. Depending on which quadrant the cable is located within, it receives a unique ID. For example, SW1 refers to the longest cable stretching towards the Southwest (SW). Note that longer cables have smaller load ratings (i.e., higher load demands) and should be prioritized for instrumentation and monitoring within the network. A bi- or triaxial accelerometer, lightweight and with lower power consumption, is recommended.



Elevation View of Cable's Accelerometers (Acc)



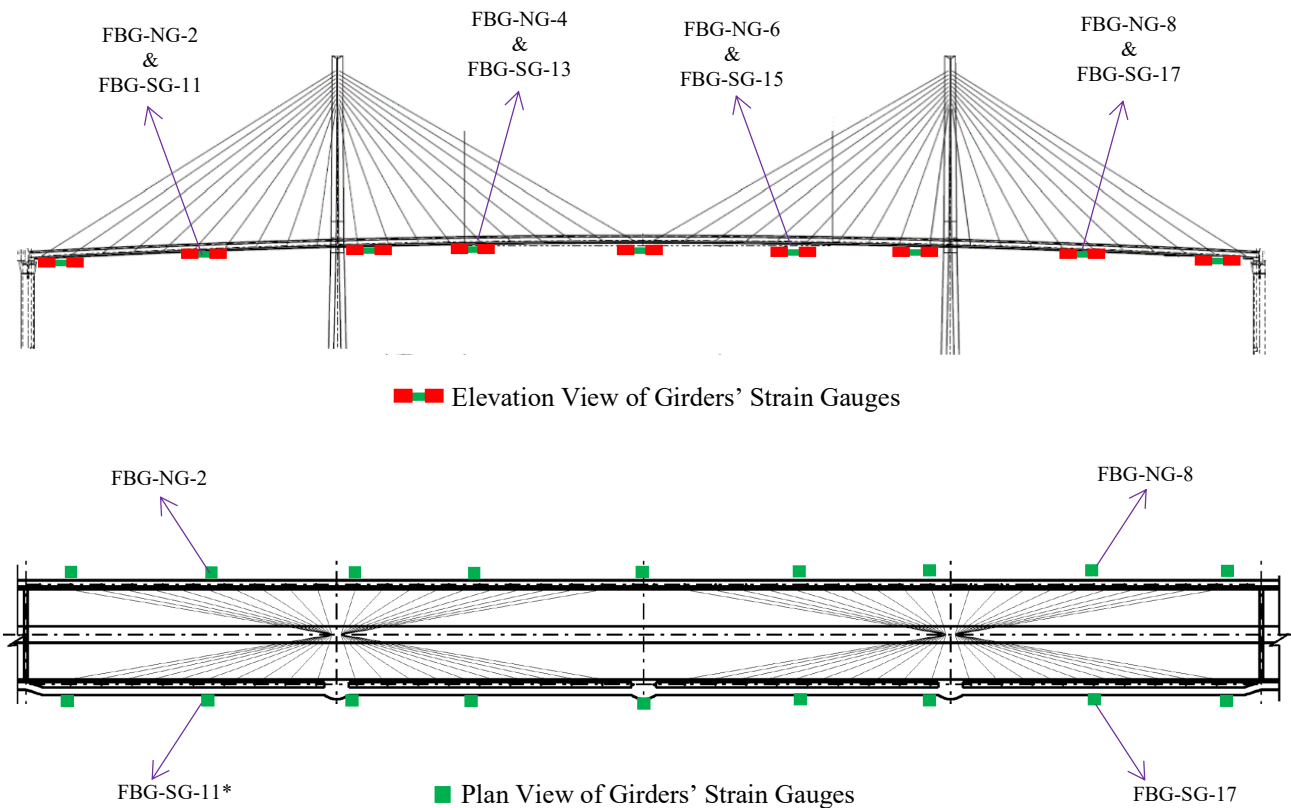
Plan View of Cable's Accelerometers (Acc)

\*Sensors' unique names are provided according to their cables' ID/name as:  
 "Acc-NW1/NE1-1 to 40" & as "Acc-SW1/SE1-41 to 80"

Figure 5.2 Recommended cables' accelerometers placement and naming convention.

### 5.2.2. Edge Girders' and Towers' Sensor Types and Placement

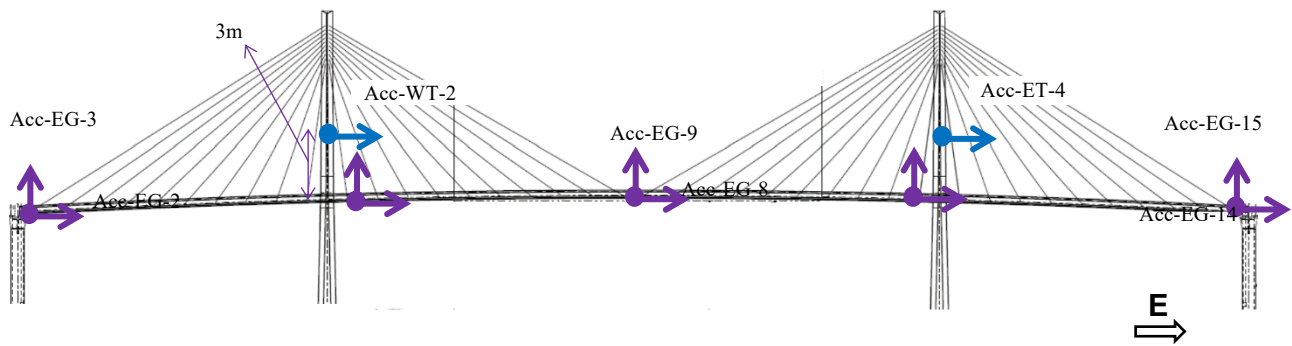
At the bridge deck, the steel girders are the most critical element to monitor, as discussed in Chapter 4. A set of Fiber Bragg Grating (FBG) strain gauges are recommended for monitoring strain, and subsequently stress, at the north and south girders. Figure 5.3 illustrates the placement of the strain gauges on the girders. It is recommended to place the sensors on the bottom flange of the girders where the most tensile stress is acting. A total of 18 FBG strain gages are recommended for girders.



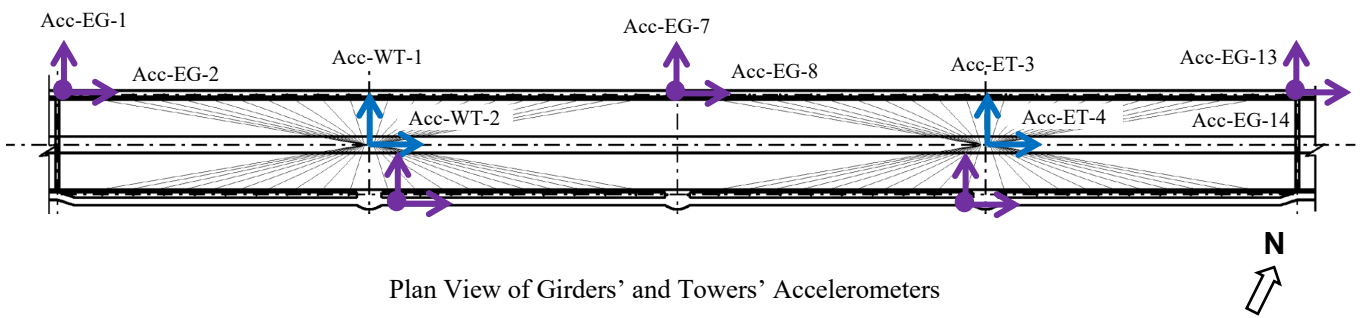
\*Strain gauges are assigned a unique name according to their locations and channel No. as:  
 “FBG-NG-1 to 9” placed on the North Girder (NG) & “FBG-SG-10 to 18” placed on the South Girder (SG)

Figure 5.3. Recommended placement for girders' strain gages and their naming convention.

A few accelerometers are recommended to be deployed on the girders and towers, as shown in Figure 5.4. As discussed in Section 4.3, the bridge comprises an existing network of 62 accelerometers deployed on the main span, east approach, and an underground geo array. The recommended accelerometers in Figure 5.4 will serve as a verification source for the existing network and will have the benefit of collecting and transmitting data shortly after an event, providing an opportunity to access real-time acceleration data. The sensors include five triaxial accelerometers (15 channels total) placed on the deck and two biaxial accelerometers (four channels total) placed on the towers.



Elevation View of Girders' and Towers' Accelerometers



Plan View of Girders' and Towers' Accelerometers

- Edge Girder Accelerometer direction  
 Acc-EG-1 to 15
- Tower Accelerometer direction  
 Acc-WT/ET-1 to 4

Figure 5.4. Layout of recommended accelerometers on girders and towers

The edge girders of the bridge were constructed by several splice joints along the bridge located at approximately 50 feet. Six LVDT sensors, three on each girder, are recommended to monitor the relative displacement at the splice joints, where large vertical deflections are expected. Figure 5.5 illustrates the location of these displacement transducers. One pair is to be installed at the center of the main span and the other two pairs to be installed at the center of the side spans.

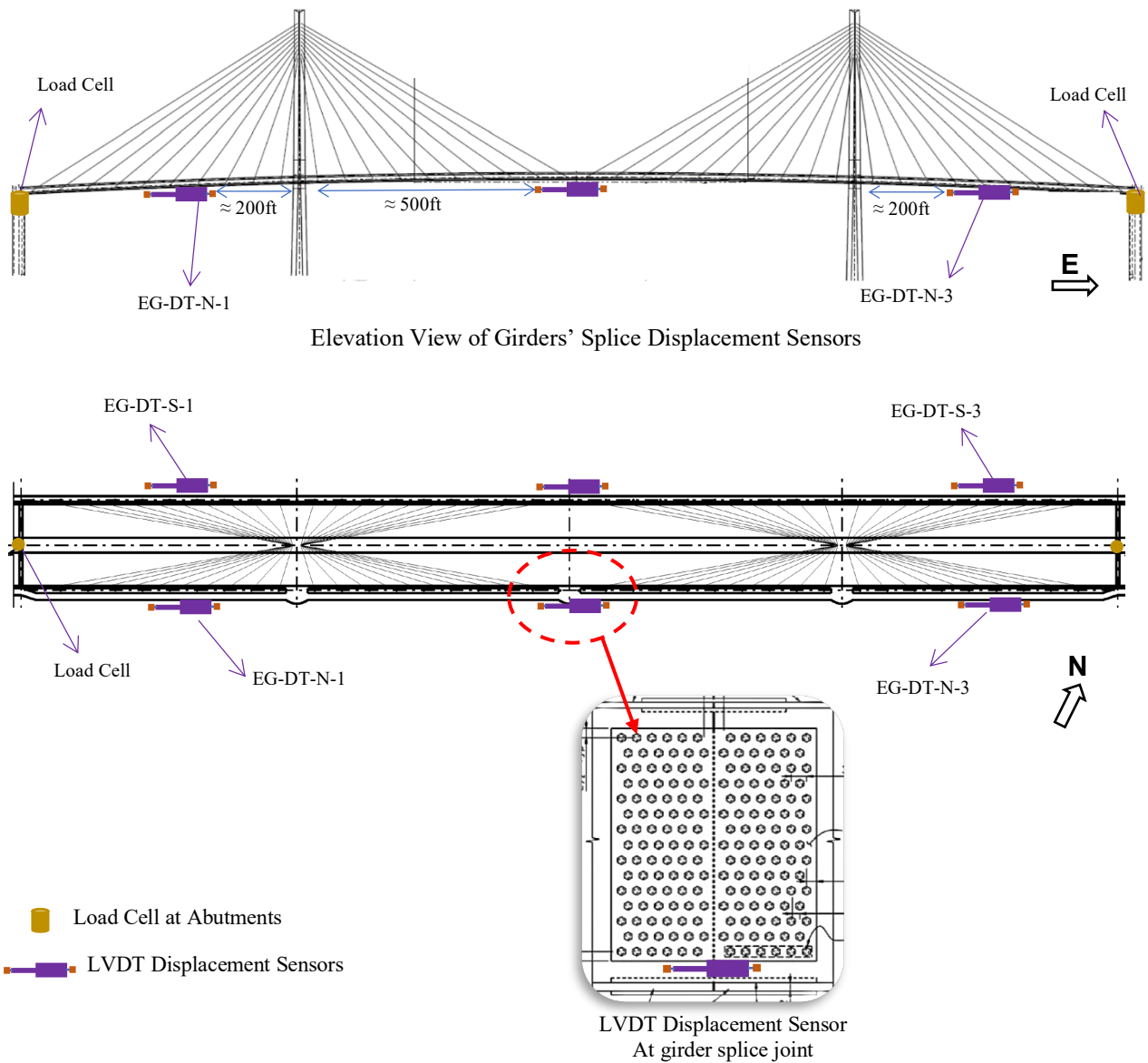
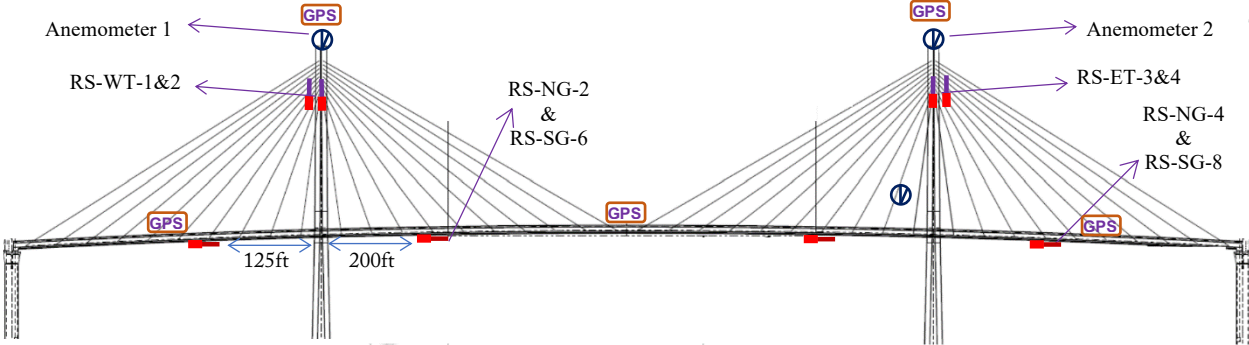
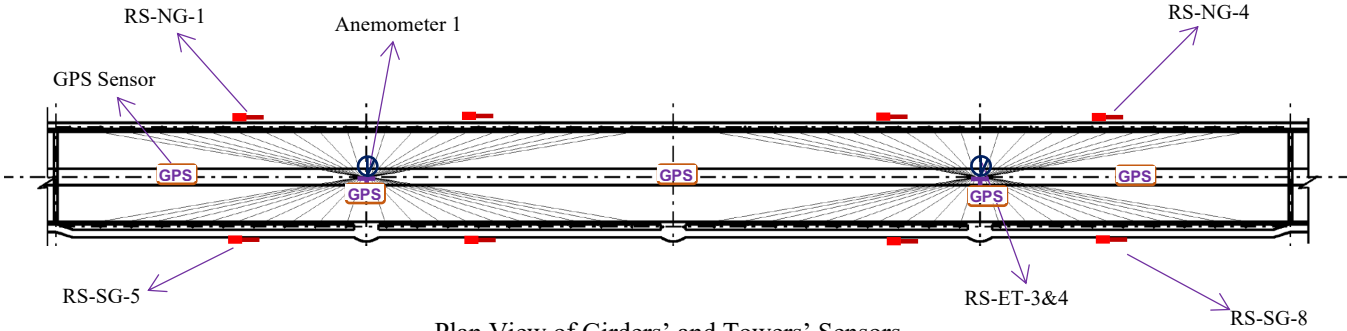


Figure 5.5. Displacement transducer at select girders' splice joints, and loadcells at the east and west bents.

Moreover, it is recommended to install two high-capacity load cells at the abutments on the east and west bents of the bridge. These loadcells will be instrumental in detecting the entry of overweight truck loads onto the bridge and in establishing a correlation between any significant response and the vehicular load. By monitoring the load at the abutments, potential overstress conditions or anomalies caused by heavy vehicles can be identified. Figure 5.6 presents additional sensing devices at the girders and towers. These include tiltmeters (rotation sensors), GPS displacement, and anemometer devices, as marked in Figure 5.6. The tiltmeters help with analyzing vertical deformation of the girders while the GPS will record lateral absolute movement of the deck.



Elevation View of Girders' and Towers' Sensors



Plan View of Girders' and Towers' Sensors

- RS-WT/ET-1 to 4 – Tiltmeters on Towers
- RS-NG/SG-1 to 8 – Tiltmeters on Edge Girders
- ⊙ Anemometer – Wind Speed and Direction
- GPS GPS Sensors at Deck and Top of Towers – Absolute Displacement readings

Figure 5.6. Tiltmeter, GPS sensor, and anemometer layout recommended for installation on the bridge girders and towers.

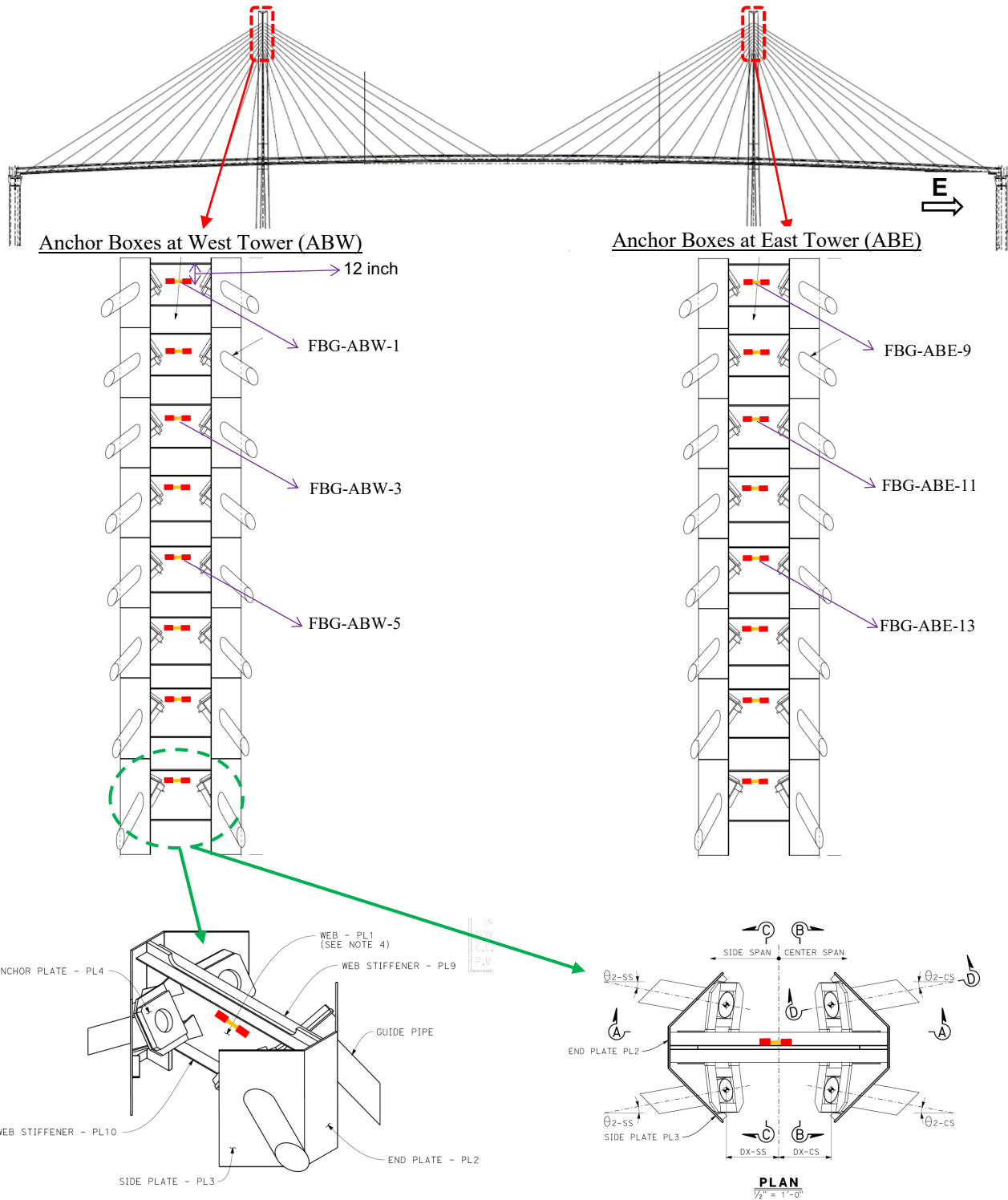
### *5.2.3. Towers' Anchor Boxes' Sensor Types and Layout*

The steel anchor boxes located at the bridge towers play a crucial role in securing the stay cables. Each anchor box accommodates four cables at the tower. It is important to monitor the strains and stresses at the anchor boxes as any cracking or failure in these steel boxes can lead to the breakout of a stay cable from the concrete wall of the tower and further cause bridge instability. Therefore, accurate and continuous monitoring of the anchor boxes is essential for ensuring the structural integrity of the bridge. Figure 5.7 illustrates recommended strain gages to be deployed on the steel anchor boxes. One FBG fiber-optic strain gage is recommended for each anchor box, installed near the top flange of their horizontal stiffener plates where tensile stress is the largest. The recorded strains could be further used to estimate the fatigue life of the steel boxes. Strain-gage readings could be impacted by temperature fluctuations inside the tower. Therefore, we recommend adding a few FBG temperature sensors at the anchor boxes or utilizing strain gages that include onboard temperature sensors. It is important to correct the strain readings for the ambient temperature for accurate assessment of the steel box's condition.

The anchor boxes are also susceptible to degradation caused by corrosion, especially in environments with higher humidity levels. As mentioned earlier, increased humidity near steel members can accelerate the rate of corrosion. Therefore, it is crucial to closely monitor the anchor boxes for any signs of corrosion. For this purpose, it is recommended to include two corrosion sensors at the anchor boxes on each tower. Figure 5.8 illustrates the location and naming of these corrosion sensors. In addition, one humidity sensor should be placed inside the tower, attached to the anchor boxes, while the other humidity sensor should be attached to the exterior face of the tower. This placement provides clues about the relative humidity between the inside and the outside of the upper segment of the tower.

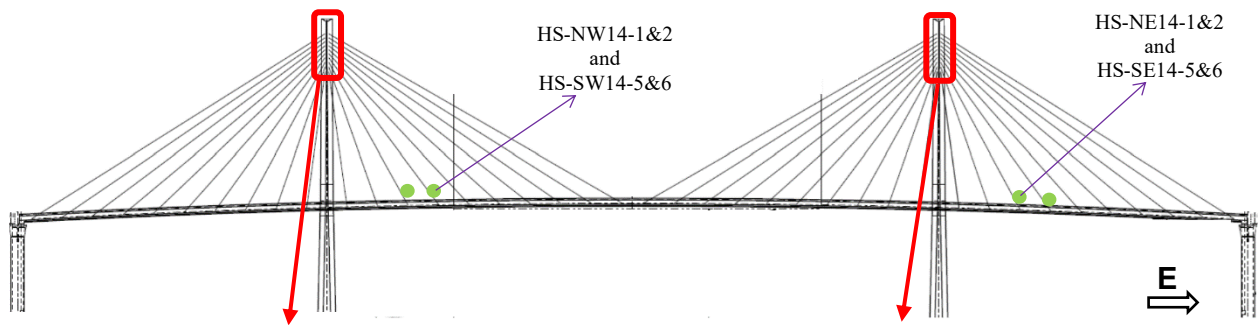
### *5.2.4. Viscous Dampers' Sensors Layout at the Bridge Deck*

The horizontal viscous dampers, connecting the deck to the towers and the bents, play a key role in dissipating seismic energy and reducing peak structural response of the bridge during a large earthquake event. Although these dampers were designed to remain inactive during service-level loads (e.g., traffic, wind, and small earthquakes), their health during a large event must be assured. It is recommended to install displacement transducers on some of the horizontal dampers in order to monitor their deformation over time. Figure 5.9 shows the layout and orientation of the recommended displacement transducers on the dampers. Any large reading at these sensors would indicate a large lateral movement of the deck, which ought to trigger an immediate inspection of the bridge.



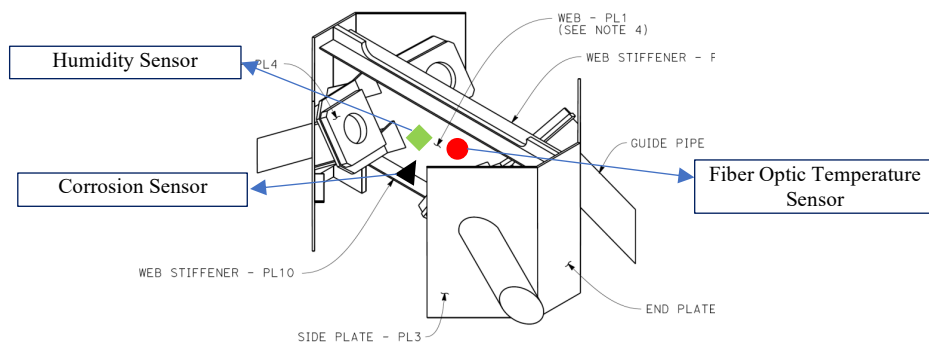
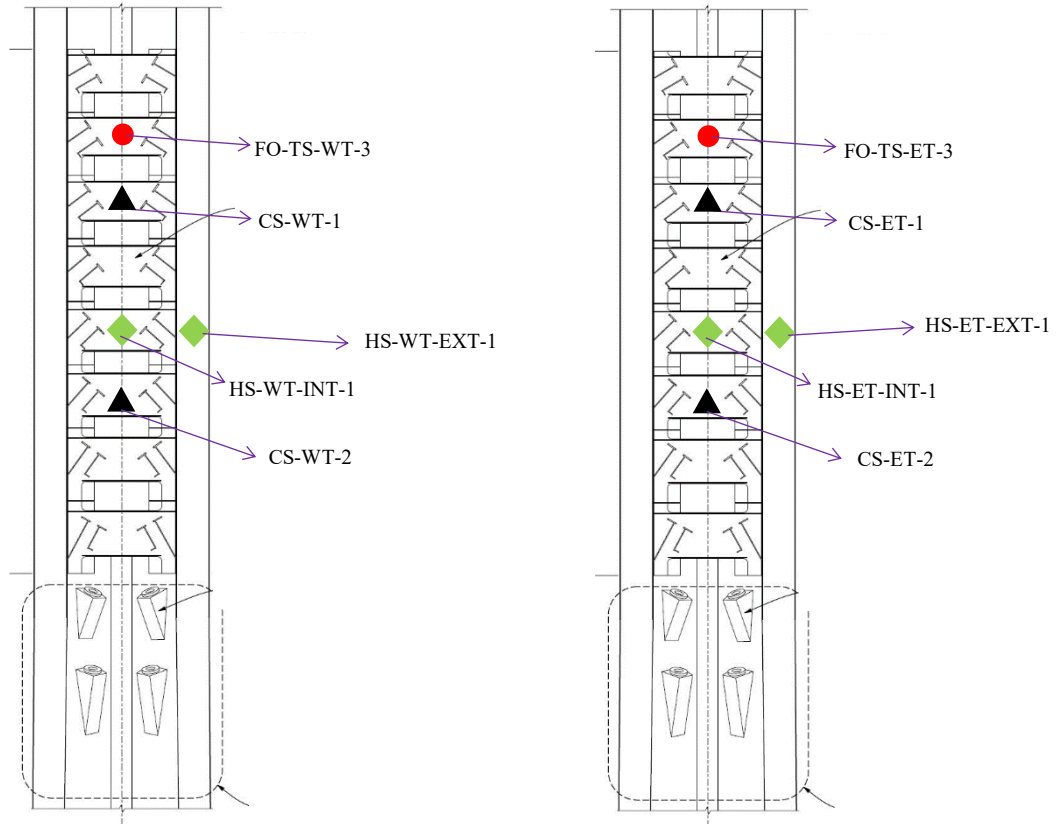
 Fiber Bragg Grating (FBG) Optical Strain Gage at Anchor Boxes (AB)  
 Sensors' unique names are as: FBG-ABW/ABE-1 to 16

Figure 5.7. Layout of FBG fiber optic strain gages recommended for the anchor boxes. The strain gages should be installed near the top flange of the stiffener plate.



Sensors on West Tower (ABW)

Sensors on East Tower (ABW)



◆ Humidity Sensors      ● Fiber Optic Temperature Sensors      ▲ Corrosion Sensors

Figure 5.8. Layout of corrosion and temperature sensors recommended at steel anchor boxes. Humidity sensors will be placed on the interior and exterior of the tower.

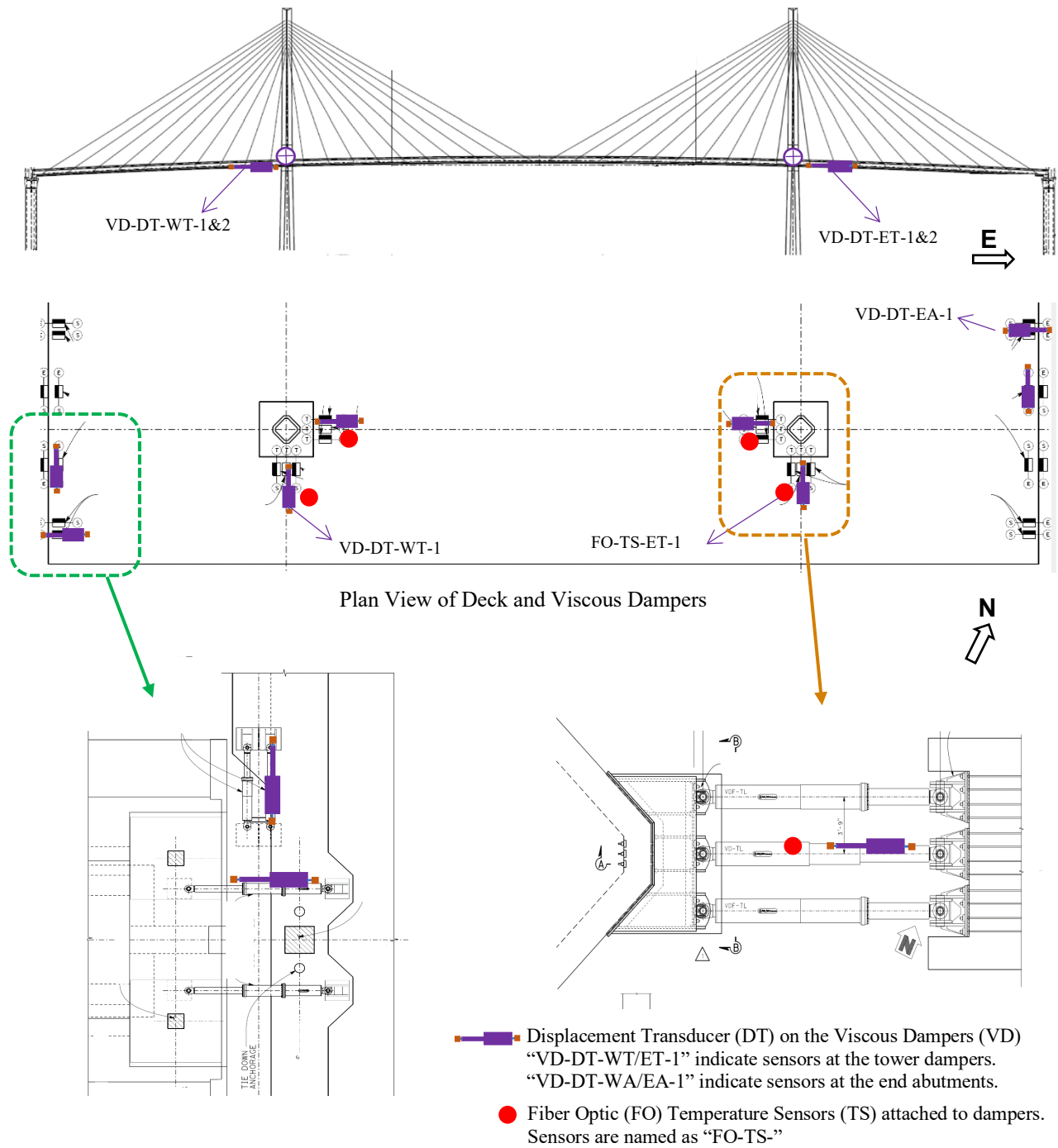


Figure 5.9. Displacement transducers for installation on the viscous dampers at deck.

### *5.2.5. Tabulated Summary of All Subnetworks, Their Corresponding Sensors, and Their IDs*

Table 5.2 presents a concise summary of all monitoring network clusters, critical elements and their associated sensors, and the sensors' unique names. The table serves as a comprehensive overview of the entire health monitoring network, allowing for a quick and comprehensive understanding of the proposed sensing network. By consolidating all relevant information, such as sensor types, sensor IDs, and their corresponding locations, the table provides a glance at the entire system.

It is important to note that the sensor IDs within each cluster (Figure 5.1 and Table 5.2) have intentionally been overlapped with adjacent clusters. This means that certain selected sensors within a subnetwork send their data to two cluster heads simultaneously. This redundancy in data acquisition provides reference points for evaluating the validity of data acquisition efforts within each cluster. By comparing the data received from overlapping sensors, any inconsistencies or anomalies can be identified, and potential false positives can be avoided. An example of utilizing the overlapping sensors is when observing large readings of cables' tension in cluster #1 while not observing similar readings in the other clusters. In such cases, the data from the overlapping sensors under cluster #1 and cluster #2 are compared to verify the validity of the large reading. This comparison helps determine whether the observed cable tension is a valid indication or if it is potentially caused by malfunctions or inconsistencies within cluster #1. By cross-referencing the data from overlapping sensors, the monitoring effort can ensure the accuracy and reliability of the measured data.

Table 5.2. Summary of the monitoring network, including critical elements, sensing clusters, and associated unique sensors' IDs

Critical Element	Base Stations				Sensor Type
	Gateway Node 1		Gateway Node 2		
	Cluster #1	Cluster #2	Cluster #3	Cluster #4	
	<i>Sensor IDs</i>	<i>Sensor IDs</i>	<i>Sensor IDs</i>	<i>Sensor IDs</i>	
Stay Cables	Acc-NW1-1 to 12	Acc-NW1-10 to 22	Acc-NE1-30 to 40	Acc-NE1-23 to 32	Accelerometer
	Acc-SW1-41 to 52	Acc-SW1-50 to 62	Acc-SE1- 70 to 80	Acc-SE1-63 to 72	Accelerometer
	HS-NW14-1&2	HS-SW14-5&6	HS-NE14-1&2	HS-SE14-5&6	Humidity sensor
Edge Girders	FBG-NG-1 to 3	FBG-NG-3 to 5	FBG-NG-5 to 7	FBG-NG-7 to 9	Fiber Optic Strain Gauge
	FBG-SG-10 to 12	FBG-SG-12 to 14	FBG-SG-14 to 16	FBG-SG-16 to 18	Fiber Optic Strain Gauge
	Acc-EG- 1 to 3	Acc-EG-4 to 6	Acc-EG-7 to 11	Acc-EG-11 to 15	Accelerometer
	EG-DT-N-1	EG-DT-N-2	EG-DT-N-2	EG-DT-N-3	Displacement Transducer
	EG-DT-S-4	EG-DT-S-5	EG-DT-S-5	EG-DT-S-6	Displacement Transducer
	RS-NG-1	RS-NG-2	RS-NG-3	RS-NG-4	Rotational Sensor (Tiltmeter)
	RS-SG-5	RS-SG-6	RS-SG-7	RS-SG-8	Rotational Sensor (Tiltmeter)
	Towers	Anemometer 1	!	!	Anemometer 2
RS-WT-1		RS-WT-2	RS-ET-3	RS-ET-4	Rotational Sensor (Tiltmeter)
Acc-WT-1 to 2		!	!	Acc-ET-3 to 4	Accelerometer
GPS-WT		!	!	GPS-ET	Global Displacement Reader
Anchor Boxes	FBG-ABW-1 to 4	FBG-ABW-4 to 8	FBG-ABE 9 to 12	FBG-ABE-12 to 16	Fiber Optic Strain Gauge
	FO-TS-WT-3	!	!	FO-TS-ET-3	Fiber Optic Temperature Sensor
	CS-WT-1	CS-WT-2	CS-ET-1	CS-ET-2	Corrosion Sensor
	HS-WT-EXT-1	!	!	HS-ET-EXT-1	Exterior Humidity sensor
	HS-WT-INT-1	!	!	HS-ET-INT-1	Interior Humidity Sensor
Viscous Dampers	VD-DT-WT-1	VD-DT-WT-1 & 2	VD-DT-ET-3	VD-DT-ET-3 & 4	Displacement Transducer
	FO-TS-WT-1	FO-TS-WT-2	FO-TS-ET-1	FO-TS-ET-2	Fiber Optic Temperature Sensor
Deck	Load Cell-1	!	!	Load Cell-2	Load cell
	GPS-1	GPS-2	GPS-3	!	Global Displacement Reader

## 6. Summary, Conclusion, and Future Work

This study presented a practical framework for instrumentation and data acquisition and aggregation of the new Gerald Desmond Bridge. The recommended instrumentation is intended to serve as the foundation for remote condition assessment of the bridge's critical elements. The bridge, located at the Port of Long Beach and completed in 2020, is California's first cable-stayed bridge that serves as a critical transportation link in the region. The iconic bridge features a unique 2000-foot-long cable-stayed segment. This very large structure demands frequent inspection and monitoring to ensure the health of its critical elements, such as the towers, girders, and stay cables. The framework presented in this study will be effective in creating a foundation for real-time or near real-time remote health monitoring of the bridge. The framework primarily targets the monitoring of critical elements of the bridge. As part of this study, a comprehensive literature review on best practices and recent advancements in both sensing technologies and instrumentation strategies utilized in similar cable-stayed bridges worldwide was performed. The framework includes, identifies, and recommends appropriate sensor types for each critical element, optimal sensor placements, and a consistent naming convention for all sensing channels across the monitoring network.

The structural system of the bridge and its design reports, such as load rating reports, have been reviewed and the existing array of 44 accelerometers on the main span of the bridge, deployed by the California Geological Survey (CGS), was discussed in detail. For reference, the response of the bridge during a local earthquake (Carson 2021) has been analyzed in the time and frequency domain. A comprehensive understanding of the load path and structural redundancy within the bridge is crucial when designing an effective monitoring regime. This knowledge allowed us to explain the failure mechanisms of critical elements and their potential impact on adjacent elements. The proposed instrumentation in this study will go beyond accelerometer arrays and encompass a wide range of cutting-edge and sustainable monitoring sensors, including Fiber Bragg Grating (FBG) friction strain gauges, displacement transducers, fiber-optic temperature sensors, FBG tiltmeters, ultrasonic anemometers, and more. Challenges associated with data acquisition for a large sensing network have been thoroughly examined, and practical solutions have been proposed to ensure the resiliency of the network.

In this study, all the crucial factors associated with the design of a successful remote monitoring system have been thoroughly examined. We gathered a set of requirements that serve as guiding principles for the design process, including (1) wireless sensing technologies and their advantages, (2) element-level local response monitoring, (3) scalability of the network, (4) cables' tension analysis, (5) energy saving and harvesting, (6) fatigue-life estimation of fracture-critical elements, (7) compensation of response for thermal effects, (8) decentralization of the data acquisition, and more. Each factor was carefully reviewed to ensure the establishment of a monitoring system for the bridge that is both reliable and resilient. Subsequently, we proposed element-specific instrumentation and layout designs tailored to the critical elements of the bridge.

Traditional visual inspection involves several challenges for a complex and exceptionally large structure like the Gerald Desmond Bridge. Some of these challenges include (1) labor intensity, (2) time consumption, (3) cost, and (4) subjectivity. Considering these challenges, alternative methods such as monitoring the bridge's critical elements using sensory data and detecting damage or deterioration in their early stages are highly desirable for inspectors and operators. Remote monitoring of bridge elements offers significant advantages in facilitating emergency response in large cities. By providing warnings for unsafe routes as soon as damage is detected, it enables fast response to ensure public safety.

Verification and calibration of the sensing network are key steps after the proposed sensors have been partially or fully deployed on the bridge. A series of recordings can be collected during heavy and light traffic hours, as well as on windy days. The recorded response of members under each sensing cluster must be reviewed, and the accuracy of the values should be confirmed. Calculated response should be compared with results obtained from the finite element model to verify and calibrate the sensor network and the post-processing algorithm based on actual on-site data. Furthermore, thresholds for healthy and anomalous responses at critical elements should be determined using the field tests. Response variabilities in the parameter of interest (e.g., strain or displacement) and their sensitivity to various environmental, operational, or non-damage related phenomena (such as creep, shrinkage cracks, thermal expansion, or contraction) should be investigated and filtered out. These verifications and calibrations are crucial for early damage warning systems, as they enhance the system's reliability and prevent future false positive alerts.

#### ***Future Work: Field Test and Verification of System Performance***

Verification and calibration of the sensing network are key steps after the proposed sensors have been partially or fully deployed on the bridge. A series of recordings can be collected during heavy and light traffic hours, as well as on windy days. The recorded response of members under each sensing cluster must be reviewed, and the accuracy of the values should be confirmed. Additionally, the acceleration of the stay cables should be analyzed to estimate their tension. The calculated value should be compared with tension forces obtained from the finite element model results to verify and calibrate the cable force calculations based on actual on-site parameters.

A simple methodology (i.e., algorithm) should be developed to interpret the collected data and infer damage for each critical element. The thresholds for healthy responses and anomalous responses at elements should be determined using the field tests mentioned above. Furthermore, a detailed analysis of variabilities in the parameter of interest (e.g., strain or displacement) and their sensitivity to various environmental, operational, or non-damage related phenomena (such as creep, shrinkage cracks, thermal expansion, or contraction) should be conducted. Any non-damage related changes in the measured parameters should be treated as noise and filtered out from the signal. The true calibration of the post-processing method may also require a series of on-site force-vibration tests where damage can be artificially induced at elements using portable masses. For example, attaching a lumped mass to a cable will decrease its fundamental frequency of

vibration, resulting in a smaller estimated tension force. The monitoring system should be capable of detecting such changes. These verifications and calibrations are crucial for early damage warning systems, as they enhance the system's reliability and prevent future false positive alerts.

# Bibliography

- Alamdari, M. M., Dang Khoa, N. L., Wang, Y., Samali, B., & Zhu, X. (2019). A multi-way data analysis approach for structural health monitoring of a cable-stayed bridge. *Structural Health Monitoring*, 18(1), 35–48.
- American Association of State Highway Officials (AASHTO). (2020). AASHTO LRFD Bridge Design Specifications, ISBN 978-1-56051-738-2.
- Ansari, F. (1997). State-of-the-art in the applications of fiber-optic sensors to cementitious composites. *Cement and Concrete Composites*, 19(1), 3–19.
- Arlin, G., & Melendez, C. (2017). Design of a Structural Health Monitoring (SHM) System for the Third Bridge Over the Panama Canal at the Atlantic Side. *Structural Health Monitoring 2017*.
- Behmanesh, I., & Moaveni, B. (2015). Probabilistic identification of simulated damage on the Dowling Hall footbridge through Bayesian finite element model updating. *Structural Control and Health Monitoring*, 22(3), 463–483.
- Betti, R., Sloane, M. J. D., Khazem, D., & Gatti, C. (2016). Monitoring the structural health of main cables of suspension bridges. *Journal of Civil Structural Health Monitoring*, 6, 355–363.
- Bischoff, R., Meyer, J., Enochsson, O., Feltrin, G., & Elfgren, L. (2009, July). Event-based strain monitoring on a railway bridge with a wireless sensor network. In *Proceedings of the 4<sup>th</sup> International Conference on Structural Health Monitoring of Intelligent Infrastructure, Zurich, Switzerland, 2224, 7482*.
- Borzok, M. J. (2022). California's First Major Vehicular Cable-Stayed Bridge. In *Structures Congress 2022*, 135–147.
- California Department of Transportation (Caltrans). (2013, April). *Seismic Design Criteria Version 1.7*.
- Catbas, F. N., Susoy, M., & Frangopol, D. M. (2008). Structural health monitoring and reliability estimation: Long span truss bridge application with environmental monitoring data. *Engineering structures*, 30(9), 2347–2359.
- Catbas, F. N., & Aktan, A. E. (2000). Modal analysis as a bridge health monitoring tool. *Advanced Technology in Structural Engineering: Structures Congress, ASCE, Reston, VA*, 1–10.

- Chen, D., Huo, L., Li, H., & Song, G. (2018). A fiber bragg grating (FBG)-enabled smart washer for bolt pre-load measurement: design, analysis, calibration, and experimental validation. *Sensors*, 18(8), 2586.
- Cho, S., Jang, S. A., Jo, H., Mechitov, K., Rice, J. A., Jung, H. J., ... & Seo, J. (2010, March). Structural health monitoring system of a cable-stayed bridge using a dense array of scalable smart sensor network. In *Sensors and Smart Structures Technologies for Civil, Mechanical, and Aerospace Systems 2010* (Vol. 7647, pp. 51–62). SPIE.
- Costa, B. J. A., Magalhaes, F., Cunha, A., & Figueiras, J. (2014). Modal analysis for the rehabilitation assessment of the Luiz I bridge. *J. Bridge Eng.*, 19(12).
- Dong, Y., Song, R., & Liu, H. (2010). *Bridges structural health monitoring and deterioration detection—synthesis of knowledge and technology* (No. AUTC# 309036). Alaska. Dept. of Transportation and Public Facilities.
- Dudek, G., & Jenkin, M. (2016). Inertial sensing, GPS and odometry. In *Springer Handbook of Robotics* (pp. 737–752). Cham: Springer International Publishing.
- Fang, Z., & Wang, J. Q. (2012). Practical formula for cable tension estimation by vibration method. *Journal of Bridge Engineering*, 17(1), 161–164.
- Fujino, Y., & Siringoringo, D. M. (2011). Bridge monitoring in Japan: the needs and strategies. *Structure and Infrastructure Engineering*, 7(7–8), 597–611.
- Ghemari, Z., Salah, S., & Bourenane, R. (2018). Resonance effect decrease and accuracy increase of piezoelectric accelerometer measurement by appropriate choice of frequency range. *Shock and Vibration*, 2018, 1–8.
- Greif, V., Sassa, K., & Fukuoka, H. (2006). Failure mechanism in an extremely slow rock slide at Bitchu-Matsuyama castle site (Japan). *Landslides*, 3, 22–38.
- Grubb, M. A., Wilson, K. E., White, C. D., & Nickas, W. N. (2015). *Load and resistance factor design (LRFD) for highway bridge superstructures—reference manual* (No. FHWA-NHI-15-047). National Highway Institute (US). <https://www.fhwa.dot.gov/bridge/pubs/nhi15047.pdf>
- Guo, C., Chen, D., Shen, C., Lu, Y., & Liu, H. (2015). Optical inclinometer based on a tilted fiber Bragg grating with a fused taper. *Optical Fiber Technology*, 24, 30–33.
- He, Z., Li, W., Salehi, H., Zhang, H., Zhou, H., & Jiao, P. (2022). Integrated structural health monitoring in bridge engineering. *Automation in Construction*, 136, 104168.

- Howell, D. A., & Shenton III, H. W. (2006). System for in-service strain monitoring of ordinary bridges. *Journal of Bridge Engineering*, 11(6), 673–680.
- Hsieh, K. H., Halling, M. W., Barr, P. J., & Robinson, M. J. (2008). Structural damage detection using dynamic properties determined from laboratory and field testing. *J. Perform. Constr. Facil.*, 22(4), 238–244.
- Huang, Q., Gardoni, P., & Hurlbaeus, S. (2011). Adaptive reliability analysis of reinforced concrete bridges using nondestructive testing. *J. of Risk and Uncertainty in Eng. Systems, Part A: Civil Eng.* 1.4 (2015): 04015014.
- Iranmanesh, A., & Ansari, F. (2014). Energy-based damage assessment methodology for structural health monitoring of modern reinforced concrete bridge columns. *J. Bridge Eng.*, 19(8), A4014004.
- Jakiel, P., & Ma! ko, Z. (2017). Estimation of cables' tension of cable-stayed footbridge using measured natural frequencies. In *MATEC Web of Conferences* (Vol. 107, p. 00006). EDP Sciences.
- Jang, S., Jo, H., Cho, S., Mechitov, K., Rice, J. A., Sim, S. H., ... & Agha, G. (2010). Structural health monitoring of a cable-stayed bridge using smart sensor technology: deployment and evaluation. *Smart Structures and Systems*, 6(5–6), 439–459.
- Jo, H., Park, J. W., Spencer, B. F., & Jung, H. J. (2013). Development of high-sensitivity wireless strain sensor for structural health monitoring. *Smart Struct. Syst*, 11(5), 477–496.
- Jo, H., Sim, S. H., Mechitov, K. A., Kim, R., Li, J., Moinzadeh, P., ... & Nagayama, T. (2011, April). Hybrid wireless smart sensor network for full-scale structural health monitoring of a cable-stayed bridge. In *Sensors and Smart Structures Technologies for Civil, Mechanical, and Aerospace Systems 2011* (Vol. 7981, pp. 45–59). SPIE.
- Kalooop, M. R., & Hu, J. W. (2016). Dynamic performance analysis of the towers of a long-span bridge based on GPS monitoring technique. *Journal of Sensors*, volume 2016. DOI: 10.1155/2016/7494817
- Kamble, V., Shinde, V., & Kittur, J. (2020). Overview of Load Cells. *Journal of Mechanical and Mechanics Engineering*, 6(3).
- Kim, B. H., & Park, T. (2007). Estimation of cable tension force using the frequency-based system identification method. *Journal of sound and Vibration*, 304(3-5), 660–676.

- Lederman, G., Wang, Z., Bielak, J., Noh, H., Garrett, J. H., Chen, S., ... & Rizzo, P. (2014, July). Damage quantification and localization algorithms for indirect SHM of bridges. In *Proc. Int. Conf. Bridge Maint., Safety Manag., Shanghai, China* (pp. 640–647).
- Lee, C. Y., & Lee, G. B. (2005). Humidity sensors: a review. *Sensor Letters*, 3(1–2), 1–15.
- Li, R. J., Lei, Y. J., Chang, Z. X., Zhang, L. S., & Fan, K. C. (2018). Development of a high-sensitivity optical accelerometer for low-frequency vibration measurement. *Sensors*, 18(9), 2910.
- Li, X. (2013). *Damage Identification of the Dowling Hall Footbridge Based on Ambient Acceleration and Strain Measurement* (Doctoral dissertation, Tufts University). <https://dl.tufts.edu>
- Liu, S., & Jiang, D. (2009, February). The application of structural health monitoring system technology using FBG to the No. 2 Wuhan bridge over the Yangtze River. In *Photonics and Optoelectronics Meetings (POEM) 2008: Fiber Optic Communication and Sensors* (Vol. 7278, pp. 159–166). SPIE.
- Massaroni, C., Saccomandi, P., & Schena, E. (2015). Medical smart textiles based on fiber optic technology: an overview. *Journal of functional biomaterials*, 6(2), 204–221.
- Melendez, G. A. C. (2017). Design of The Structural Health Monitoring System for The Third Bridge Over the Panama Canal. In *Proc. PLANC-World Congress in Panama City, Panama*.
- Meng, N., Treacy, M., Adam, S., Paciacconi, A., & SA, M. (2019). New SHM applications in cable-supported bridges—Case studies. In *Proceedings of the 5th conference on Smart Monitoring, Assessment and Rehabilitation of Civil Structures* (pp. 27–29).
- Mosquera, V., Smyth, A. W., & Betti, R. (2012). Rapid evaluation and damage assessment of instrumented highway bridges. *Earthquake Engineering & Structural Dynamics*, 41(4), 755–774.
- Noel, A. B., Abdaoui, A., Elfouly, T., Ahmed, M. H., Badawy, A., & Shehata, M. S. (2017). Structural health monitoring using wireless sensor networks: A comprehensive survey. *IEEE Communications Surveys & Tutorials*, 19(3), 1403–1423.
- Noman, A. S., Deeba, F., & Bagchi, A. (2013). Health monitoring of structures using statistical pattern recognition techniques. *J. Perform. Constr. Facil.*, 27(5), 575–584.
- Ntotsios, E., Papadimitriou, C., Panetsos, P., Karaiskos, G., Perros, K., & Perdikaris, P. C. (2008). Bridge health monitoring system based on vibration measurements. *Bull Earthquake Eng.* 7, 469–483.

- O'Connor, S., Kim, J., Lynch, J. P., Law, K. H., & Salvino, L. (2010, January). Fatigue life monitoring of metallic structures by decentralized rainflow counting embedded in a wireless sensor network. In *Smart Materials, Adaptive Structures and Intelligent Systems* (Vol. 44168, pp. 751-759). ASME.
- Rahmani, M., Ebrahimian M., & Todorovska, M. I. (2015). Time-wave velocity analysis for early earthquake damage detection in buildings: Application to a damaged full-scale RC building. *Earthq. Eng. Struct. Dyn.*, *44*, 619–636. DOI: 10.1002/eqe.2539.
- Rahmani, M., & Todorovska, M. I. (2014). 1D system identification of a 54-story steel frame building by seismic interferometry. *Earthquake Engng Struct. Dyn.*, *43*(4), 627–640.
- Rahmani, M., & Todorovska M. I. (2021). Structural health monitoring of a 32-storey steel-frame building using 50 years of seismic monitoring data. *Journal of Earthquake Engineering and Structural Dynamics*, *50*(6), 1777–1800.
- Rizzo, P., & Enshaiean, A. (2021). Challenges in bridge health monitoring: A review. *Sensors*, *21*(13), 4336.
- Said, M. N. A., Duchesne, D., Maurenbrecher, A. P., Ibrahim, K., Lumsdon, C., & Stephenson, D. (2005). Monitoring the long-term performance of the Peace Tower in Ottawa. *APT bulletin*, *36*(1), 53–59.
- Seo, J., Hu, J. W., & Lee, J. (2015). Summary review of structural health monitoring applications for highway bridges. *J. Perform. Constr. Facil.*, *30*(4), 04015072.
- Son, H., Pham, V. T., Jang, Y., & Kim, S. E. (2021). Damage localization and severity assessment of a cable-stayed bridge using a message passing neural network. *Sensors*, *21*(9), 3118.
- Soyoz, S., Feng, M. Q., & Shinozuka, M. (2009). Utilization of seismic response measurement for damage detection and capacity estimation of bridge. *Technical Conf. on Lifeline Earthquake Engineering Conf., ASCE, Reston, VA*, 1–8.
- Subandi, A., Idris, I., & Ahmad, A. S. (2007). Experimental study of an Aluminum-Polysilicon Thermopile for Implementation of Airflow Sensor on Silicon Chip. *Journal of Engineering and Technological Sciences*, *39*(2), 98–108.
- Vossoghi, A., & Saiidi, M. S. (2010). Seismic damage states and response parameters for bridge columns. *International Concrete Abstracts Portal*, 29–46.
- Wang, T., Yuan, Z., Gong, Y., Wu, Y., Rao, Y., Wei, L., ... & Wan, F. (2013). Fiber Bragg grating strain sensors for marine engineering. *Photonic Sensors*, *3*, 267–271.

- Woszczyński, M., Rogala-Rojek, J., & Stankiewicz, K. (2022). Advancement of the Monitoring System for Arch Support Geometry and Loads. *Energies*, 15(6), 2222.
- Xiao, F., Chen, G. S., & Hulse, J. L. (2017). Monitoring bridge dynamic responses using fiber Bragg grating tiltmeters. *Sensors*, 17(10), 2390.
- Ye, X. W., Ni, Y. Q., Wong, K. Y., & Ko, J. M. (2012). Statistical analysis of stress spectra for fatigue life assessment of steel bridges with structural health monitoring data. *Engineering Structures*, 45, 166–176.
- Zhang, L., Qiu, G., & Chen, Z. (2021). Structural health monitoring methods of cables in cable-stayed bridge: A review. *Measurement*, 168, 108343.
- Zhou, Z., Wegner, L. D., & Sparling, B. F. (2007). Vibration-based detection of small-scale damage on a bridge deck. *J. Struct. Eng.*, 133(9), 1257–1126.
- Zui, H., Shinke, T., & Namita, Y. (1996). Practical formulas for estimation of cable tension by vibration method. *Journal of structural engineering*, 122(6), 651–656.

# About the Authors

## **Mehran Rahmani, PhD, PE**

Dr. Mehran Rahmani is an Associate Professor in the Civil Engineering and Construction Management (CECEM) Department of California State University Long Beach (CSULB). He earned a PhD in Structural and Earthquake Engineering from the University of Southern California (USC) in 2014, an MS in Electrical Engineering (with an emphasis in Signal Processing) from USC in 2013, and an MS in Structural Engineering from Sharif University of Technology (Iran) in 2009. Prior to joining CSULB, Dr. Rahmani, a registered Professional Engineer (PE) in the state of California, worked as a Senior Engineer and as a Project Engineer in the structural engineering industry from 2014 to 2017.

Dr. Rahmani's research focuses on structural system identification, structural health monitoring, and earthquake damage detection of buildings and bridges using sensory data. His PhD research focused on developing a wave-based methodology for remote post-earthquake structural damage detection that is robust when applied to actual structures and is calibrated using data from full-scale buildings. The research project was funded by the National Science Foundation (NSF). He was instrumental in the advances in wave-based structural identification and monitoring in the past 15 years.

## **Vesna Terzic, PhD**

Dr. Vesna Terzic is an Associate Professor in the CECEM department at CSULB. Dr. Terzic has conducted research related to transportation infrastructure for the past 15 years. Her research focuses on experimental and analytical investigations of the seismic performance of highway bridges. Dr. Terzic has vast experience in developing robust and high-fidelity nonlinear models of overpass bridges. She has significantly contributed to developing analytical models for evaluating the traffic capacity of bridges in damaged conditions. She has recently developed a novel method for probabilistic evaluation of the post-earthquake functionality of bridges.

## **Andrea Calabrese, PhD**

Dr. Andrea Calabrese is an Associate Professor in the CECEM department at CSULB. Dr. Calabrese earned his PhD in Construction Engineering with an emphasis in Structural Engineering in 2013. He was a visiting research fellow at the Pacific Earthquake Engineering Research Center (PEER) from 2010–12 and a postdoctoral researcher of the ReLUI Consortium, The Italian Network of University Laboratories in Earthquake Engineering, from 2013–2014. He worked as a Structural Engineer at Foster & Partners, London, and has been a registered engineer in Italy since 2009 and a Chartered Engineer (CEng) and Full Member of the Institution of Civil Engineers (MICE) in the UK since 2017. Dr. Calabrese's current research interests are in the fields of experimental testing, structural dynamics, base isolation, vibration

engineering and in the development of novel low-cost devices for the seismic protection of bridges and buildings.

**Brittany Campbell, BS. CE**

Brittany Campbell received her BS in civil engineering from California State University, Long Beach. She served as a Research Assistant on this project. Brittany will commence her Master's in Business Administration (MBA) at the CSULB in the Fall 2023.

# MTI FOUNDER

---

**Hon. Norman Y. Mineta**

## MTI BOARD OF TRUSTEES

---

**Founder, Honorable Norman Mineta\*\*\***  
Secretary (ret.),  
US Department of Transportation

**Chair, Jeff Morales**  
Managing Principal  
InfraStrategies, LLC

**Vice Chair, Donna DeMartino**  
Retired Transportation Executive

**Executive Director, Karen Philbrick, PhD\***  
Mineta Transportation Institute  
San José State University

**Rashidi Barnes**  
CEO  
Tri Delta Transit

**David Castagnetti**  
Partner  
Dentons Global Advisors

**Maria Cino**  
Vice President  
America & U.S. Government  
Relations Hewlett-Packard Enterprise

**Grace Crunican\*\***  
Owner  
Crunican LLC

**John Flaherty**  
Senior Fellow  
Silicon Valley American  
Leadership Form

**Stephen J. Gardner\***  
President & CEO  
Amtrak

**Ian Jefferies\***  
President & CEO  
Association of American Railroads

**Diane Woodend Jones**  
Principal & Chair of Board  
Lea + Elliott, Inc.

**Priya Kannan, PhD\***  
Dean  
Lucas College and  
Graduate School of Business  
San José State University

**Will Kempton\*\***  
Retired Transportation Executive

**David S. Kim**  
Senior Vice President  
Principal, National Transportation  
Policy and Multimodal Strategy  
WSP

**Therese McMillan**  
Retired Executive Director  
Metropolitan Transportation  
Commission (MTC)

**Abbas Mohaddes**  
CEO  
Econolite Group Inc.

**Stephen Morrissey**  
Vice President – Regulatory and  
Policy  
United Airlines

**Toks Omishakin\***  
Secretary  
California State Transportation  
Agency (CALSTA)

**April Rai**  
President & CEO  
Conference of Minority  
Transportation Officials (COMTO)

**Greg Regan\***  
President  
Transportation Trades Department,  
AFL-CIO

**Rodney Slater**  
Partner  
Squire Patton Boggs

**Paul Skoutelas\***  
President & CEO  
American Public Transportation  
Association (APTA)

**Kimberly Slaughter**  
CEO  
Systra USA

**Tony Tavares\***  
Director  
California Department of  
Transportation (Caltrans)

**Jim Tymon\***  
Executive Director  
American Association of  
State Highway and Transportation  
Officials (AASHTO)

**Josue Vaglienty**  
Senior Program Manager  
Orange County Transportation  
Authority (OCTA)

\* = Ex-Officio  
\*\* = Past Chair, Board of Trustees  
\*\*\* = Deceased

---

## Directors

**Karen Philbrick, PhD**  
Executive Director

**Hilary Nixon, PhD**  
Deputy Executive Director

**Asha Weinstein Agrawal, PhD**  
Education Director  
National Transportation Finance  
Center Director

**Brian Michael Jenkins**  
National Transportation Security  
Center Director

